Portable Energy for the Dismounted Soldier

Study Leader:
Nathan S. Lewis

Contributors:
Henry Abarbanel
Lars Bildsten
Paul Dimotakis
Freeman Dyson
Douglas M. Eardley
Stanley M. Flatté
Dick Garwin
Jeremy Goodman
Robert Grober
Jonathan Katz
Steve Koonin
Richard Muller
Malvin Ruderman
Ellen D. Williams

June 2003

JSR-02-135

JASON
The MITRE Corporation
7515 Colshire Drive
McLean, Virginia 22102-7508
(703) 883-6997

REPORT DOCUMENTATION PAGE

Form Approved
OMB No. 0704-0188

1. AGENCY USE ONLY *(Leave blank)*	2. REPORT DATE	3. REPORT TYPE AND DATES COVERED
	June 2003	

4. TITLE AND SUBTITLE

Portable Energy for the Dismounted Soldier

5. FUNDING NUMBERS

13039021-DC

6. AUTHOR(S)

Nathan S. Lewis, et al.

7. PERFORMING ORGANIZATION NAME(S) AND ADDRESS(ES)

The MITRE Corporation
JASON Program Office – W950
7515 Colshire Drive
McLean, Virginia 22102

8. PERFORMING ORGANIZATION REPORT NUMBER

JSR-02-135

9. SPONSORING/MONITORING AGENCY NAME(S) AND ADDRESS(ES)

Office of Defense Research and Engineering (ODDR&E)
Plans and Programs
3030 Defense Pentagon
Room 3D108
Washington, DC 20301-3030

10. SPONSORING/MONITORING AGENCY REPORT NUMBER

JSR-02-135

11. SUPPLEMENTARY NOTES

12a. DISTRIBUTION/AVAILABILITY STATEMENT

Approved for public release; distribution unlimited

12b. DISTRIBUTION CODE

13. ABSTRACT *(Maximum 200 words)*

In response to the study charge, the JASONs focused primarily on fuel cells for portable electrical energy production. Fuel cell technologies that were evaluated included high temperature fuel cells such as solid oxide fuel cells and molten carbonate fuel cells, and low/mid temperature (80-200 °C) fuel cells including phosphoric acid fuel cells, alkaline fuel cells, and polymer electrolyte membrane fuel cells. In addition, direct methanol fuel cells were evaluated.

14. SUBJECT TERMS

15. NUMBER OF PAGES

135

16. PRICE CODE

17. SECURITY CLASSIFICATION OF REPORT	18. SECURITY CLASSIFICATION OF THIS PAGE	19. SECURITY CLASSIFICATION OF ABSTRACT	20. LIMITATION OF ABSTRACT
Unclassified	Unclassified	Unclassified	

Standard Form 298 (Rev. 2-89)
Prescribed by ANSI Std. Z39-18
298-102

Contents

1 EXECUTIVE SUMMARY

This study addresses technologies that have the potential to provide high gravimetric energy densities (> 1000 W-hr/kg) at 20 W mean output power levels for use by a dismounted soldier. For such missions, soldiers currently carry approximately 15-20 kg of batteries, so lighter electrical energy sources are highly desirable.

In response to the study charge, the JASONs focussed primarily on fuel cells for portable electrical energy production. Fuel cell technologies that were evaluated included high temperature fuel cells such as solid oxide fuel cells and molten carbonate fuel cells, and low/mid temperature (80-200 °C) fuel cells including phosphoric acid fuel cells, alkaline fuel cells, and polymer electrolyte membrane fuel cells. In addition, direct methanol fuel cells were evaluated.

Additional technologies that were evaluated include carbon-air batteries, thermophotovoltaics, alkali-metal-thermal-to-electric converters, and four types of microengines: micro two-stroke engines, microdiesels, microturbines, and microswing engines.

A variety of fuels were explored, including methods of storing and generating hydrogen for direct use in fuel cells. Additionally, propane, diesel fuel, methanol, and ammonia were considered as fuels either for use directly in fuel cells or for input to a fuel processing unit to produce an output fuel that could be used as the fuel cell feedstock.

We find that several technologies have legitimate potential, at 20 W power levels for long duration missions, to significantly outperform existing battery packs. Specifically, we find that:

- all such systems are hybrids with secondary batteries or supercapacitors to meet peak power demands;

- hybrid battery packs composed of two different types of batteries can significantly reduce soldier battery pack mass for certain missions, from a total mass of 20 kg to a mass of 6-7 kg;
- engineering considerations, as opposed to fundamental physical constraints, dictate the actual performance of fielded systems;
- this application space is unique to the military, and there does not appear to be a significant commercial market for 1 kg convertors that provide 20 W of portable power for 7-10 day periods;
- demonstrated H_2 polymer electrolyte membrane 20 W fuel cells and H_2 gas tankage can provide significant improvement in energy density relative to current primary battery technology;
- direct methanol fuel cell systems seem especially promising for this application, having demonstrated energy densities that are 10-fold greater than current primary batteries;
- 100-500 W microdiesel engines seem well-suited for rapid multi-battery charging using JP-8 provided that there is an acceptable logistical mission for such an approach;
- engineering trade-offs become severe as the overall system volume and mass decrease, or as the required power capacity per unit of mass or volume increases.

1.1 Recommendations

The following recommendations are offered in response to the following three specific questions in the study charge to the JASONs:

- Address technology options to mitigate the current limitations to the use of fuel cells (for example, current fuel cells can operate at temper-

atures of nearly 1000 degrees C; this presents an unacceptable risk in the modern battlefield).

- Provide insight into the question: Should the Department dramatically invest in fuel cells, or is some other energy generation technology more appropriate.

- If fuel cells are used, what ancillary technology is required for them to operate in a non-detectable manner?

We recommend that for 20 W mean power levels on extended missions, direct methanol fuel cells receive significant investment to further their technological development. Both direct methanol fuel cells and polymer electrobte membrance (PEM)/H2 fuel cells operate at 100 degrees C, thereby mitigating against safety limitations that might arise from high temperature operation. Both types of fuel cells can be operated with low signatures and made essentially non-detectable. However, direct methanol fuel cells avoid the storage and safety issues associated with use of H2, and for extended duration missions offer practical achievable energy densities that are superior to PEM/H2 systems and which are superior to current and projected battery systems.

We also recommend that investment be made into materials and systems that enable "passive" fuel cell operation with fewer active control loops. This would greatly simplify the balance of plant in fuel cell systems.

We recommend that funding be allocated to address the safety and packaging requirements and associated limitations for the fieldability of various fuels.

We recommend that fuel cell prototypes be evaluated rapidly with field personnel so that feedback as to the ultimate utility of what is being developed can be obtained in an expedient fashion.

At the DoD 6.1 level, we recommend that research be sustained towards:

- improving the performance at fuel cell cathodes (oxygen reduction). All of the fuel cells suffer kinetic overpotential losses at the cathode and improved cathode catalysts would have a global impact on the efficiency of such devices.

- development of improved anodes for methanol oxidation in DMFCs. Higher energy efficiencies would obviously be obtained if the kinetic overpotential for methanol oxidation could be reduced to levels comparable to that of H2 in a PEM fuel cell

- development of CO and S-tolerant H2 PEM catalysts. Such catalysts would avoid the need for water-gas shift and preferential oxidation catalysts and thereby could significantlysimplify systems that used steam reforming in conjunction with PEM fuel cells.

2 INTRODUCTION

This JASON report addresses a component of the Power and Energy initiative being undertaken by the DDR&E's office. The charge to JASON for this study reads as follows:

> The US military is currently challenged by a recognized deficiency to safely generate power in and to forward deployed locations and critically important, but austere accommodating environments i.e.: space, desert, jungle. JASONs shall provide an assessment and analysis of technologies including the viability and limitations of fuel cell technologies, and provide a detailed objective analysis, a comprehensive annotated report and oral presentation of the potential for power generation under described scenarios. The JASONs shall survey planned fuel cell technologies, and specifically hydrogen based fuel cells, in sufficient detail to allow a detailed business case to be made to guide investment in fuel cells for military use. The JASONs shall deliver a comprehensive report and annotated briefing that includes the following:

- Describes emergent fuel cell technology
- Describes (objectively) the power generated as a function of expendable supplies/materials
- Describes a viable architecture for their employment in the tactical battlespace of the future
- Addresses technology options to mitigate the current limitations to the use of fuel cells (for example, current fuel cells can operate at temperatures of nearly 1000 degrees C; this presents an unacceptable risk in the modern battlefield).

- Provide insight into the question: Should the Department dramatically invest in fuel cells, or is some other energy generation technology more appropriate.

- If fuel cells are used, what ancillary technology is required for them to operate in a non-detectable manner?

In response to this charge, the JASON's undertook a study in summer 2002 of power and energy for the military. The study topic was narrowed to address primarily portable power for dismounted soldiers, specifically for special operations types of missions, on which soldiers currently might carry 15-20 kg of batteries.

The study received briefings from the following people:

Jack Taylor & John Pellegrino, DDR&E (Energy and Power overview)

Scott Feldman, Army/Natick (Land Warrior overview)

Robert Hamlin, Army-Ft. Monmouth (Batteries)

Jeff Schmidt, Ball Aerospace (H_2 and methanol fuel cell systems)

Dave Bloomfield, Analytic Energy Systems (H_2 generators and NH_3 cracking)

William Acker, MTI (Direct methanol fuel cells)

Jerry Hallmark, Motorola (Direct and reformed methanol fuel cells)

Dan Palo, DOE-PNNL (micro methanol reformers)

Rich Masel, U. of Illinois (microreactors for NH_3 cracking)

Klavs Jensen, MIT (microchemical reactors)

John Cooper, LLNL (carbon-air batteries)

Ed Mussi & Tom Hunt, Ampsys (alkali-metal thermal to electric convertors)

Werner Dahm, U. of Michigan (microswing engines)

Kurt Annen, Aerodyne (micro two-stroke engines)

Alan Epstein, MIT (microturbines)

Paul Dev, D-Star Engineering (micro two-stroke engines)

In addition, the following people were consulted on the telephone and provided additional resources for this study:

Rao Surampudi, NASA-JPL (Direct methanol fuel cells)

Jeff Rinker, BP/Amoco/Arco (H_2 storage/utilization)

Mike Heben, DOE-NREL (H_2 storage)

Bob Nowak, DARPA (Palm Power Program)

Richard Paur, ARO (Portable Power)

Brian James/Ira Kuhn, Directed Technologies (H_2 storage)

Joe Stockel, USG (Power Sources and battery technology)

M. Amy Ryan, NASA-JPL (Alkali metal (AMTEC) thermionics)

David Wilt, NASA-Glenn-AFOSR (Thermophotovoltaics)

We acknowledge, and are grateful to, all of these briefers for their valuable input, that made this study possible.

The study exclusively considered local generation of portable power accompanying the soldier, and did not consider approaches such as battery recharging using solar power, or beaming of microwave or other electromagnetic power forms to the soldier. The study also did not address the use of nuclear reactions, in any form, for portable power generation.

3 POWER AND ENERGY DEMANDS

The JASONs did not receive detailed information on the current electrical power and energy budgets of soldiers. This lack of information in part is apparently due to the wide variability in power and energy demands that exist for the various different types of missions.

An estimate of the needed power demand was obtained, however, from the Army Land Warrior program [1, 2]. This program represents the next generation system of equipment for Army soldiers. The Land Warrior package includes advanced electronics and contains an integration of some of the power systems of the various electronics components.

The target mean power load for the Land Warrior package is $\approx$ 20 W. The current power budget has a higher value ($\approx$ 50 W), which is broken down to 14.8 W for the computer, 6.4 W for the flat-panel display, 7.4 W for the soldier radio (6.0 W transmit and 1.4 W receive), 14.0 W for the squad radio (12.0 W transmit and 2.0 W receive), 1.5 W for GPS, 5.6 W for the helmet and sighting system, and 6.0 W for the weapon system (5.5 W for the thermal weapon sight) [1]. The JASON study did not address possible demand reduction through redesign of the electronics, as this topic has been covered in depth in a recent National Research Council report on Energy for Dismounted Soldiers [1]. We anticipate some interplay between the estimated power demand budget and the power supply budget, so to set the scale of the problem we will use a 20 W value as a working estimate of the mean power load to be delivered by the energy conversion unit.

For a 7 day mission, the 20 W mean power load implies that a total energy budget of 3.4 kW-hr (12 MJ) must be supplied in the form of electrical energy to the soldier. We will also assume that all systems will be hybrids of some type, in which peak power loads are provided by a rechargeable battery, with the remainder of the system selected to provide the high energy needed

to recharge the secondary battery at a mean load of 20 W for the duration of the mission.

4 BATTERY PERFORMANCE

4.1 Theoretical and Practical Energy Densities of Battery Technologies

Table 1 lists the energy densities available from several different types of battery technologies [1]. The table includes values for primary (non-rechargeable) batteries as well as secondary (rechargeable) battery systems.

Table 1: Battery Performance Characteristics

	Anode	Cathode	W-hr/kg, Theoretical	W-hr/kg, Actual
Primary	Li	SO_2	1175	260
	Li	$SOCl_2$	1489	320
	Li	SO_2Cl_2	1405	450
	Li	MnO_2	1001	230
Secondary	Zn	MnO_2	358	85
	Ni	Ni-H	278	70
	Zi	MnO_2	330	55
	Li	Mn_2O_4	510	140
	Li	CoO_2	750	95

The theoretical values are obtained by considering only the masses of the materials used to make the anodes and cathodes of a battery cell. These values neglect the mass of the electrolyte, separator, packaging, and of any of the other components of a real battery. The theoretical values thus can not be achieved in any actual implementation of a packaged battery. The "actual" values listed in Table 1 are the energy densities of various packaged batteries that are available at the present time.

Of specific interest is the Li/SO_2 battery designated as the Army BA 5590 (Table 2).

Table 2: Battery Performance Characteristics

Battery Name	Type	W-hr/kg	$/kW-hr
Army BA5590	Li/SO_2(P)	170	344
Army BA390	Ni/MN (R)	47	
L.W.v.0.6	Li-MnO_2(P)	285	
L.W.v.0.6	Li-ion (R)	118	

The energy density of this battery is in the range of the other battery technologies displayed in Table 1, and thus is consistent with the order-of-magnitude estimate of the performance of current lithium battery technology for this application. The Li/SO_2 battery is an extensively packaged battery (for safety purposes) and also provides a high current (i.e., a high discharge rate) so that it can deliver high power densities as well as moderately high energy densities.

Table 2 also displays energy densities for the next generation of military batteries, the so-called Land Warrior v 0.6 Li/MnO_2 and Li-ion batteries [2]. The former is a primary battery, and the latter is a secondary battery. The values of interest are 285 W-hr/kg for the packaged primary battery and 118 W-hr/kg for the rechargeable battery.

When considering replacing an existing technology with an alternative option that is yet to be developed, it is always necessary to evaluate the rate at which the existing technology is improving with time. In this fashion, one can estimate the performance that will be provided by the existing system at the time at which the alternate technology might be actually deployable in the field. Figure 1 displays the energy density of various different rechargeable battery technologies over a 15 year period up to 1999.

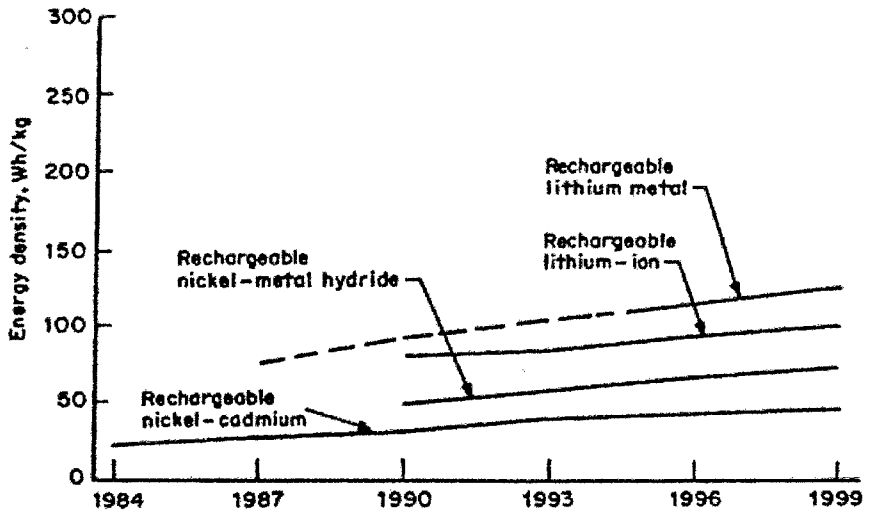

Figure 1: Battery performance characteristics.

This plot shows that battery technology has been improving only modestly over the past 15-20 years. We therefore will take as a working estimate an energy density of 300 W-hr/kg for battery technology for military applications, i.e. a value which is slightly higher than the next generation Land Warrior battery, as the value with which one will have to compete through introduction of any new technology in the next 5–10 year period.

4.2 Trade-offs between Power Density and Energy Density: Ragone Plots

Figures 2 and 3 depict plots of the power density available from various types of battery technologies as a function of the energy density of such batteries. All battery technologies exhibit a trade-off between high power density and high energy density. This tradeoff reflects the losses in deliverable capacity when batteries are discharged at a high rate. These losses fundamentally arise from resistive losses in the battery as well as kinetic and thermodynamic losses that are incurred when higher current densities are

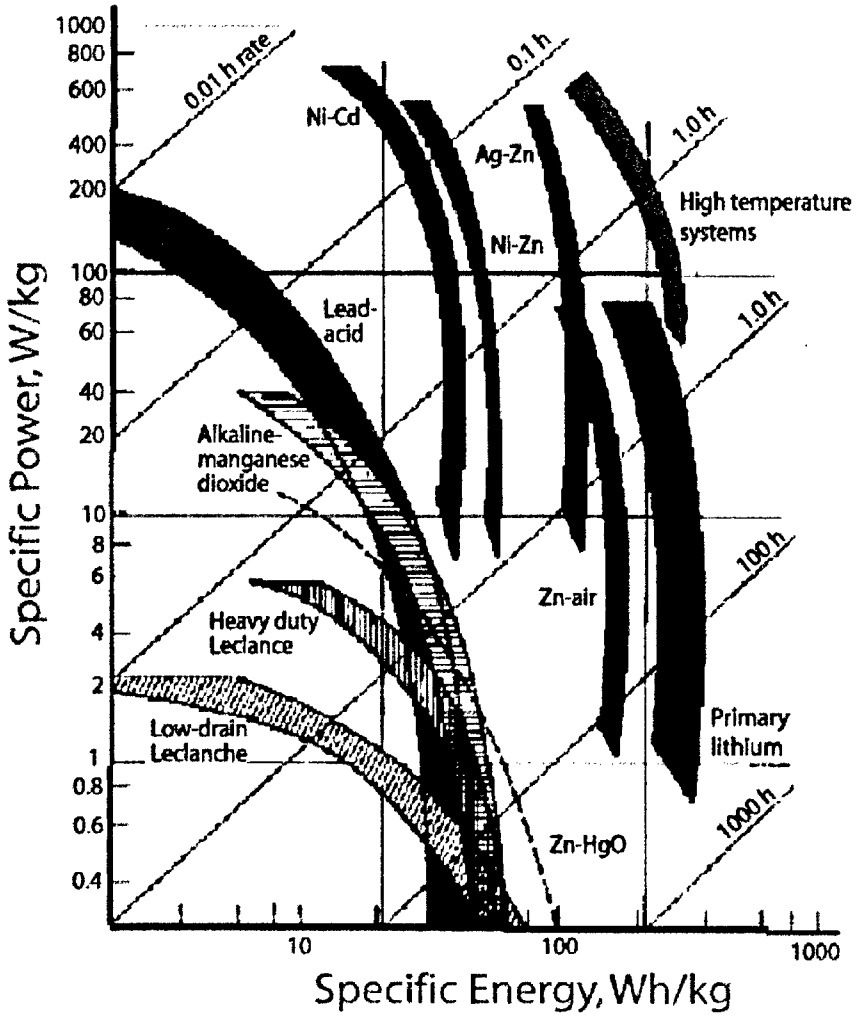

Figure 2: Battery performance characteristics.

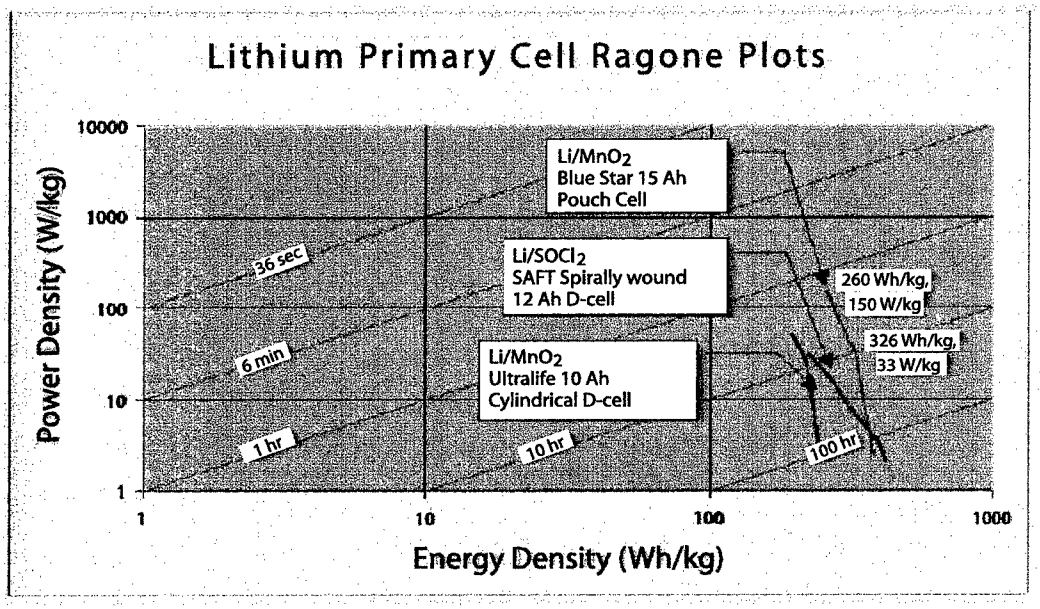

Figure 3: Battery performance characteristics.

passed through the electrochemical cell that forms the battery system. The data in Figure 2 are for various types of batteries, while those in Figure 3 are specifically for three types of lithium batteries.

A point of interest is that a battery pack which is optimized to perform well at moderate-to-high power densities will not provide optimum energy density performance at low discharge rates. Hence this tradeoff suggests the use of hybrid battery systems for the extended mission application of concern, in which the peak power is supplied by a relatively small mass of high power density secondary batteries and the energy density demands are satisfied by a larger mass of primary batteries operating at a low output power density. The constraint is of course that the total mass of both battery types must be sufficient to provide a mean load of 20 W and that the battery pack should simultaneously be capable of providing, at minimum, the target of 3.4 kW-hr of total energy at a 20 W discharge rate.

It appears possible to meet these two targets simultaneously through use of a hybrid battery/battery system. Several candidates are available for the high energy density batteries, which would be run at relatively low rate. Candidate technologies include lithium-air batteries, zinc-air batteries, and Li/carbon monofluoride batteries. We will describe the hybrid battery/battery approach with the Li/CF battery as an example primarily because the specifications for this battery system were available to the JASONs during the course of this study [3].

Li/CF batteries of the type designated X702 are manufactured for the U.S. Government and are available for use over a reasonable temperature range [3]. They are available in DD size (with a mass of 0.18 kg) and are a relatively low rate battery, providing 0.5 A at 2.7 V. A sample specification sheet for these batteries is reproduced as Table 3, and sample discharge characteristics are displayed in Figure 4 [3].

Obtaining 3.4 kW-hr of output energy requires 6.1 kg of such batteries. This mass would produce a mean rated power of 45 W, which is sufficient for the 20 W baseload power demand and could additionally provide surge capacity. Alternatively, the primary batteries could be used in conjunction with a power management system (having a mass not estimated but which is not expected to be greater than 0.2 kg) to recharge a secondary battery that would be used to produce high peak power loads as needed. In this hybrid system, essentially all of the energy is provided by the high energy density Li/CF batteries. Hence the total system mass would be reduced from 20 kg of BA-5590 batteries to 6.1 kg of Li/CF batteries (assuming an actual energy density of 500 W-hr/kg of such batteries as opposed to the 550-590 W-hr/kg performance that these batteries can actually provide according to the specification sheet). Thus, as depicted in Figure 5, a significant portion of the mass of the battery pack of BA-5590 batteries could be eliminated through use of the hybrid battery pack approach.

Table 3: Characteristic of a Li/CF battery.

TYPICAL CAPACITIEES (aH) FOR x702c (LATE MARCH 2001) to a 2.00 V Cutoff Volate (VCO)									
Nominal		TARGET	CELLS DISCHARGE AT THE FOLLOWING TEMPERATURES °C °F)						
TIME	CURRENT	RESISTOR	-40 (-40)	-20 (-4)	0 (32)	24 (75)	50 (122)	70 (158)	90 (194)
0.50 h									
1.00 h									
2.00 h									
3.16 h									
5.00 h									
10.0 h									
10.0 h									
20.0 h	1.95A	1.38 m Ω	-	0.00	0.00	18.57	26.03	30.10	
31.6 h									
500 h h	78.0 mA	34.6 Ω	26.17	33.75		38.62			
100 kh	39.0 mA	69.0 Ω	28.25	35.12	38.20	39.58	39.30	38.95	36.29
P2.00 kh	19.5 mA	138 Ω		35.62 P	39.92 P	39.52 P	39.02 P	38.63 P	29.79
3.16 kh									
500 kh	7.80 mA	346 Ω	33.01	38.76	40.18	39.81	38.48	33.84	11.77
10.0 kh	3.90 mA	690 Ω				R	R		
20.0 kh	1.95 mA	1.39 Ω			R	R	R		
31.6 kh	1.23 mA	2.19 Ω				R,P			
50.0 kh	780 μA	3.46mk Ω				R			
100 kh	390 μA	6.90 k Ω				R,P			
R - Test is still running		P - Occasional Pulses Were Superimposed But Their Capacity is Not Included							

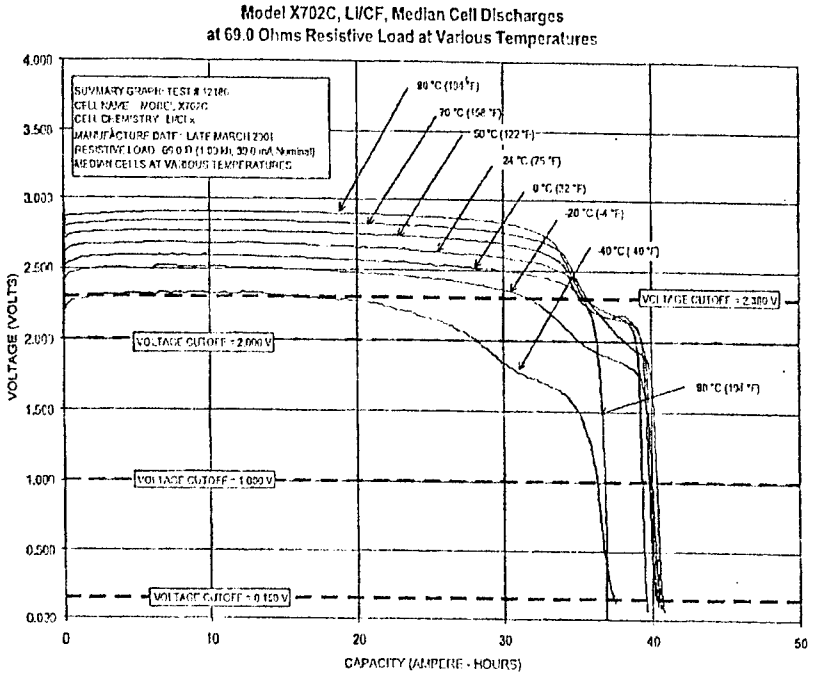

Figure 4: Capicity vs temperature of a Li/CF battery.

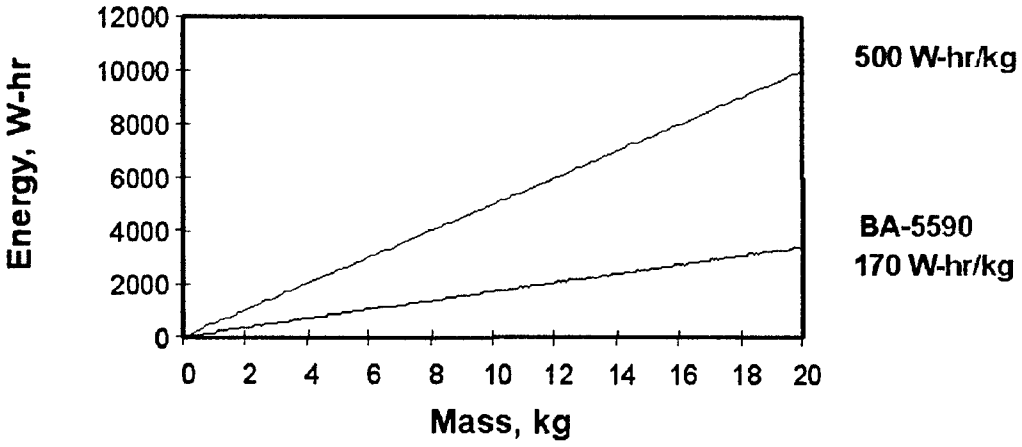

Figure 5: Energy vs mass of Li/CF and Li/SO_2 batteries.

This hybrid approach does not cover missions in which many radios or other devices simultaneously need to be powered, for which the total mean power load is in excess of 45 W. In that case, higher rate, lower energy density batteries would be required, and at sufficiently high power densities, the system performance will asymptotically approach that of a system consisting solely of BA-5590 batteries, due to the need to provide a high discharge rate as well as a high energy density.

5 COMPARISON OF ENERGY DENSITIES OF FUELS AND BATTERIES

Table 5 displays the energy densities theoretically available from various fuels [1, 4]. The values listed are based on the lower heating values (enthalpies of combustion forming water vapor as opposed to liquid water) for the combustion of the various fuels under standard temperature and pressure conditions. The value for propane is a good approximation to the value for diesel fuel; diesel fuel is primarily hydrocarbons and the energy density produced by combustion of the hydrocarbons is very similar, on a mass basis, for propane and diesel fuel (the lower heating value for a typical diesel fuel is $\approx$ 11,900 W-hr/kg) [1].

Table 4: Energy density of various fuels

			for 4 kW-hr	
Fuel	W-hr/kg	W-hr/L	kg	L
H2	33,300	755 (5,000 psi)	0.12	5.2
Gasoline	12,000	8,600	0.33	0.46
Methanol	5,500	4,400	0.72	0.91
Ammonia	5,800	603	0.69	6.6
Propane	12,800	6,400	0.32	0.64
Li/SO2 (cell)	900			
LiMnO2(P)	285	456	14.0	8.8

The theoretically obtainable values listed in Table 5 are not attainable in any practical system, much as the theoretical battery energy densities of Table 1 are not attainable in a packaged battery. Nevertheless, the theoretically available energy density of fuels is obviously over an order of magnitude, and almost two orders of magnitude, greater than the energy density delivered by packaged batteries. This large difference between actual battery performance and theoretical fuel energy density is the fundamental reason why fuel cells have attracted much recent attention as energy delivery systems: a fuel cell

system that converted even 10% of the energy density theoretically available in hydrogen, for example, or that converted 20% of the energy density theoretically available in diesel fuel, would have a 10-fold higher energy density than that of the next generation Land Warrior v0.6 Li/MnO_2 battery.

It is equally apparent, however, that engineering and packaging losses must be carefully considered before any robust comparison between theoretical values and actual energy densities of fuel cell systems can be made. The reason why these engineering-related losses are not expected to lower the practical energy densities of fuel cell systems below that of batteries is that fuel cell systems have a fundamental advantage for energy delivery applications relative to batteries. Batteries must contain both the reactants and the products of the electricity-generating reaction (excluding the special case of lithium-air or zinc-air batteries). In contrast, fuel cells need only carry one of the reactants, whereas the oxidant (oxygen from the air) as well as the products (generally carbon dioxide and water) are not carried in the energy production unit and therefore do not contribute to the mass of the electricity-producing system.

Several different technology approaches can be envisioned to achieve the conversion of the energy content of the fuels of Table 5 into electrical energy. One approach (Figure 6, bottom) would utilize a combustion process to run an engine (e.g., either a microturbine, an internal combustion engine, or an external combustion engine), and the mechanical energy would then be converted into electrical energy using a generator. The efficiencies of such systems are considered in Section 14.3 of this report. A second approach avoids limitations imposed by Carnot cycles and the need for a generator, and utilizes a fuel cell to directly produce electrical energy from a liquid chemical fuel. This option (Figure 6, top) is discussion in Sections 10.1 and 13 of the report. A third approach is to utilize a gaseous species, such as H_2, as the feedstock of the fuel cell, with the H_2 obtained either by chemically converting hydrocarbon-based liquid fuels partially in to H_2 (reforming), or

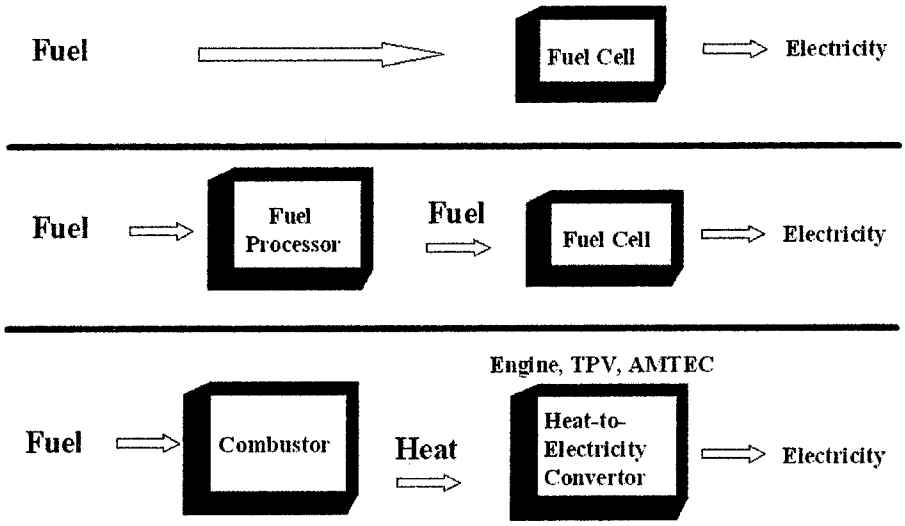

Figure 6: Options for electricity production.

through storing H_2 either in its compressed gas or liquid forms (Figure 6, middle). This approach is discussed in Sections 10.6 and 12 of the report.

6 BASIC PROPERTIES OF FUEL CELLS

In this section we review the fundamental physical chemistry of fuel cells and describe the processes that contribute to the power losses of an actual fuel cell [4, 5]. Figure 7 presents a schematic description of a fuel cell along with the fuel source that comprises the energy-production system. All of the fuel cells considered in this report utilize atmospheric pressure oxygen as the oxidizing component of the fuel stream. This avoids an energy density penalty associated with having to carry the oxidant along with the fuel. The second, chemically reduced component, of the fuel mixture is introduced as required into the other compartment of the fuel cell.

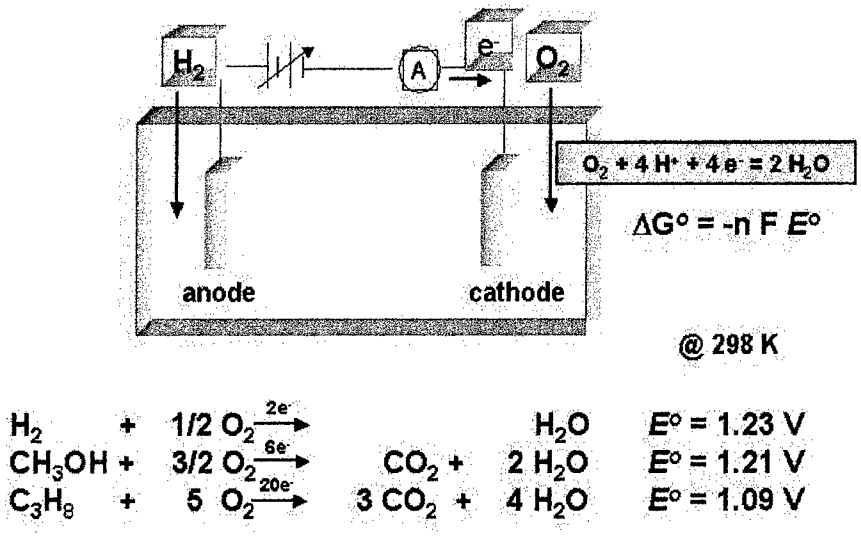

Figure 7: Principles of fuel cell operation.

The electrochemical potential difference between the two different chemical components of the fuel cell produces a flow of electrical current such that electrons leave the compartment containing the fuel and enter the compartment containing the oxygen. The electrode in the oxygen-containing compartment is therefore the cathode and the other electrode is the anode. The

flow of current produces an oxidized species in the anode compartment and a reduced species in the cathode compartment. Generally the reduced species is water, whereas the oxidized species is CO_2 for hydrocarbon fuels and is solvated protons for H_2 as the fuel. Charge neutrality in both the anode and cathode compartments during sustained discharge of the fuel cell requires flow of a charge-compensating species across a membrane (separator). The charge-compensating species is generally a solvated proton. The high solubility of protons in water, as well as the high diffusion coefficient of solvated protons relative to other chemical species, minimizes electrical resistive losses arising from transport of these species through the separator.

The performance of a fuel cell is characterized by three key parameters. The open-circuit potential is a function of the electrochemical potential difference between the chemical components present in the anode and cathode compartments of the cell. The short-circuit current density of the cell represents the current flow in the absence of an external load. This current generally reflects the mass transport limit of reagents supplied to one of the compartments of the fuel cell. No power is produced under either of these two conditions; in the first condition, no current flows, while in the latter condition, no voltage is produced by the cell. Under load, the current is reduced from its short-circuit value until no current flows at open circuit. The desired operating point of the fuel cell is the maximum power point, i.e. the point at which the I-V product of the cell is maximized.

The losses in the cell that occur during current flow can be broken down by where the losses originate physically. One loss occurs as a result of the electrical resistance of the electrolyte, and is generally Ohmic in form. A second loss process arises from Ohmic resistance losses across the separator. The losses from Ohmic resistance in the external leads and contacts to the electrodes are ignored, as these are generally negligible in a well-designed fuel cell system. The remaining losses are electrochemical in nature and arise at the electrode/electrolyte interfaces of the cell. One loss is thermodynamic in

nature, and arises due to the so-called concentration polarization produced by current flow at any electrode/electrolyte interface. For a reduced/oxidized (redox) species pair in charge transfer equilibrium with a metallic electrode, the potential relative to a reference potential (generally the normal hydrogen electrode, NHE) is given by the Nernst equation [6]:

$$E = E^{\circ'} + (\mathrm{RT/nF})\, \ell n\, \{[Ox]/[Red]\} \tag{1}$$

where [Ox] represents the concentration of the oxidized form of the redox pair, [Red] represents the concentration of the reduced form of the redox pair in this compartment of the electrochemical cell, E° is the potential under standard-state conditions, E is the actual potential developed by the electrode, R is the gas constant and F is the charge on a mole of electrons.

When current flows through the interface, the concentrations of oxidized and reduced species at the electrode/electrolyte interface are not equal to their concentrations in the bulk of the solution. Sustaining this current produces an unavoidable loss due to the nonuniform concentration profiles of the reduced and oxidized species in this compartment of the cell. This loss, the so-called concentration polarization loss, is thermodynamic in origin, and can not be avoided. Concentration polarization of an anode can be shown to be of the following form [5, 6]:

$$(\mathrm{RT/nF})\, \ell n\, \{i/(i_{1,a} - i)\} \tag{2}$$

where $i_{1,a}$ equals the limiting current density at the anode. The limiting current density is obtained when the concentration of reagent at the electrode surface is zero, and hence is a function of the concentration of analyte supplied to the solution and the thickness of the boundary layer in the electrolyte.

A second loss is a function of the chemical kinetics of electron exchange between the species in the electrolyte and the electrode material. This loss is a function of the electrode material as well as the chemical transformation

that is being accomplished, and produces a so-called kinetic overpotential loss. In other words, some voltage must be sacrificed in order to overcome the activation energy to produce a desired rate of electron exchange between the electrons in the electrode and the redox-active reagent in the solution.

The form of the kinetic overpotential loss is generally:[5, 6]

$$i = i_o \exp\{[\alpha nF/RT][E - E^o]\} \tag{3}$$

where α is the so-called Tafel coefficient, a unitless parameter between zero and 1 that expresses the fraction of the overvoltage that reduces the activation energy for the electron-transfer process at the electrode surface, and i_o, is the exchange current density that expresses the tendency of the reaction to exchange electrons with the electrode under equilibrium conditions.

The kinetic overpotential is ohmic in form only at very small overpotentials, where the exponentials can be expanded and hence the current-voltage relationship linearized, producing:

$$\frac{V}{i} = \left(\frac{RT}{\alpha\, n\, F i_o}\right) \tag{4}$$

with $RT/(\alpha nFi_o)$ being defined as the charge transfer resistance of the electrode/electrolyte interface of interest [5, 6].

The fuel cells of interest will use one of three fuels: hydrogen, methanol, or hydrocarbons. Figure 7 presents representative chemical reactions that occur in these types of fuel cells. In each case, the full chemical reaction is a combustion reaction with air to produce H_2O and CO_2 (as appropriate). In a fuel cell, the combustion process is separated into two different compartments, with the reaction in the cathode compartment being the reduction of oxygen to water, and the reaction in the anode compartment being the oxidation of the fuel fed into the fuel cell. The entire chemical reaction can be described by two separate "half-reactions" that describe the chemical and electron flow in each compartment of the fuel cell. In the cathode compartment, each mole of oxygen that is reduced will form two moles of water.

This will require consumption of four moles of protons, which in turn implies consumption of four moles of electrons. Hence one can deduce the number of electrons that are produced in the external circuit of the fuel cell by realizing that 4 moles of electrons are required to reduce each mole of O_2.

The different fuel types of course require different molar amounts of oxygen to consume the fuel stoichiometrically. Balancing the chemical equations reveals the amount of oxygen needed, and therefore also reveals the number of moles of electrons that will be produced in the external circuit of the fuel cell during the course of the chemical reaction. Hence, two electrons are produced for every mole of H_2 consumed at the anode of a hydrogen/oxygen fuel cell, 6 moles of electrons are produced for every mole of methanol consumed at the anode of a methanol/oxygen fuel cell, and 20 moles of electrons are produced for every mole of propane consumed at the anode in a propane/oxygen fuel cell.

The theoretical voltage produced by these three types of fuel cells differs relatively little, however. The theoretical voltage can be obtained through use of the well-known relationship:

$$\Delta G^\circ = -n\,F\,E^\circ \tag{5}$$

where ΔG° is the standard free energy change per mole of reactants [5, 6].

Thus, if standard free energy of the reaction is known, the open-circuit potential under standard state conditions of the fuel cell can be calculated. The ideal open-circuit voltages for the three reactions of interest are very similar to each other. This similarity is not fortuitous but arises fundamentally because chemical bonds are worth on the order of 1-2 eV/bond. Although the three fuel cell reactions of interest have different free energies, they also produce different numbers of electrons per mole of combusted fuel. Each cleaved bond produces two electrons flowing through the external circuit at approximately the same potential per electron; hence the overall free energy

energy reflects primarily the number of bonds cleaved in the various fuel cell oxidation reactions of interest.

In practice, catalysts are needed to obtain high exchange current densities, and thereby to minimize kinetic overpotential losses at the fuel cell electrodes. For example, the exchange current density of H_2 oxidation at various metals ranges from a value of 2×10^{-13} A/cm^2 for a Pb anode, to in excess of 10^{-3} A/cm^2 for a Pd electrode. A similar situation exists at the cathode for reduction of oxygen, in which catalysts are needed to accelerate the reaction by reducing the kinetic barrier to reduction of oxygen by four electrons to form water [4, 5].

The mass transport limited current density of an air-breathing fuel cell cathode is based on the diffusion coefficient of oxygen, and is on the order of 0.2-2 A/cm^2 [2, 4, 5]. Hence this value dictates the current density at which one ideally wants to operate an air-breathing fuel cell. Since the Tafel coefficient is typically on the order of 0.5, [4, 5] each factor of 10 increase in actual current density relative to the exchange current density requires a voltage of approximately 120 mV at each electrode. Thus, obtaining the best catalysts for fuel cell electrodes is of critical importance to fuel cell technology, otherwise the output voltage of the device is significantly reduced because of the need to drive the anode and cathode reactions to the desired potentials in order to utilize all of the fuel supplied to the cell.

The output of a fuel cell depends significantly on temperature. The value of the ideal fuel cell potential for the reactions of interest generally decreases with temperature. Since the number of electrons produced by the reaction does not change with temperature, but the free energy becomes less negative as temperature increases, equation 1 indicates that the ideal cell voltage for the reactions of interest must decrease as temperature increases. Hence this component of fuel cell output declines with increases in temperature. However, generally the value of i_o increases significantly with

increases in temperature, hence kinetic overpotential losses are less at higher temperatures. Since this increase is often exponential with temperature, and because increases in i_o are achieved at both the anode from the cathode as the temperature is raised, increased temperature generally leads to significant improvement in the overall power output of a given fuel cell. A third effect of raising temperature is to increase the conductivity of the electrolyte in the fuel cell; in some fuel cell technologies, in fact, the resistive losses in the membrane/electrolyte that separates the anode and the cathode dominate the overall fuel cell voltage losses, and in this case increases in temperature are also beneficial to fuel cell power performance.

A final point about basic fuel cell properties involves fuel utilization. At each point on each of the two electrodes of the fuel cell, the basic equations above govern locally the behavior of the solid/liquid/gas interface. As fuel is utilized, the reactions will be driven towards higher concentrations of products and lower concentrations of reactants. Hence the concentration overpotential will increase and the ideal electrode potential will decrease to reflect this shift in concentration of fuel away from the value in the stream of gas that is supplied to the electrode surface. Because of this overpotential, fuel cells are not generally operated at full fuel utilization, because this would require very large overvoltages which would degrade the overall energy conversion performance of the fuel cell system. Further details on the tradeoffs involved in temperature, fuel utilization, and other design properties of fuel cells can be found in reference texts on the subject.

Fuel cells produce voltages in the range of 0.5-1.0 V, which are relatively low voltages to supply to electronic devices. Thus, fuel cells are generally connected physically in series, in a configuration denoted as a fuel cell stack. In some cases fuel cells are wired together in parallel, to enable face-breathing operation, however this comes at a sacrifice in packaged power density of the fuel cell system. Generally stacks are formed, as shown in Figure 8. The basic fuel cell unit consists of the membrane electrode assembly (MEA),

which consists of the cathode and anode separated by a thin membrane that

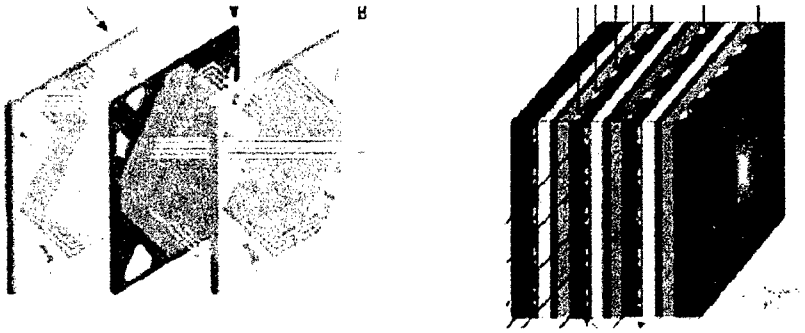

- Stacks required to increase V_{total}
- MEA is 20% of mass of stack, bipolar plate 80%
- Bipolar plates provide gas supply, cooling air/water, water management
- Most engineering tradeoffs in design of stack

Figure 8: Fuel cell stacks.

will contain the electrolyte. The needed catalysts for the electrodes are also contained in, or deposited onto, the MEA. Each MEA is then surrounded by two conducting structural elements, called bipolar plates. The bipolar plates contain grooves or other means for directing the fuels to the individual fuel cells, for removing the product gases and liquids for the fuel cell, and a means of delivering either air or water for thermal management of the heat produced by the operation of the fuel cell stack. The bipolar plates obtain their name because in a stack they are connected to the anode of one fuel cell and the cathode of the next fuel cell, in an analogous fashion to electrodes of a battery pack in which the batteries are connected electrically in series. Most of the engineering and design tradeoffs in fuel cell technology involve the details of the design of the bipolar plates and the exact structure of the flow fields that supply reactants and remove products from the fuel cell as

well as the details of the thermal management schemes of the fuel cell stack [4, 5].

After considering the loss mechanisms as described above, the energy efficiency of a fuel cell can be simply defined as:

$$\text{Energy efficiency} = (\text{electrical energy output}) \quad (6)$$
$$/(\text{lower heating value of fuel input})$$

In this fashion, the fuel cell is considered a "black box" that converts the energy content of fuel into electrical energy. The energy efficiency of this "black box" conversion module simply represents the ratio of the energy content of the output electrical energy to the input energy contained in the fuel fed into the fuel cell, along with any parasitic losses and energy inputs that are required to achieve efficient operation of the fuel cell-based energy conversion module.

7 TYPES OF H_2/O_2 FUEL CELLS

We now discuss the various types of fuel cells that have been developed into fuel cell power production systems. We first discuss hydrogen/oxygen fuel cells, and then discuss direct methanol fuel cells. The general operating principles, as well as engineering limitations, of each different type of fuel cell are described separately. The five types of fuel cells to be discussed are alkaline, phosphoric acid, polymer electrolyte membrane, molten carbonate, and solid oxide fuel cells. The latter two are high temperature fuel cells, which the former three fuel cells operate at low to moderate (80-200 °) temperatures.

7.1 Alkaline Fuel Cells (AFC)

Alkaline fuel cells (Figure 9) are well-developed technologically [5, 7]. They were used in the Apollo space program and have also been used on the

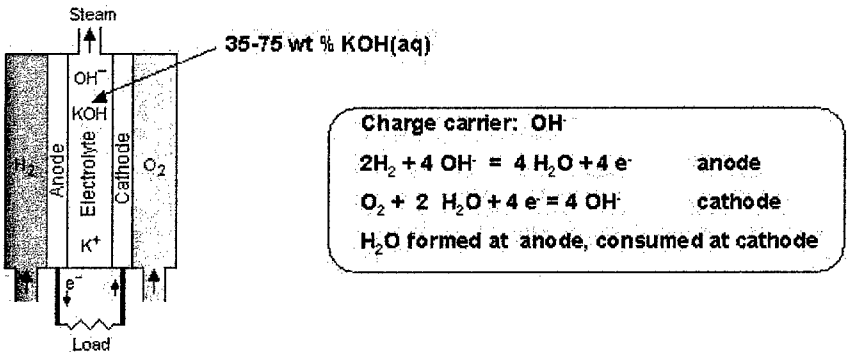

Figure 9: Alkaline H_2 Fuel Cell

Space Shuttle. They are the system of choice in these applications because the water management is especially simple and the catalysts are inexpensive and well-developed.

The alkaline fuel cell consists of a concentrated (35-75 wt%) of KOH in water as the electrolyte. The electrode kinetics for the reduction of oxygen in basic solutions are relatively rapid, so inexpensive non-noble metal catalysts, such as NiO, suffice at the cathode to produce acceptable losses in kinetic overpotential for oxygen reduction. The catalyst at the anode is generally Ni. Such fuel cells operate at 80 100 °C, although they can operate at up to 250 °C if the higher weight fractions of KOH are used in the electrolyte.

The power density of these types of fuel cells is ≈1.5 kW/kg [5, 7]. The overall energy efficiency of the fuel cell is 50-70%, depending on the operating temperature. The remaining loss is predominantly at the cathode in the oxygen reduction process. Water management in these fuel cells is especially simple because the water simply evaporates at the high temperatures used in the fuel cell operation. Since water is formed at the anode and consumed at the cathode in the chemical reactions of the hydrogen/oxygen fuel cell under basic conditions, the product water can be allowed to evaporate with no other required water management issues in the system.

The main operational drawback of alkaline fuel cells is that they are not air breathing, because they are intolerant of CO_2. The CO_2 in the air gets sorbed into the basic aqueous electrolyte, forming carbonates that precipitate in the cell and deleteriously affect its operations. Hence such fuel cells are available, but generally have been limited in use to applications in which pure oxygen is available at the cathode, such as on the space flight missions.

7.2 Phosphoric Acid Fuel Cells

A second type of fuel cell avoids the CO_2 sensitivity issues of alkaline fuel cells by using a highly acidic electrolyte (Figure 10). The electrolyte of choice is concentrated phosphoric acid. In this system, water is formed at the cathode but is not destroyed at the anode. It does, however, evaporate

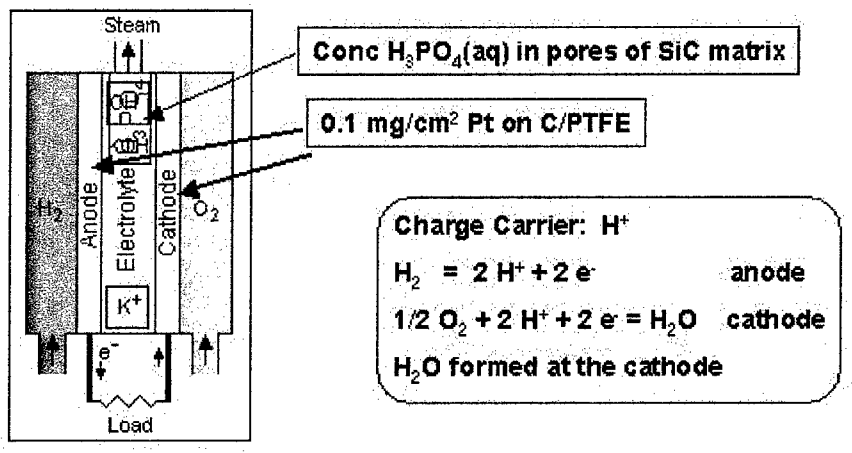

Figure 10: Phosphoric acid fuel cell.

as steam due to the very low vapor pressure of water over hot phosphoric acid. Hence water management is also simple in such fuel cells. Phosphoric acid fuel cells (PAFC's) are the most advanced fuel cells technologically, and are often found in hospitals, computer facilities, and other locations where reliable back-up power supplies are needed [4, 5].

The electrodes in such systems are Pt, because the reactions in acid require different catalysts under the basic conditions of the alkaline fuel cells discussed above. A drawback of using noble metal catalysts is that they are poisoned by the carbon monoxide that is present in the output feed stream of a methanol or hydrocarbon reforming unit (vide infra). However, the higher temperature operation of a phosphoric acid fuel cell allows the system to tolerate up to 1% of CO in the anode feed stream.

Since concentrated phosphoric acid freezes at 42 °C, PAFC's must be preheated to obtain significant conductivity in the electrolyte and therefore produce net output power. This limits their operating temperature range in practice to 150–200 °C to obtain good electrode kinetics and acceptable resistance losses in the electrolyte.

PAFC's exhibit very good energy conversion efficiencies, operating at 0.6–0.8 V at current densities of 150–400 mA/cm^2. This translates into an energy conversion efficiency of 50–55%. The remaining losses are predominantly at the cathode, with anode overpotentials only about 10 mV and resistive losses in the electrolyte only about 10–15 mV. Hence the remaining 400 mV of losses are predominantly at the cathode in the reduction of oxygen to water.

Phosphoric acid is relatively dense compared to water. This, along with other factors, produces a power density of PAFC fuel cells that is approximately a factor of 10 lower than that of AFC's. A second disadvantage of PAFC's is that they must be run under load because at open circuit the carbon support in the MEA's corrodes under the operating conditions and temperatures of the fuel cell. Finally, PAFC's have poor start-up times because of the requirement of preheating the system to obtain net power output.

7.3 PEM Fuel Cells

The third low-to-moderate temperature fuel cell technology is PEM fuel cells (Figure 11). These are considered the fuel cells of choice at the current time for most low/mid range power applications (power levels below 10 kW) [4, 5].

The heart of a PEM fuel cell is the separator membrane (Figure 12) [8]. This membrane consists of Nafion, a version of perfluorinated polyethylene (Teflon) that additionally has side groups that contain sulfonic acid residues. The Teflon backbone regions form hydrophobic domains in the membrane material, while the ionic sulfonate residues agglomerate into hydrated, hydrophilic pools. The hydrophilic pools are interconnected by a network of hydrophilic channels throughout the membrane. Nafion membranes transport protons well but do not transport negative ions in water. Nafion membranes

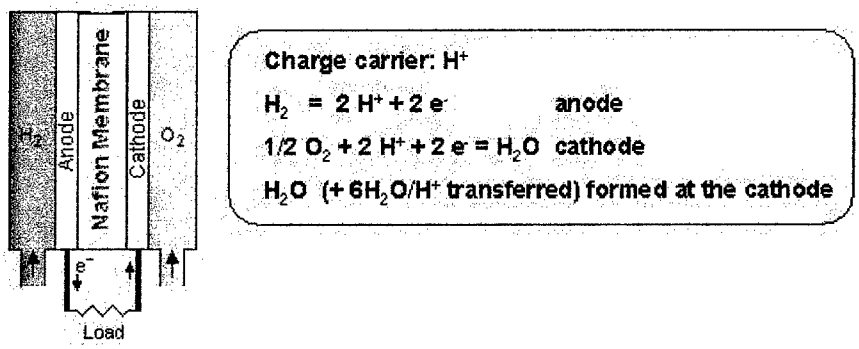

Figure 11: PEM fuel cell.

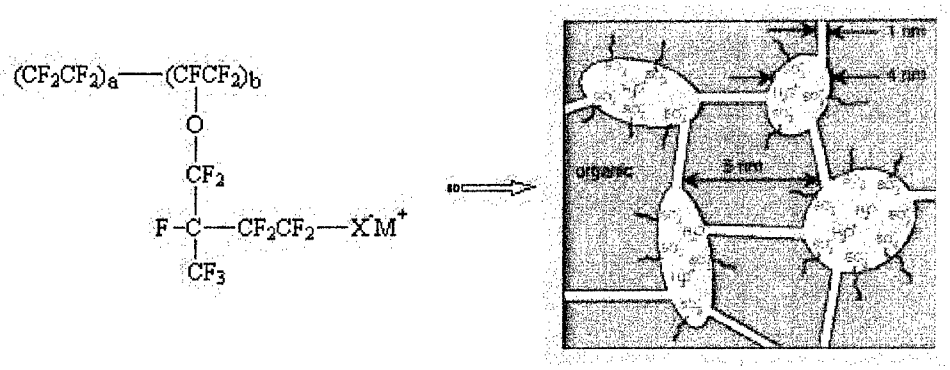

Figure 12: PEM fuel cell membrane.

also effectively transport water (and methanol) but do not transport larger organic molecules.

The anode and cathode catalysts in a PEM fuel cell are noble metals, and a great deal of effort has gone into optimization of the dispersion, wetting properties, and morphology of the MEA's of such systems to obtain optimum fuel cell performance at minimum catalyst loadings [4, 5]. Figure 13 displays the progress that has been made in the performance of such systems through such optimization, in which the power output has increased 10-fold since 1984 while the catalyst loadings have decreased by a factor of 100.

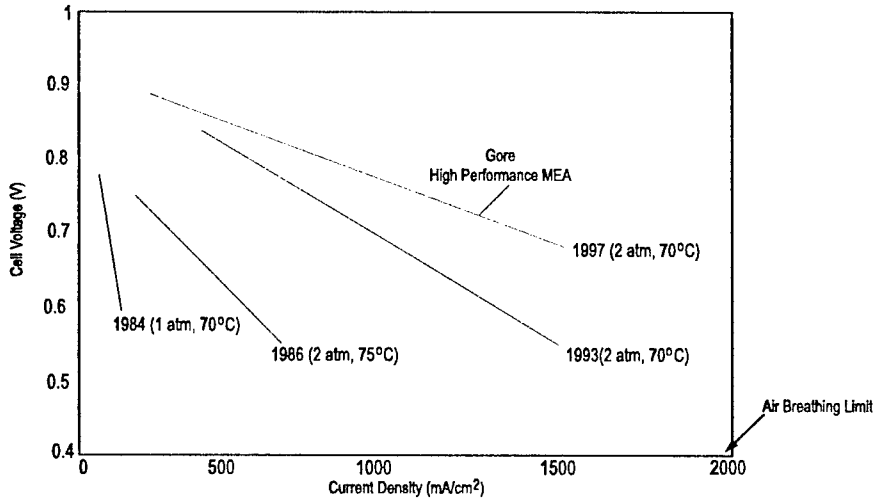

Figure 13: Improvement of PEM fuel cell properties vs time.

PEM fuel cells operate at 0.7 V at 1 A/cm^2, for an overall energy conversion efficiency of 50–60%. As is the case in PAFC's, the remaining losses are primarily at the cathode in the kinetic overpotential for the reduction of oxygen to water. Power densities are comparable to those of AFC's, and are $\approx$ 1 kW/kg.

Costs of PEM fuel cells can be obtained from estimates for their use in vehicular transportation applications. A report to the California Air Re-

sources Board summarizes these costs, which have been estimated to be $4–8/kW for the electrodes, and $80–100/kW for Nafion, for a total of $50–100/kW for the cells in mass production [9].

Drawbacks of PEM fuel cells involve their intolerance to CO and the need for very precise water management [4, 5, 8, 9]. The moderate temperatures involved in PEM fuel cell operation ($< 100°C$ is required or the Nafion membrane irreversibly dries out and becomes destroyed) make the noble metal catalysts intolerant to > 100 ppm of CO. This places severe restrictions on the composition of feed gases from a reformer unit, as described in section 11.

The second drawback is the sensitivity to dehydration of the membrane and the need for precise water management of the fuel cell. Water is formed at the cathode, however additionally water is transported across the Nafion membrane when current flows. The reason for this is that since protons are the charge carriers, charge neutrality requires the movement of protons from the anode to the cathode when the fuel cell is producing current. Due to electro-osmotic drag, approximately three waters accompany each proton through the Nafion membrane [10]. This process therefore tends to deplete the anode compartment of water. If this depletion process were allowed to continue, the Nafion would dry out and the fuel cell would cease to operate. Hence, water must be recovered from the cathode compartment and recycled into the anode compartment. The water recovery and distribution processes must be done both temporally and spatially over the anode to insure that the membrane does not dry out, and additionally to insure that the fuel cell electrodes are not "flooded" i.e., that they do not become too hydrophilic and thereby preclude effective access to the catalyst by the gaseous fuels that need to react at the electrode/electrolyte/gas interface of the electrodes in the fuel cell. The need for both thermal management and water management in PEM fuel cells adds complexity to the balance of plant (the auxillary

components needed to control and operate the fuel cell) in a PEM fuel cell system, as will be described further in Section 9 below.

7.4 Molten Carbonate Fuel Cells (MCFC's)

A fourth fuel cell technology is molten carbonate fuel cells (Figure 14). In this system, the electrolyte is a molten alkali metal carbonate, typically potassium carbonate. The charge carrier is the carbonate ion, and the fuel cell reactions are:

$$H_2 + CO_3^{2-} = H_2O + CO_2 + 2e^- \qquad \text{anode} \tag{7}$$

$$1/2O_2 + CO_2 + 2e^- = CO_3^{2-} \qquad \text{cathode} \tag{8}$$

These fuel cells require temperatures in excess of 600 °C in order to melt the carbonate salt and thus to provide conductivity through the electrolyte [11]-[13].

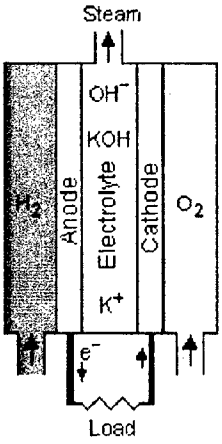

Charge carrier: CO_3^{2-}

$H_2 + CO_3^{2-} = H_2O + CO_2 + 2e^-$ **anode**

$1/2\ O_2 + CO_2 + 2e^- = CO_3^{2-}$ **cathode**

Figure 14: Molten carbonate fuel cells.

An advantage of molten carbonate fuel cells is that the high temperatures allow use of relatively inexpensive, non-noble, metal catalysts (typically Ni is used). In addition, CO is a fuel, so MCFC's can be run directly off of

the output feed of a hydrocarbon reforming unit. MCFC's produce output voltages of 0.65–0.70 V at current densities of 200 mA/cm^2, and are typically between 50–55% energy efficient.

Disadvantages of MCFC's are that they require high temperatures, involve a corrosive liquid electrolyte, require that CO_2 must be supplied actively to the cathode in order to make up for the CO_3^{2-} that is transported across the membrane during fuel cell operation, and have relatively low power densities, of 0.15 kW/kg, due to the high density of the electrolyte. Their use of inexpensive catalysts and high current densities, however, makes them attractive for certain high power, fixed installation, applications.

7.5 Solid Oxide Fuel Cells (SOFC's)

A fifth fuel cell technology is solid oxide fuel cells (Figure 15) [4, 5, 11, 14]. In this approach, an oxygen-conducting ceramic serves as the membrane of the fuel cell. A typical membrane material would be zirconia (ZrO_2) that contains 10% yttria (Y_2O_3). Such materials at high temperatures are ionic conductors of O^{2-}, and this ion is the charge carrier of the SOFC.

The reactions in a SOFC are:

$$H_2 = 2\,H^+ + 2\,e^- \qquad \text{anode} \tag{9}$$

$$1/2\,O_2 + 2\,H^+ + 2\,e^- = H_2O \qquad \text{cathode} \tag{10}$$

SOFC's must be heated to high temperatures (> 700 °C) to produce sufficient O^{2-} mobility through the membrane. Figure 16 displays the resistance losses that plague such systems even at temperatures as low as 600–700 °C. At high temperatures, though, the SOFC's can run at 0.775 V at a current density of 160 mA/cm^2, and display energy conversion efficiencies of 50–55%.

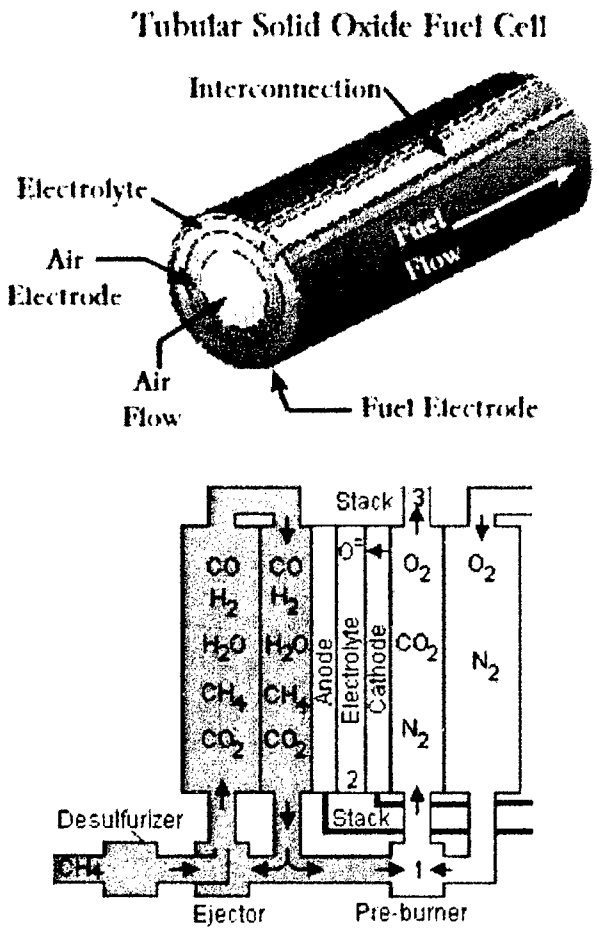

Figure 15: Solid Oxide Fuel Cells.

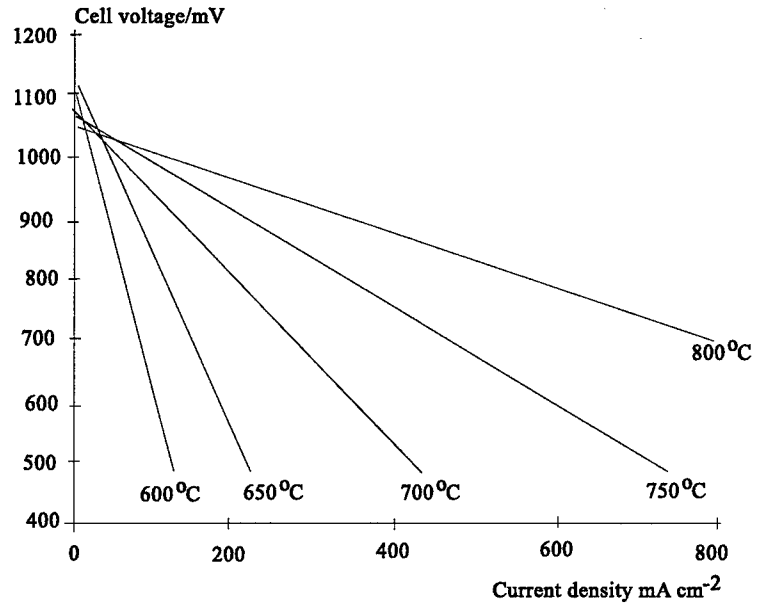

Figure 16: Solid oxide fuel cell performance versus temperature.

SOFC's also can accept the output feed of a hydrocarbon reforming unit, because CO is also a fuel for SOFC's. The ceramic materials are however expensive to extrude and present significant materials integration issues to achieve compatibility with other parts of a fuel cell system. Recent work has claimed that SOFC's can run directly on butane or propane, although the remainder of the system components form coke deposits after 48 hours of operation.

8 RANGE OF FUEL CELL APPLICATIONS

Figure 17 summarizes the typical range of fuel cell applications, segmented by the power level required by the application [5]. For low power applications including portable electronics, cars, etc., PEM fuel cells are favored due to their low operating temperature, relatively simple components, and tolerance of atmospheric feed at the cathode. At higher power levels, where the overhead associated with CO_2 scrubbing can be tolerated, alkaline fuel cells are favored. At still higher power levels, more fixed costs and space can be allotted to the balance of systems in the fuel cell installation, and operating at high temperatures can be achieved as a tradeoff for obtaining enhanced fuel cell performance or avoiding the need for expensive noble metal electrode catalysts. Hence at higher power levels PAFC's are the technology

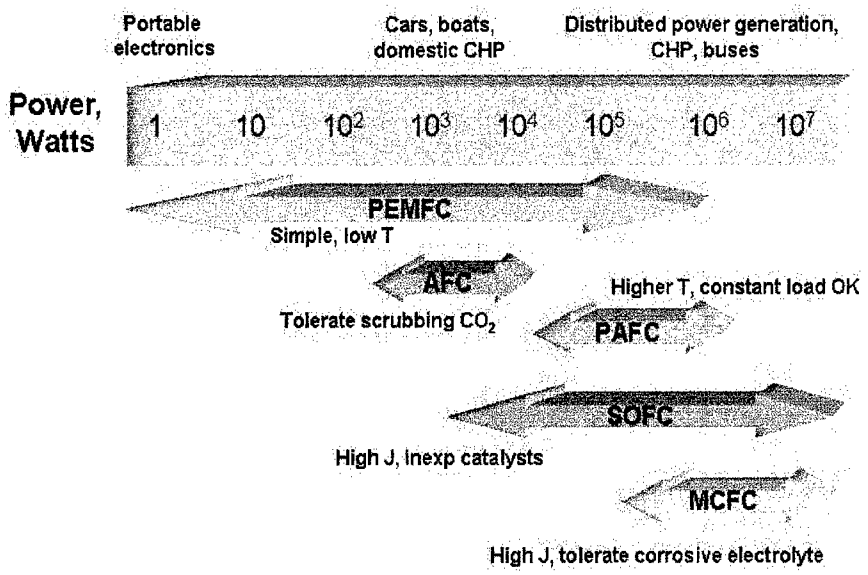

Figure 17: Range of fuel cell applications.

of choice. Finally at the highest power levels, SOFC's and MCFC's dominate due to their inexpensive catalysts in addition to the ability to extract

still further efficiency improvements through use of a fuel cell system in a combined heat and power (CHP) application, in which the waste heat in the output stream of the fuel cell is used to produce additional power by acting as the feedstock for a turbine, for example, in a bottoming cycle of a CHP facility. Hence for the remainder of the discussion below, we will focus on PEM fuel cells at the 20 W level for the soldier portable power application.

9 FUEL CELL SYSTEMS

The fuel cell and fuel cell stack form the basis for, but do not comprise the complete components of, an actual fuel cell power system. The system requires a balance of plant for feeding the gaseous fuels to the fuel cell, maintaining closed loop feedback control on the various parts of the fuel cell stack, and providing other engineering functions to the operation of the fuel cell under a variety of operating conditions. Such conditions include orientation independence, functioning over a variety of altitudes (and hence oxygen partial pressures in the cathode feed stream), and functioning over a range of temperatures. In addition, user-related functions such as system status, connections for fuel supply, output voltage convertors and selectors, a battery back-up, load following hardware, and appropriate field packaging (dust filters for the air intake, water exhaust outputs, handles and clips, etc.) must be included. Consideration of the mass and volume of the balance of plant and of the packaging into a power production module must be considered before any fuel cell technology can be compared robustly to that of battery-powered systems.

An excellent system for examining the scaling of fuel cell systems with output power capacity is provided by the series of PEM products and demonstrators that have been produced by Ball Aerospace[15, 16]. These units are depicted in Figure 18, with the initial demonstrator designated the Snorkler and subsequent units designated as personal power sources (PPS) accompanied by the appropriate numerical rated power capacity level. We discuss in this section how the mass of such fuel cell systems scales with power capacity, to understand the fixed mass burden that would be involved if a PEM fuel cell were used for electrical energy production from fuel.

A theoretical limit on the power density can be obtained by considering the power that is produced by an air-breathing PEM fuel cell, and dividing

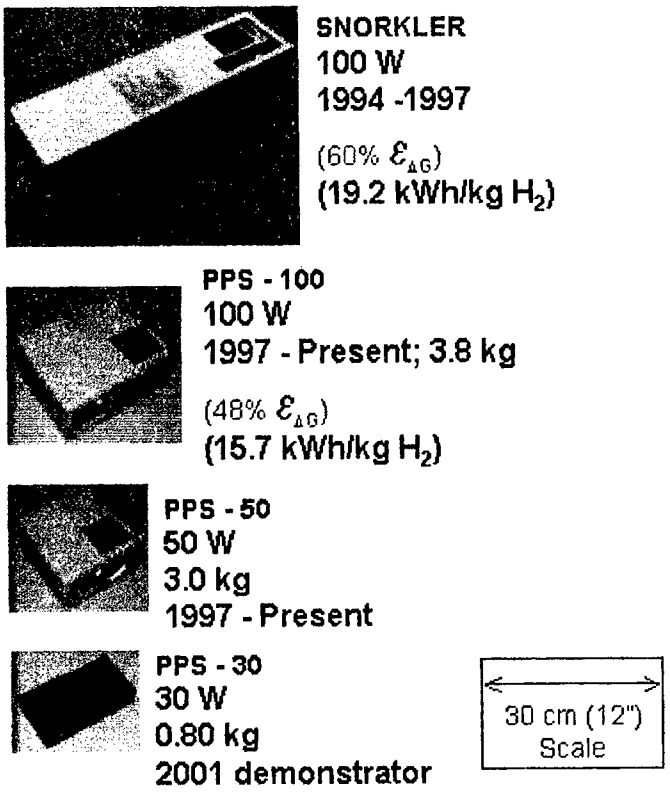

Figure 18: H_2 PEM fuel cell systems.

that power only by the mass of the MEA. For a low pressure air-breathing PEM fuel cell, a typical current density of 0.2 A/cm^2 is obtained at a voltage of 0.7 V. A typical MEA thickness of 0.05 cm, and a density of 2.0 g/cm^3, then produces a specific power density of 1.4 kW/kg under such conditions [15].

However, the fuel cell must also be incorporated into a fuel cell stack, which requires the addition of the bipolar plates. For real 2.0 mm thick bipolar plate assemblies including flow fields and the MEA, the ideal specific power is reduced to 0.350 W/kg. Additionally, incorporation of thermal management requires additional mass. A mature H-Power, Inc. 50-watt PEM stack cooled by forced air convective cooling provides a guide as to the

expected cooling mass burden, and in that instance a 25 cm^2 MEA with 32 cells has a mass of 500 g, for a power density of 100 W/kg [16].

Finally, one must add the balance of plant and the packaging. The Ball Aerospace system is especially well-engineered to minimize mass while not compromising on the parasitic efficiency losses incurred in the balance of plant, and the PPS-30 has a total mass of 0.8 kg at a rated power of 30 W. Hence, the real system has a power density of 37.5 kW/kg (with an actual power density of 25 W/kg because typically the fuel cell system is run at less than rated capacity to be most efficient). Thus, the actual packaged mass of a 20 W PEM H_2/O_2 fuel cell is approximately 0.8 kg for the soldier portable power application. The PPS-30 also has a back-up battery, and is load-following up to its rated output power [15, 16].

10 FUELS FOR H_2 FUEL CELLS

The fuel cell power conversion unit discussed above at the 20 W level has a 50–55% energy conversion efficiency, and the total mass of such a packaged fuel cell system is 0.8 kg. Therefore, since the energy density in H_2 is 33,000 W-hr/kg, it would be a relatively easy task to compete with batteries *if* the H_2 fuel could be stored efficiently as a percentage by weight of its container. However, in practice, storing H_2 in significant mass fractions is not easy. In this section we review the various options for H_2 storage, and estimate the overall energy conversion performance of the resulting fuel and fuel cell system for portable power production.

10.1 Compressed Gaseous H_2

Arguably the best approach technically for storing hydrogen at the present time on a mass basis is through the use of compressed H_2 gas in a storage cylinder [17]. Significant effort has gone into reducing the weight of hydrogen tanks for vehicular applications, and the portable power effort can leverage these advances directly into its program.

At 5000 psi, H_2 does not behave as an ideal gas. The appropriate pressure vs volume relationship under these conditions is displayed in Figure 19 citeJames. The mass of H_2 required to produce 3.4 kW-hr of electricity from a 50% energy efficient PEM fuel cell is 0.21 kg. This amount of H_2 occupies a volume of 8.8 liters at 5000 psi.

The key question is what kind of tankage is to be used for the storage of the H_2(g). Steel tanks that have current Department of Transportation (DOT) approvals only store 2% H_2 by weight, however carbon–lined epoxy tanks that are available from specialty manufacturers and can store up to 6% H_2 by mass [9, 15]. Such tanks maintain a safety factor of 2.25, where

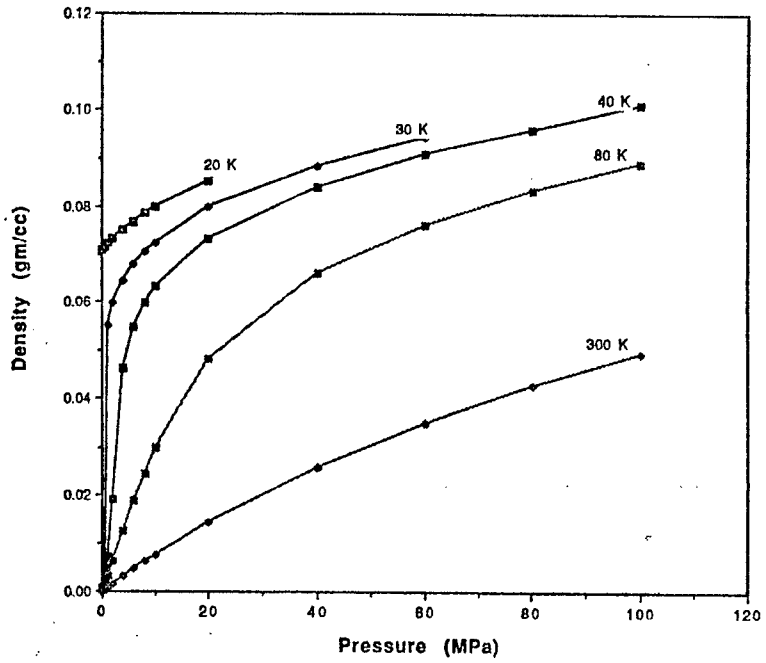

Figure 19: Density vs Pressure of Gaseous H_2.

the safety factor is the ratio between the burst pressure of the tank and the rated pressure of the gas that is to be stored in the tank during operation. Assuming the use of these lightweight tanks, approximately 3.5 kg of tankage and fuel would be required to store the needed 0.21 kg of H_2. The total volume of the tankage and fuel is thus approximately 10 L.

The system weight is therefore $\approx$ 4.5 kg (3.5 kg for tank and fuel, 1.0 kg for the PEM fuel cell and valving etc.). The system therefore has a fixed "dead" mass of approximately 1.0 kg, and at 50% energy conversion efficiency in the fuel cell, produces an incremental energy density of 1000 W-hr/kg for each kg of H_2 carried if we assume a stored mass fracture of 6.0% H_2 in the tank. The comparison between this energy system, the hybrid battery/battery system, and BA-5590 Li/SO_2 Army batteries at 170 W-hr/kg, is shown in Figure 20. Clearly, the use of H_2 in conjunction with the PEM fuel cell system would result in a reduced mass even compared to

the hybrid battery pack, with a total system mass being reduced from 20 kg for the BA-5590's, to 6.1 kg for the hybrid battery pack, to 4.5 kg for the H_2/PEM fuel cell system combination.

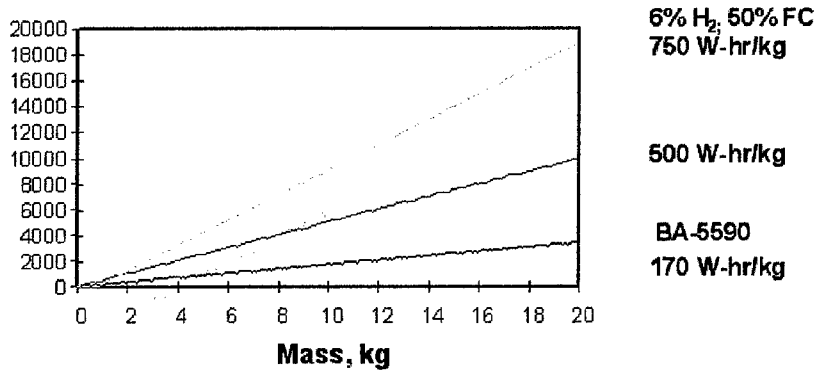

Figure 20: Energy vs mass of stored H_2 with a PEM Fuel Cell vs batteries and hybrid battery packs.

10.2 Cyrogenic H_2 Storage

The method providing the most storage by mass of H_2 is storage of liquid hydrogen at cryogenic temperatures. This approach has been taken by BMW and some other automakers in constructing demonstrators for fuel-cell powered vehicles [9]. We discuss the technical aspects of cryogenic H_2 storage in this section.

Cryogenic H_2 storage requires temperatures of 20 K, and is generally accomplished using double-walled steel dewars. A significant amount of the energy density of the H_2 is consumed in liquifying the H_2 from the gas. Loss rates as low as 0.5% of the stored volume per day have been achieved by automakers on 3 kg quantities of cryogenically-stored H_2 [9, 17].

To our knowledge, no system has been implemented for cryogenic H_2 storage on a scale compatible with soldier portable power requirements. Using vehicular H_2 storage as an estimate, 3 kg of H_2 requires a total mass of

21.7 kg (14% by mass H_2) for the tankage, and occupies a volume of 85 liters, 50 of which is the H_2 fuel [9, 17]. We estimate that storing 0.21 kg of H_2 will therefore require 1.5–3 kg, and a volume of 7–10 liters. This would produce a net energy density of 33,000 W-hr/kg * 0.14 * 0.5 = 2,200 W-hr/kg. However, although technically feasible, we do not see how this approach could be readily implemented on the battlefield logistically to provide power to soldiers.

10.3 Glass Microspheres for H_2 Storage

This approach to H_2 storage is based upon technology used to prepare targets for fusion research. Glass microspheres are heated up to a temperature at which H_2 can diffuse through the glass, and the spheres are filled with H_2 under high pressure. The temperature is then lowered and the gas is trapped inside the microspheres. To release the gas, the spheres are either then heated up (requiring significant energy input) or are mechanically crushed. The latter is the preferred method for portable power applications.

This approach has been explored in some depth by W. J. Schafer Associates, Inc. in Livermore, CA as well as by Robert J. Teitel Associates, Inc. [18, 19]. The claim is that the use of glass microspheres is possibly safer and more convenient than direct storage of the compressed gas in a tank. A drawback, however, is that the approach imposes a volume density penalty due to the 50% excluded packing fraction of spheres that store the gas. Stored mass fractions of H_2 are $\approx$ 3–5%, but values as high as 8–10% have been claimed to be possible through the use of very low defect density, high strength, custom designed glasses. Crushing mechanisms similar to unpeeling a roll of film through a crusher, with the film coated on both sides with a layer of the glass spheres, have been conceptualized and constructed at the demonstration stage. Lawrence Livermore National Labs estimated that a fully engineered system, including auxiliary heaters, manifolds, and

containers would be 4–4.5% H_2 by weight (at 6.8 kg of H_2 storage) and would have a volume density of 8–9 kg of H_2/m^3 [17].

The final technology limitations of this approach are not known at the present time, nor is the cost. The fact that the mass fractions are not superior to that of compressed gas, and that one pays a volumetric energy density penalty to use the microspheres, along with the added complexity of delivering the gas as needed by crushing the spheres, are likely impediments to further development of this approach at the present time.

10.4 Metal Hydrides for H_2 Storage

A variety of metal hydrides have been investigated as H_2 storage media. Solids that have been investigated include magnesium and its alloys, as well as mixed alloys of elements selected from: Ti, V, Cr, Mg, Fe, Co, or Ni, mixed with elements selected from: Zr, La, or "mischmetal": (Ce/Pr/Nd) [17].

The net energy density output available from hydride-based systems has recently been estimated considering the energy inputs needed to desorb the H_2 during the heating cycle. A summary of the properties of these systems for vehicular transportation applications is available in the report by James and co-workers [17]. Despite much work on improving the mass fraction of H_2 stored in these materials, at present maximum values are less than 2% by weight H_2 for low-temperature metal hydrides, in which the H_2 can be desorbed at moderate temperatures. The "high temperature" hydrides store as much as 4% H_2 by weight, but require parasitic losses of the stored H_2 through combustion to generate sufficient heat to desorb the remaining H_2 stored in the metal hydride.

While mature technologically, use of these materials in conjunction with a 50% energy efficiency fuel cell module would provide a maximum net en-

ergy density from the fuel of 33,000 W-hr/kg * 0.02 * 0.5 = 330 W-hr/kg. This value is less than the 500 W-hr/kg that can be obtained from hybrid battery pack systems described in Section 4.2 above and also is less than that obtainable from gaseous H_2 in state-of-the-art tankage (Section 10.1 above).

10.5 Carbon Adsorbents and Carbon Nanotubes for H_2 Storage

Carbon adsorbents have also been investigated as H_2 storage media. H_2 is stored both in the void spaces of the sorbent and by adsorption onto the carbon. Stored mass fractions as high as 5% by weight have been claimed, but reproducible values in independent laboratories are typically in the range of 3–4% or less. Carbon nanotubes have also been claimed to afford H_2 storage densities >5% H_2 by mass, but again values reproduced in various laboratories are lower and are in the range of 1–3% H_2. State-of-the-art tankage is needed to confine the H_2 sorbed into the void spaces of the sorbent at minimal mass penalty. In addition, the higher storage fractions require maintaining the sorbent at low temperatures (150 K). The desorption requires a heating cycle and adsorption requires a cooling cycle; even discounting the parasitic energy losses needed to accomplish this process, the available H_2 that can be desorbed at room temperature by mass is generally less than that in H_2 cylinders at 5000 psi [17].

10.6 Hydrogen Generators

Another approach to providing H_2 for fuel cells is to carry the fuel as a reagent, or set of reagents, that generate gaseous H_2 as the result of a chemical reaction. In this respect, the charge of H_2 would be analogous to the electrical charge provided by a primary battery in that in both systems, the chemicals would need to be replaced after a full single discharge. Systems

that are not acceptable for consumer applications (which demand secondary battery technology, for example, or extremely inexpensive, available, and safe primary H_2 charge materials) might still be acceptable for military uses, hence such systems are examined below in further detail.

Table 5 lists several examples of H_2 generation systems. In one generic approach, main group metal hydrides of the form $Y(ZH_4)_m$ are reacted with a hydrogen-containing reagent, with the reaction producing residual solid as well as the desired H_2 gas [20]. When elements having a relatively low

Table 5: Properties of Hydrogen generating compositions.

	H_2 Generating Formation	H_2 yield per reactant weight	Stability	Comments
1	$NH_4B_4H_4$	20.7%	dec. -40°C	unstable
2	NH_3BH_3	19.6%	dec. ~100°/50°C	Mix: fine solids, high burn rate, high T
3	$BH_2(NH_3)_2BH_4$	19.6%	dec. < 95°C	Mix: fine solids, high burn rate, high T,
4	$NH_3(B_3H_7$	17.8%	dec. 74°C	unstable.
5	$N_2(H_4)x2BH_3$	16.9%	dec. ~100°C	Mix: fine solids, high burn rate, el stat.
6	$Mg(BH_4)_2x2NH_3$	16.0%	dec. ~100°C	Mix: fine solids, high burn rate, high T,CO/NH_3.
7	$Li + H_2O$	4.0%	not stable	not pursued
8	$LiH + H_2O$	8.0%	not stable	not pursued
9	$LiBH_4 + H_2O$	10.5%	not stable	not pursued
10	$NH_4F + LiBH_4$	13.5%	dec.~40°C	unstable (DSC)
11	$NH_4F + NaBH_4$	10.7%	dec.~45°C	unstable (DSC)
12	$NH_4F + LiAlH_4$	10.7%	dec.76°C	unstable (DSC)
13	$N_2H_6Cl_2 + LiBH_4$	9.4%		no react.up to 400°C(DSC)
14	$NH_4Cl + LiBH_4$	10.6%	dec.60°C	unstable
15	$NH_4F + NaAlH_4$	8.7%	dec.107°C	not pursued - NH_4F toxicity
16	$Li_3AlH_6 + NH_4F$	11.0%		compound not available
17	$Li_3AlH_6 + NH_4Cl$	9.0%		compound not available
18	N_2H_4 x $2BH_3$ — $LiAlH_4$	13.0%		compound not available
19	N_2H_4 x $2BH_3$ — MgH_2	13.9%		compound not available
20	N_2H_4 x $2BH_3$ — NH_4Cl + $3LiAlH_4$	10.3%		compound not available
21	$NH_4Cl+2LiAlH_4$	8.5%	dec.~100°C	onset of dec at 75°C
22	$NH_4Cl + NaAlH_4$	7.4%	dec.~170°C	very stable
23	$NH_4Cl + 3LiAlH_4$	8.4%	unknown	being evaluated
24	$NH_4Cl + 1.2LiAlH_4$	7.3%	unknown	being evaluated
25	$NH_4Cl + NaAlH_4+$ $2LiAlH_4$	7.6%	unknown	being evaluated

atomic number are used as the main group metal, > 10% H_2 by mass can be theoretically produced from such processes, assuming that the mass of the H_2 gas formed is divided into the mass of the reactants and other residual

products of the chemical reaction. Hence such H_2 generation systems have potential theoretically to provide relatively high mass fractions of storable H_2 [20].

One must consider carefully however the actual engineering issues involved in construction of such a H_2 generation system on a soldier-type power level. At least two concrete examples of the implementation of such systems were presented to the JASONs. One such system was built by Dave Bloomfield of Energy Conversion Systems,[21] and the other system was built by Research Triangle Institute and Hydrogen Components Inc. as subcontractors to Ball Aerospace [15].

A practical system must consider first the inadvertent discharge of hydrogen, at least from the chemistries that only involve one reagent as the reactant. Figure 21 shows the decomposition temperatures of such systems

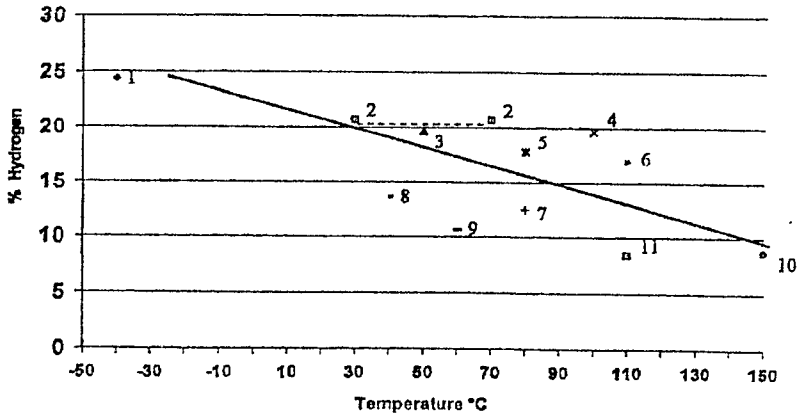

1. NH_4BH_4 (pure cpd)
2. $NH_4B_3H_8$ (pure cpd)
3. NH_3BH_3 (pure cpd)
4. $BH_3(NH_3)_2BH_4$ (pure cpd)
5. $NH_2B_3H_7$ (pure cpd)
6. $N_2H_4 \cdot 2BH_3$ (pure cpd)
7. $Mg(BH_4) \cdot 2NH_3$ (in formulation)
8. $LiBH_4 + NH_4F$ (in formulation)
9. $LiAlH_4 + NH_4F$ (in formulation)
10. $NaAlH_4 + NH_4Cl$ (in formulation)
11. $2LiAlH_4 + NH_4Cl$ (in formulation)

Figure 21: H_2 storage technologies.

as a function of the stored mass fraction of H_2 [20]. The expected relationship is roughly obeyed in that the systems that display the highest H_2 mass fractions are also the most reactive and therefore unstable towards de-

composition. An actual system must either be safe to decomposition over reasonable temperature excursions or must have a containment vessel that would be capable of holding the discharge pressure of a temperature-induced discharge of the stored H_2. The latter option requires tankage, which lowers the net stored H_2 mass fraction below that of gaseous H_2 itself, and hence is not a reasonable design approach. One must therefore either use safe, single reagents or must employ a chemical reactor that mixes binary reagents, at least one of which is a solid. Both such approaches involve engineering constraints that significantly reduce actual H_2 mass fraction to below the theoretical values listed in Table 5.

An example of the binary approach that involves the mixing of two solids is the reaction of NH_4Cl and $NaBH_4$ to produce NaCl, BN and 4 H_2 [15, 20, 21]. This process has a theoretical H_2 stored mass fraction of 8.8%. The reactants are stable at T<80 °C for safety reasons, and hence pellets can be constructed in which both materials co-exist, along with a binder. Detonation of each pellet using an electrical spark initiates the reaction and produces a charge of H_2 gas.

Practical implementation of the entire system necessary to achieve the detonation, isolate the pellets from each other, etc. results in a system that in actuality produces only <3% stored H_2 by mass [21]. Another feature to note is that this system was constructed on a scale much larger than that required for solider power, and hence will be better in mass fraction of stored H_2 than a smaller scale system due to the need for a certain amount of fixed mass in the balance of systems and packaging in both cases.

The other exemplary system presented to the JASON's mitigates, to some extent, some of the engineering difficulties encountered when two solids must either be mixed or combined and then detonated. The chemistry involves $NH_3 + LiAlH_4$ to form hydrogen gas and Al nitrides [15]. One reactant in this reaction is a gas, NH_3, and thus can be fairly readily delivered to the

solid, $LiAlH_4$, to initiate the reaction to form H_2. A demonstration system using this chemistry has been built by Hydrogen Components Inc. on a scale sufficient to produce 400 W-hr of H_2. As shown in the mass budget of Table 6, the theoretical H_2 mass fraction is significantly reduced during the practical

Table 6: Empty Ammonia – Hydrogen Generator Mass Breakdown

Ammonia Tank	
Subassembly	**Grams**
NH_3 Relief Valve (not including the boss in the tank head)	1.63
NH_3 Schrader-type Outlet Valve (not including the boss in the tank head)	4.79
Polycarbonate 1/4-Turn Half-Coupling (locks NH_3 tank to reactor)	14.94
Pressure Vessel (2 heads with valve bosses and the cylinder)	69.43
Fiberglass Cloth (used to bond the lock ring to the pressure vessel)	0.38
Epoxy Glue (used to bond the lock ring to the pressure vessel)	1.63
Weld Filler Rod (estimated by difference between total and part weights)	1.90
Paint (self-etching primer plus camouflage colors)	2.07
Total NH_3 Tank Weight (empty)	96.77
Reactor	
Subassembly	**Grams**
Reactor Cap with Quick Disconnect, Filter and O-ring	25.43
Polycarbonate 1/4-Turn Half-Coupling (locks reactor to NH_3 tank)	25.36
Reactor Relief Valuve (includes boss that gets welded to head)	3.52
Teactor Check Valve (not including integral boss in head)	2.03
8" Pressure Vessel (head with check valve boss, cylinder, support ring)	99.79
or	
12" Pressure Vessel (head with check valve boss, cylinder, support ring)	142.82
Fiberglass Cloth (used to bond the lock ring to the pressure vessel)	0.38
Epoxy Glue (used to bond the lock ring to the pressure vessel)	1.63
Weld Filler Rod (estimated by difference between total and part weights)	1.00
8" Paint (self-etching primer plus camouflage colors)	2.28
or	
12" Paint (self-etching primer plus comouflage colors)	3.03
Total 8" Reactor Mass (empty)	161.31
Total 12" Reactor Mass (empty)	205.09

implementation of such a system. After consideration of the needed tankage to store the NH_3, along with the ancillary valving, containment vessel for the solids, valves and materials to provide protection against an H_2 overpressure being formed during the reaction, metering of the reagents to provide a constant H_2 production rate, and active control over the system to compensate for possible variations in external temperature at which the system might be operated, the final system was 2–3 % H_2 by mass [15]. Hence on the soldier

power scale, such a system apparently has less mass percentage of H_2 than does storing H_2 in its gaseous state at 5000 psi in carbon-fiber lined tankage. The hydrogen generation system might be perceived to be safer (due to the lower pressure of H_2 at 200–300 psi) or alternatively, might be perceived to be more dangerous (due to the presence of $LiAlH_4$ and NH_3) than a H_2 cylinder.

A significant portion of the engineering challenges involved in implementation of the above H_2 generation systems involves issues related to manipulation of solid reagents (the main group metal hydrides). Two other H_2 generation systems attempt to minimize these problems by dealing with liquid-based H_2 sources. The technology developed by Millenium Cell, Inc. primarily for vehicular transportation applications involves use of an aqueous solution of $NaBH_4$ [22]. The solution is stable under basic conditions, but when passed over a suitable catalyst, H_2 is liberated and sodium borate is formed.

The limitation of this approach at the present time is the concentration of $NaBH_4$ that can be dissolved and handeled as a stable aqueous solution. The Millenium Cell approach uses 25% by weight solutions of $NaBH_4$ in H_2O. The reaction chemistry generates 4 moles of H_2 for each mole of $NaBH_4$, hence the solution effectively contains 3.5% available H_2 by mass. For vehicular applications, the competing technology is secondary batteries, and large quantities of Li batteries may not be accepted by consumers. Thus, it is not unreasonable to suggest that the $NaBH_4/H_2O$ approach might have merit for transportation applications, where non-Li secondary batteries have energy densities of 50–100 W-hr/kg. An issue for transportation (but not perhaps for military) applications is that recycling of the system requires reconversion of sodium borate back into sodium borohydride. The key point for soldier power system applications is that the solution of 3.5% by mass of H_2, used in conjunction with a 50% energy conversion efficiency fuel cell, produces an energy density of 580 W-hr/kg with no mass burden for the bal-

ance of plant involved with the H_2 generation and delivery system. Hence, this approach does not appear to offer significantly better performance than the hybrid battery/battery system described above and currently has less mass percentage of available H_2 than storage of the gas at 5000 psi.

An alternative approach to liquid-based H_2 generation is the work of S. Narang and S. Sharma at SRI, who have explored the use of organosilanes as H_2 generators [23]. The silanes are very hydridic in that the Si-H bond is polarized to form a partial positive charge on the Si and a partial negative charge on the H; in this respect, their chemistry is similar to that of alkali metal hydrides and alkaline earth hydrides in that H_2 is liberated upon addition of the reagent to H_2O. Quite high theoretical H_2 mass fraction values are obtained from the reaction chemistry alone, and in this respect such systems are encouraging (Figure 22, Table 7). At the present time, however,

Table 7: Efficiency of Hydrogen Production

Silanes	
$C(SiH_3)_4$	9.8
$(H_3Si)2C=C(SiH_3)_2$	9.4
$H_3Si\text{-}C\equiv C\text{-}SiH_3$	8.6
$C_6(SiH_3)_6$	8.6
$HC\equiv CSiH_3$	7.2
$C_6H_3(SiH_3)_3$	7.2
$C_6H_4(SiH_3)_2$	6.2
$C_6H_5SiH_3$	4.4
Metal hydrides	
$LiBH_4$	8.6
$NaBH_4$	7.3
$NaAlH_4$	6.4

the actual H_2 yields are significantly lower than the theoretical values, due to the fact that gel-like siloxanes form during the mixing process and impede complete reaction of the reagent with the stoichiometric amount of water indicated by the theoretical reactions indicated in Figure 22 [23]. These sys-

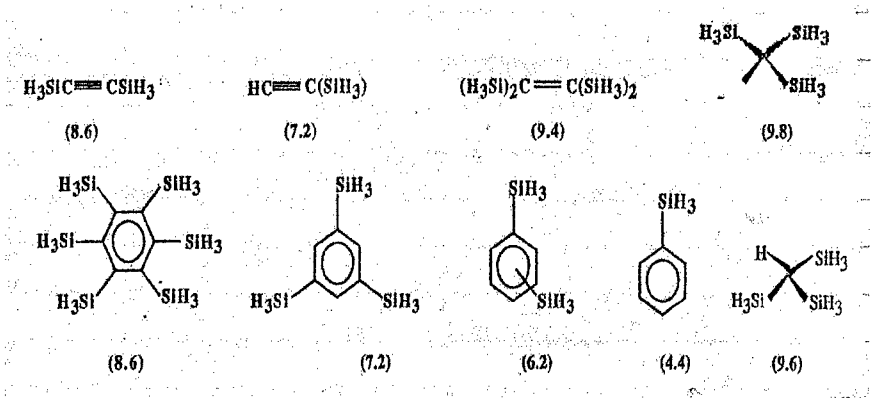

Figure 22: Proposed silanes and theoretical H_2 mass fractions (in parenthesis).

tems might make promising H_2 generation systems for military applications if these engineering-related problems can be mitigated on the desired scale and if the mass burden of the balance of plant required to perform the chemical reaction and insure the safety of the system under a wide range of operating conditions can be minimized. At present, 4% by mass of H_2 is the best value that has been obtained;[23] hence in conjunction with a 50% energy conversion efficient PEM fuel cell, this would provide a gross energy density of 660 W-hr/kg without including any mass burden for the balance of systems or packaging of the reaction components.

11 REFORMING HYDOCARBON FUELS FOR USE IN CONJUNCTION WITH H_2 FUEL CELLS

Another approach to H_2 generation from liquid sources is to reform liquid hydrocarbon fuels, such as methanol, gasoline, or diesel fuels, generating H_2 as a reaction product. These reactions are practiced industrially on large scales, and hence a great deal is known about the reaction chemistry [24, 25]. In this section we discuss the technology issues related to the use of reformers for soldier-level energy generation. The reformer unit alone is not the entire system needed to produce the pure H_2 that is required as a fuel for the PEM fuel cell, and the entire required unit is designated as a fuel processor.

Two main routes to generation of H_2 from methanol or diesel fuel (exemplified by the reaction chemistry of octane in Figure 23) , are steam reforming

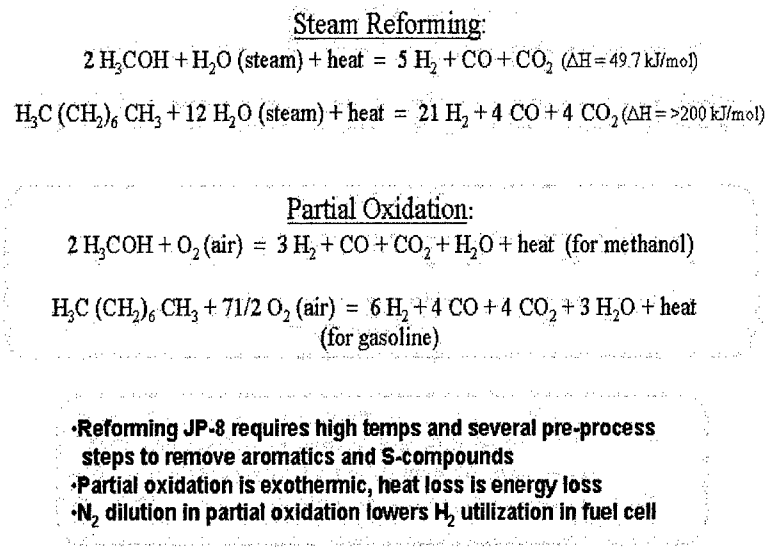

Figure 23: H_2 storage technologies: reforming organic fuels.

or partial oxidation. Steam reforming involves the use of the hydrocarbon, water supplied as steam, and heat, and produces H_2, carbon monoxide (CO),

and carbon dioxide (CO_2) as reaction products. The balanced chemical reactions for steam reforming of methanol and of octane are depicted in the top portion of Figure 23.

The second main route to generation of H_2 from methanol or hydrocarbons such as octane is partial oxidation. In this process, O_2 from air, along with heat, is supplied to the system, and H_2, CO, CO_2, and H_2O are produced as products. Exemplary balanced reactions for methanol and octane partial oxidation are depicted in the lower panel of Figure 23.

Several points are of importance regarding these two reaction processes. First, reforming reagents containing C-C bonds, such as diesel fuel, requires much higher temperatures than are needed to reform methanol. This can be seen by the fact that steam reforming is much less endothermic for methanol than for octane. Hence, much larger energy inputs are required to perform steam reforming of diesel fuel than of methanol, greatly favoring the latter as a fuel. A second point favoring use of methanol as the fuel for reforming is that military diesel fuel, JP-8, contains aromatics and sulfur-containing compounds which are not compatible with the reforming catalysts. Thus, use of JP-8 as the fuel would require several pre-reforming process steps to remove these chemicals from the fuel stream this would greatly complicate the overall process flow and would require significant additional mass and energy inputs. A third point is that partial oxidation generates less H_2 per mole of hydrocarbon input into the system than does steam reforming, because some of the H_2 is produced from the H in the water used as a reagent in the steam reformer. A fourth point is that partial oxidation reactions are exothermic, and the heat loss is an energy loss relative to the energy content of the fuel itself. Finally, the N_2 dilution that is needed to run a partial oxidation reaction lowers the H_2 utilization of the PEM fuel cell, further reducing the entire system efficiency. Taken together, these factors clearly favor the use of steam reforming and methanol as a fuel as the system of choice for generating H_2, at least on small scale systems.

World-class reformers can be over 80% energy efficient for production of H_2 relative to the energy inputs of the fuel and the heat provided to run the endothermic reaction at an acceptable rate. Smaller scale reformers are expected to be less efficient due to larger heat losses to the environment. The PNNL (Pacific Northwest National Laboratory) microreformer, depicted in Figure 24, is currently ≈50% energy efficient, for example [26, 27].

A significant drawback of the reforming chemistry is, however, the need for further fuel processing before the reformate is suitable for use as a feed into the anode of a PEM fuel cell. The reason for this is that the reforming reaction produces CO as well as H_2, and CO is a poison for the Pt-based electrode catalysts used in PEM fuel cells. Figure 25 presents the equilibrium concentration of reactants and products in the reforming of CH_4 for example. Although there is some dependence on temperature, significant amounts of CO are produced over the entire temperature range [5, 24, 25]. PEM fuel cells can not tolerate more than 100 ppm of CO; hence the reformate product stream must be "cleaned up" prior to use in a PEM fuel cell.

The first chemical process for reduction of the CO content of the fuel is the water-gas shift reaction. This reaction is depicted in the middle panel of Figure 26. It is relatively thermoneutral, and can be run in either direction depending on the conditions used. In the water-gas shift process, reaction of steam with CO produces H_2 and CO_2. If this reaction could be driven sufficiently towards CO_2 and H_2 product formation, it could be used to clean-up the reformate directly. However, due to the near-equilibrium nature of the reaction, residual levels of CO of 0.25–0.5% remain in the product stream of a water-gas shift reactor.

These levels of CO are too high to be fed into a PEM fuel cell, so yet another chemical process step is required. In a subsequent step, a preferential oxidation reaction is performed, in which oxygen is reacted with the CO to produce CO_2. Specific catalysts are required to perform the preferential

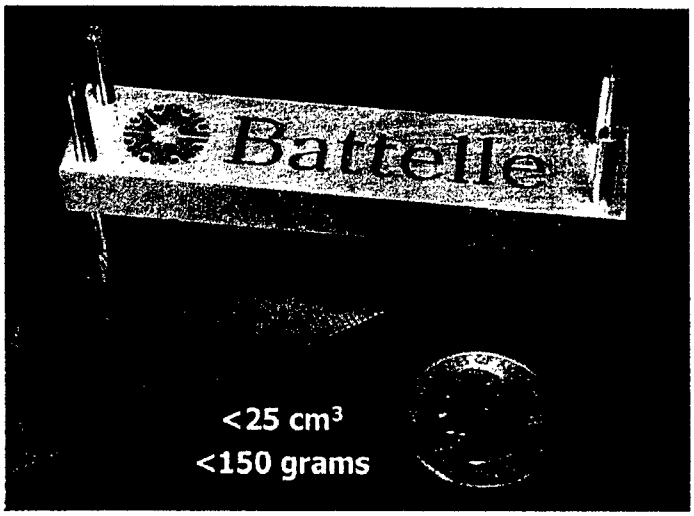

Figure 24: PNNL microreformer.

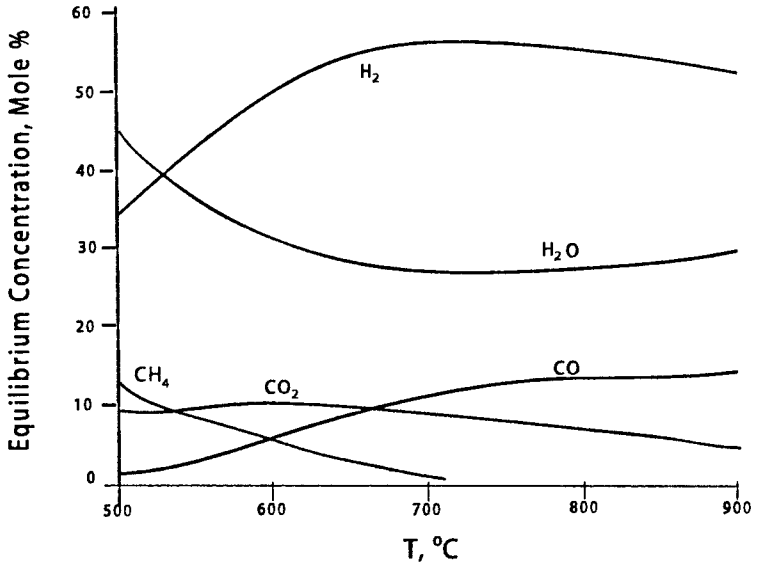

Figure 25: Composition of CH_4 steam reformate vs temperature.

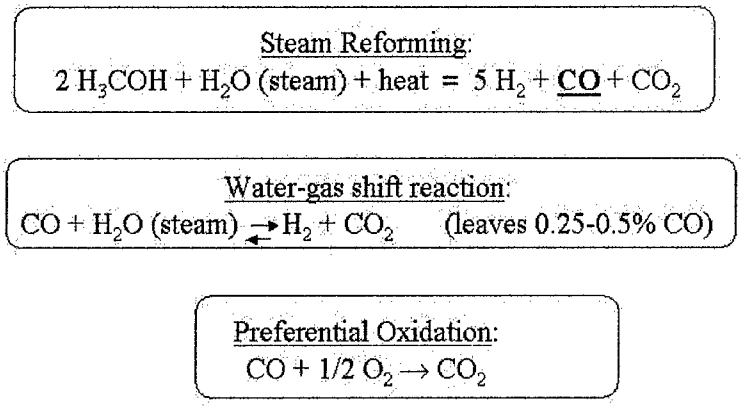

Figure 26: H_2 storage technologies: reforming organic fuels

oxidation of CO with the O_2 in the presence of much higher concentrations of H_2; in practice the selectively for CO is not ideal and some H_2 is sacrificed during this process. Use of the water-gas shift reformate output as the input to a preferential oxidation reactor can, however, produce a final gas stream output having CO levels of less than 50 ppm, which can be fed into a PEM fuel cell without irreversibly degrading the fuel cell performance.

The full process stream of a typical methanol reformer-based fuel processor for use in a PEM fuel cell is presented in Figure 27 [9]. The balance

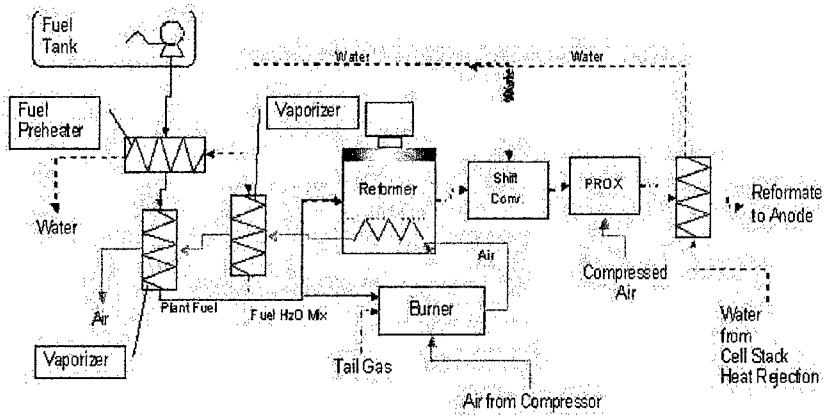

Figure 27: Process stream for a methanol reformer-based fuel processor.

of plant includes process flows for effective utilization of waste heat and for recycling of water through the various parts of the system. The fuel processing system is clearly complicated by the need for the various clean-up steps integrated into the basic reforming reactor process.

To our knowledge, no complete fuel processing system has been constructed on a 20 W power level scale using microfluidics and micromachining approaches to fabricate the needed parts. Thus, we can only estimate what the energy conversion efficiency of such a system might be. The scaling laws of small chemical reactors are fairly well-known; units become less thermally efficient in general as they get smaller. The fundamental reasons for this are that the heat lost to the environment is proportional to the reactor area, A, multiplied by the temperature difference between the inside and outside regions of the reactor:

$$K\,A(T_{\text{in}} - T_{\text{out}})$$

Furthermore, reactors are typically operated at a throughput that is dictated by the amount of catalyst in their catalyst bed, such that the flow velocity, v, is the number of bed volumes V, per sec (i.e., the flow velocity is limited by the inherent activity of the catalyst in the reaction of interest). Hence the heat loss per unit of reactor throughput scales as:

$$\frac{K\,A(T_{\text{in}} - T_{\text{out}})}{K'V} = \frac{K''}{\ell}$$

where K, K' and K" are constants and ℓ is the scaling dimension of the reactor size. Thus, smaller reactors are less energy efficient (if the design is held constant while the reactor is scaled down).

The key variable in evaluating the overall conversion efficiency of a microreformer system is whether the water needed for the reforming and water gas shift reactions will be carried as a co-fuel, or whether it will be recovered from the waste of the fuel cell cathode. If the water is carried as a co-fuel mixed with the methanol, the advantage is that the fuel processor and fuel

will still operate below 0 °C, where water would otherwise freeze. The disadvantage is of course a weight penalty on the energy content of the fuel. Water recovery from the fuel cell avoids having to carry the extra water as a co-fuel, but adds complexity to the balance of plant and adds another control system to the fuel cell system.

When water is to be carried, the steam reforming and water gas shift reactions require together a mass of water that is approximately equal to the mass of the methanol that is to be reformed into H_2. Hence, the 5500 W-hr/kg energy density of methanol is diluted in practice by 50% due to the auxiliary required water, and therefore in practice produces an available energy density of 2700 W-hr/kg of fuel. Taking an overall energy conversion efficiency of 50% for the fuel processor, and a 50% energy conversion efficiency for the fuel cell thus produces a net energy available electrical energy density of 685 W-hr/kg based on the fuel input into the fuel processing/fuel cell system. This calculation assumes no mass burden for the balance of plant or the packaging of the fuel processor.

If water is to be recycled, we can refer to a design proposed by Ball Aerospace and PNNL for an integrated fuel processor/fuel cell unit for reformed methanol for an estimate of the overall energy conversion efficiency that might be obtainable in a highly optimized system. They project a net energy density of approximately 1000 W-hr/kg, with the gain due primarily to the advantages of not having to carry the water and a slight penalty in parasitic power losses and increased mass of the entire unit to operate the more complex balance of plant that is required in this approach [28].

12 CRACKING OF AMMONIA AS A SOURCE OF H_2 FOR FUEL CELLS

The complexity of reforming methanol and hydrocarbons has led some researchers to search for a simpler fuel processing system. Again a liquid fuel is sought, but one which simplifies the fuel processing demands in its conversion to a stream of H_2 suitable for introduction into a PEM fuel cell. Such considerations have led several groups to propose cracking of ammonia for this purpose.

As displayed in Table 4, ammonia has an energy density of 5,800 W-hr/kg, based on the mass fraction of H in ammonia (3/17) and the equivalent of 33,000 W-hr/kg for the H_2 that could be obtained from that NH_3. Furthermore, ammonia has a higher H density than liquid H_2; 100 million tons of NH_3 are produced domestically per annum at a cost of approximately \$0.06/pound; the U.S. DOT classifies ammonia as non-flammable, and ammonia cracking technology is well-developed industrially and is relatively simple. Hence NH_3 is an attractive potential alternative H_2 source to methanol reformate.

Ammonia cracking is being pursued vigorously by at least two research teams, one led by Klavs Jensen at MIT and the other by Rich Masel at the University of Illinois, Urbana-Champaign. Both groups briefed the JASON's on their work and progress to date.

Masel's team has made impressive progress in fabricating microscale ammonia crackers capable of feeding a 20 W_e (where W_e is watts of electricity) output PEM fuel cell (Figure 28). A 2.5 cm^3 microreactor constructed of microposts loaded with a catalyst has been shown to be capable of producing sufficient H_2 for the 20 W_e fuel cell. The energy balance of the system is that 40 W of NH_3 (as computed from the rate of fuel flow and heat of combustion of NH_3) is input into the reactor, and the H_2 output is equivalent to 45 W

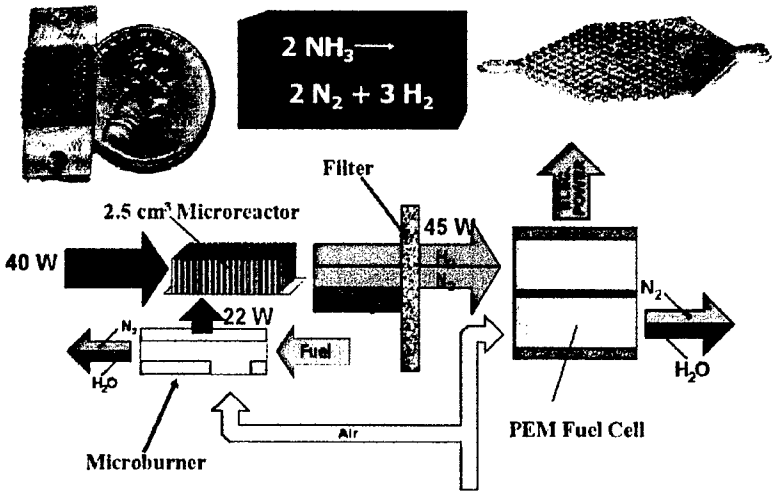

Figure 28: NII_3 cracking for hydrogen production.

of power density. Additionally, 22 W of heat must be input into the reactor, and 17 W of heat is lost to the environment. Hence the overall energy conversion efficiency of the current reactor design is 45/62 = 72%. Additionally, the output stream must be either purified or processed in a separate process step, because PEM fuel cell catalysts can not tolerate even relatively low levels of ammonia, which also acts as a poison to the electrode catalysts. Either carbon sorbent cartridges (that would be disposed of or recycled), palladium tubes, or other types of filters are likely suitable for this process at minimal parasitic power loss.

Jensen's team is now addressing methods for reduction of the heat transfer losses of such microreactors. In this approach, a micromachined chemical reactor is essentially fully released from the substrate except for a zone where good heat transfer is desired (Figure 29). Two fuel stream loops are available, one to combust fuel to produce heat and the other to absorb the heat and perform the fuel processing reaction. A combustion catalyst is cleverly placed, into the heat transfer zone using a micromachined wick, so that the combustion region can be controlled to insure effective heat generation only

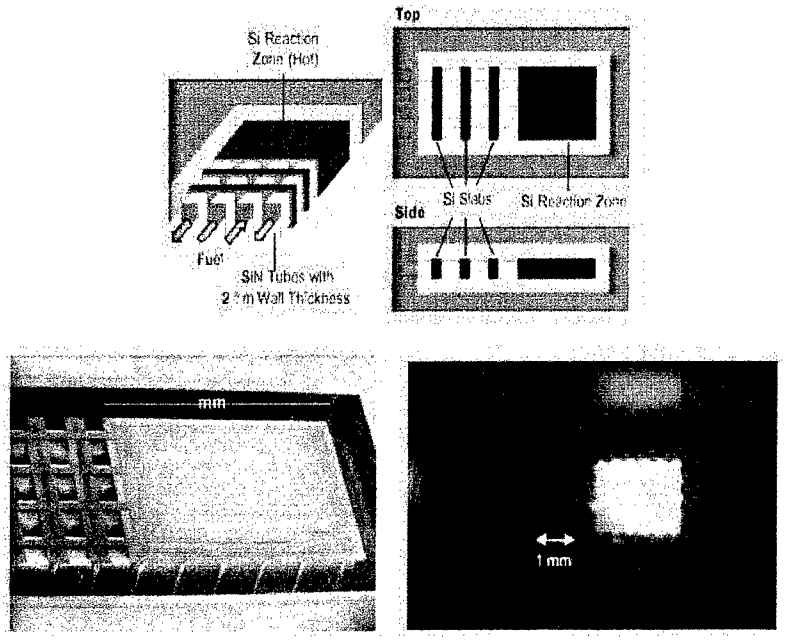

Figure 29: MIT Microchemical Reactor.

in the heat transfer zone of the microreactor. Some recuperation is also available due to micromachined strips being fabricated normal to the flow paths of both flow loops.

The system to date has been demonstrated using propane as the combustible gas, transferring its heat of combustion to the second flow loop that contains ammonia for cracking. The scale of the system is sufficient that enough H_2 is made to provide 1 W_e output from a PEM fuel cell. The heat transfer efficiency of this microreactor is an impressive 90% from one loop to the other loop. This high efficiency requires maintaining a vacuum between the microreactor body and the substrate on which it was micromachined and released. Whether such vacuum encapsulation can be made rugged enough to survive in the field remains to be evaluated.

We can now estimate the possible performance of a PEM fuel cell coupled to a NH_3 cracker as the fuel processing system for H_2 generation. The crackers are between 72% and 90% energy efficient, and have relatively little mass. However, we must also derate the energy density of the NH_3 by the mass of the associated tankage, analogous to the procedure that is used to derate the density of H_2 gas by the mass of its tankage. A ruggedized NH_3 tankage system has been constructed by Ball Aerospace for use in their binary H_2 generation system involving $LiAlH_4$; for our purposes we only consider the portion of the system that houses and delivers the NH_3 [15]. The tank was constructed from 6061 Al alloy, and was designed to sustain a 1300-1400 psi burst pressure at 70 °C in order to obtain a safety factor of 2.0 at this temperature. The vessel was 69 g, the relief valve is 2 g, the polycarbonate coupler and associated components is 15 g, and in total 100 g of tankage and associated components were required to store 150 g of NH_3. This design therefore requires derating the energy content of the NH_3 from 5800 W-hr/kg (based on the H_2 energy contained in the NH_3 assuming 100% energy efficiency in cracking) by the 60% mass fraction of NH_3 in the tankage. A more aggressive tankage design would involve use of carbon-fiber wrapped tanks similar to those used for H_2storage; however the fixed mass of the auxiliary components is not likely to be reduced by very much. We estimate an upper limit of the mass fraction of NH_3 of 90% of the total mass of fuel and tankage. The lower value of 60%, combined with a 50% energy efficient PEM fuel cell and a 72% efficient NH_3 cracker, produces an overall available energy density from the fuel of 1200 W-hr/kg. Optimization of the tankage mass and improvements in cracker efficiency to 90% energy efficiency can lead to an approximate upper limit of 1500 W-hr/kg that might be obtained in an advanced engineered system with NH_3 as the fuel source.

13 DIRECT METHANOL FUEL CELLS

A final option for conversion of liquid fuels using fuel cells or fuel processors that was considered by the JASON's is the direct methanol fuel cell (DMFC). In this approach, a PEM fuel cell configuration is used, with Nafion as the membrane. Methanol instead of H_2 is directly oxidized at the fuel cell anode while the cathode still performs the reduction of O_2 to form H_2O. Fuel cells that use methanol directly, while less energy efficient than those that use H_2 as the fuel, represent a one-step approach to the conversion of the liquid fuel, methanol, into electrical energy.

DMFC technology has advanced rapidly in the past decade. Methanol oxidation is kinetically much more difficult than oxidation of H_2, and classic anode catalysts exhibit large overpotentials for the oxidation of methanol, wasting energy and reducing the energy efficiency of the fuel cell to values below 20%. Another very significant issue is that methanol is soluble in the Nafion membranes of PEM fuel cells, and therefore fuel crossover is significant. Both of these issues must be managed in order to obtain an effective energy conversion system from the DMFC approach.

The main DMFC technology advances have been achieved in the 1990's by work at Los Alamos National Laboratory (LANL) and the Jet Propulsion Laboratory (JPL) [29, 30]. Workers at JPL have shown that the crossover issues can be minimized through use of a 1.0 M solution of methanol in water [29]. In such an instance, at a sacrifice of some voltage, the methanol can be oxidized at a rate faster than it can diffuse to and through the membrane. Crossover can thus be minimized if the pure methanol is metered appropriately, using a closed loop sensing and control system, into the fuel cell to maintain a 1.0 M solution of CH_3 OH in water, while the anode potential is controlled as well (Figure 30). Secondly, the catalysts have been changed from Pt to a Pt/Ru alloy, which exhibits much lower overpotentials

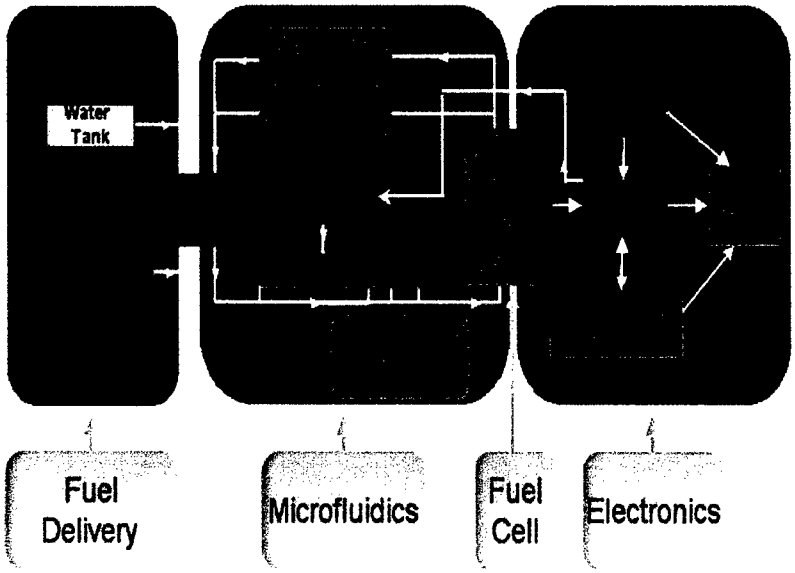

Figure 30: Direct methanol fuel cell system diagram.

for methanol oxidation than what had been reported previously in DMFC systems. At 70–80 °C, the anode losses have been sufficiently minimized in such systems that the overpotentials at the cathode and anode are approximately equal, and the overall energy conversion efficiency of such DMFC's is approximately 40%. An example of the I-V behavior of such a system is depicted in Figure 31.

The DMFC cells exhibit lower energy efficiencies than their H_2-fueled PEM counterparts, primarily due to the increased overpotential for oxidation of methanol at the anode. Power densities are reduced to $\approx$0.2 kW/kg, and the higher catalyst loading leads to increased catalyst costs by approximately a factor of 50 relative to H_2-fueled PEM fuel cells. In addition, the need for control over the methanol content of the anode solution, along with the usual water management issues of PEM fuel cells, leads to a rather complex balance of plant required for current DMFC's [15].

An early LANL DMFC stack that includes liquid/evaporative cooling

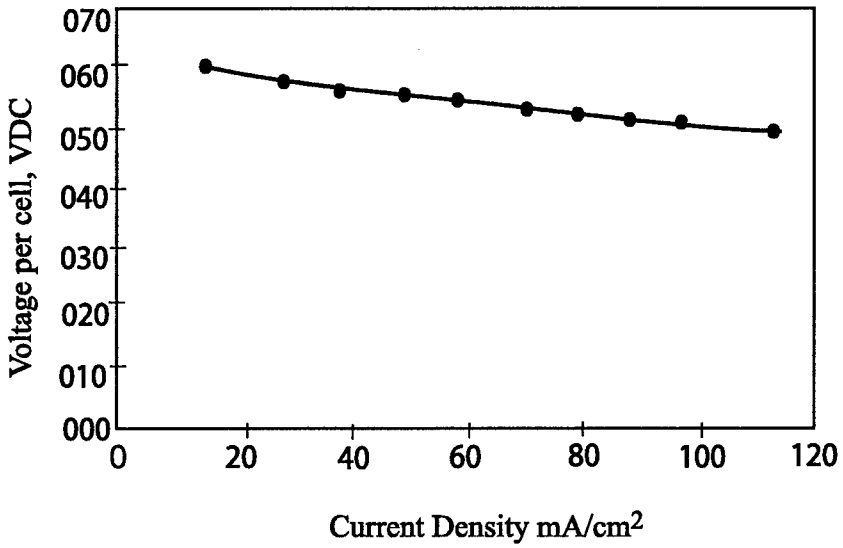

Figure 31: V-I Properties of a direct methanol PEM fuel cell.

weighs 500 gm, and has an power output density of 40 W/kg, as compared to 100 W/kg for a more mature H_2-powered PEM system [15]. This lower power density reflects the inferior performance of the DMFC fuel cell relative to the H_2-fueled PEM counterpart. In addition, the more complex balance of plant adds more mass to the overall fuel cell system. The Ball Aerospace 20 W_e output DMFC has a mass budget of 1.1 kg and meeting this mass budget is proving to be difficult, but a reasonable goal of 1.5 kg would present relatively little risk to construct as a prototype. The high efficiency balance of plant components lead to relatively low parasitic power losses, so the overall system exhibits an energy efficiency that is 90% of the value of the fuel cell itself. Thus, energy conversion efficiencies of 30–36% are reasonably expected in a load-following DMFC system that can operate at a range of temperatures, altitudes, etc. and has a system fixed mass of 1.5 kg. The available energy density of the fuel in such a DMFC is therefore 5500 W-hr/kg * 0.30–0.36, or 1650–2000 W-hr/kg.

Another issue is the scaling of the DMFC fuel cell system with power density. Since the catalyst costs are much more significant for DMFC's than

for PEM's, DMFC fuel cells cost about $200/kW. This is much too high for use in vehicular transportation systems, which require a 50 kW power plant and hence would require $10,000 in catalyst costs alone for the fuel cell. At low power applications, such as cellphones and laptop energy conversion units, catalyst costs are not significant but the limited space available in such devices and the lower power density of DMFC's relative to H_2-PEM fuel cells necessitates implementing engineering tradeoffs between the size and efficiency of the balance of plant, the amount of fuel that can be carried, and the complexity of the control systems that can be implemented. Significant efforts are being made in the commercial sector to advance DMFC technology to the point where it can compete effectively with secondary batteries in cellphone and laptop power devices, but at present the overall energy densities are inferior to those provided by consumer-purchaseable Li batteries [31]. Significant effort is also being made to construct DMFC-based systems that are simpler and involve less control loops in the balance of plant; to the extent that such efforts are successful, DMFC technology will be still more attractive to the military for use in soldier portable power applications.

14 TECHNOLOGIES FOR CONVERTING HEAT FROM COMBUSTED FUEL INTO ELECTRICITY

A fundamentally different set of technological approaches to obtaining power from fuels is to combust the fuel, producing heat, and then convert the heat into electrical power using some type of device for this purpose. Thermoelectrics are notoriously inefficient, so some other technology must be used to be competitive with batteries or with the emerging fuel cell technologies described above. The technologies that the JASON's evaluated for this purpose included thermophotovoltaic devices, alkali metal thermal energy conversion (AMTEC) systems, and microengines. We describe the status of each of these approaches to portable power generation, at the 20 W power level, in this portion of the report.

Most of the technologies proposed for soldier power and energy are quite old. For example, AMTEC (alkali metal thermal energy conversion) was invented at Ford in 1968, and swing engines were patented in 1903. For each technology, it is necessary to ask what is new. In some cases (certain fuel cells) it is a new catalyst, in others (MEMS microturbines) a new fabrication technology and in others (microdiesels) simply the development at small scale of a technology previously employed only at larger scales. In each case it is necessary to ask "What's new?" to decide if there is a prospect that this technology will perform better in the future than it has in the past. If nothing significant is new, then little improvement can be expected.

14.1 Thermophotovoltaics

Thermophotovoltaic convertors of heat to electrical energy rely on small band gap (0.5 eV) photovoltaic (PV) cells to absorb relatively low energy

photons and thereby produce electrical current. Materials of choice to date are from the III-V semiconductor family, in particular GaSb, with a band gap of ≈ 0.7 eV [32]. Typically, selective emitters or other types of radiation filters are placed between the heat source and the PV cells, to obtain better spectral matching between the photons that strike the PV cell and the band gap of the PV cell material.

A thermophotovoltaic energy conversion unit includes a combustor to convert the fuel into heat, a chamber to allow the photons from the heat bath to impinge on an array of photovoltaic cells, a method for air circulation, and often some heat recuperation (Figure 32). The system mass is affected by the masses of all of these components. At present, 20–25 W TPV systems have masses of approximately 2.6 kg.

Many design factors contribute to loss mechanisms in thermophotovoltaic approaches to converting the energy contained in fuel into electrical energy. Heat from the combustion of the fuel must be transferred effectively onto the selective emitter. The emitter must efficiently convert (or pass through, if a filter) photons of the desired energies and reflect others back into the heat source area. Finally, the PV cell must convert absorbed photons directly into electrical energy.

At present, gross efficiencies (i.e., not including parasitic losses needed to operate the system such as fans, etc.) are no higher than 2%. Table 8 presents a breakdown of the losses in a 20 W TPV system, for example [32]. The burner has a radiative efficiency of approximately 29% for producing useful photons from the heat of combustion of the fuel, only 30% of those photons are above the band gap of the PV cells, and the cells themselves have a conversion efficiency of absorbed photon energy into electrical energy of approximately 30%. The conversion efficiency of the cells is near the upper limit because the band gap is sufficiently small that the dark current is quite large, and hence the operating voltage suffers in such systems. The radiative

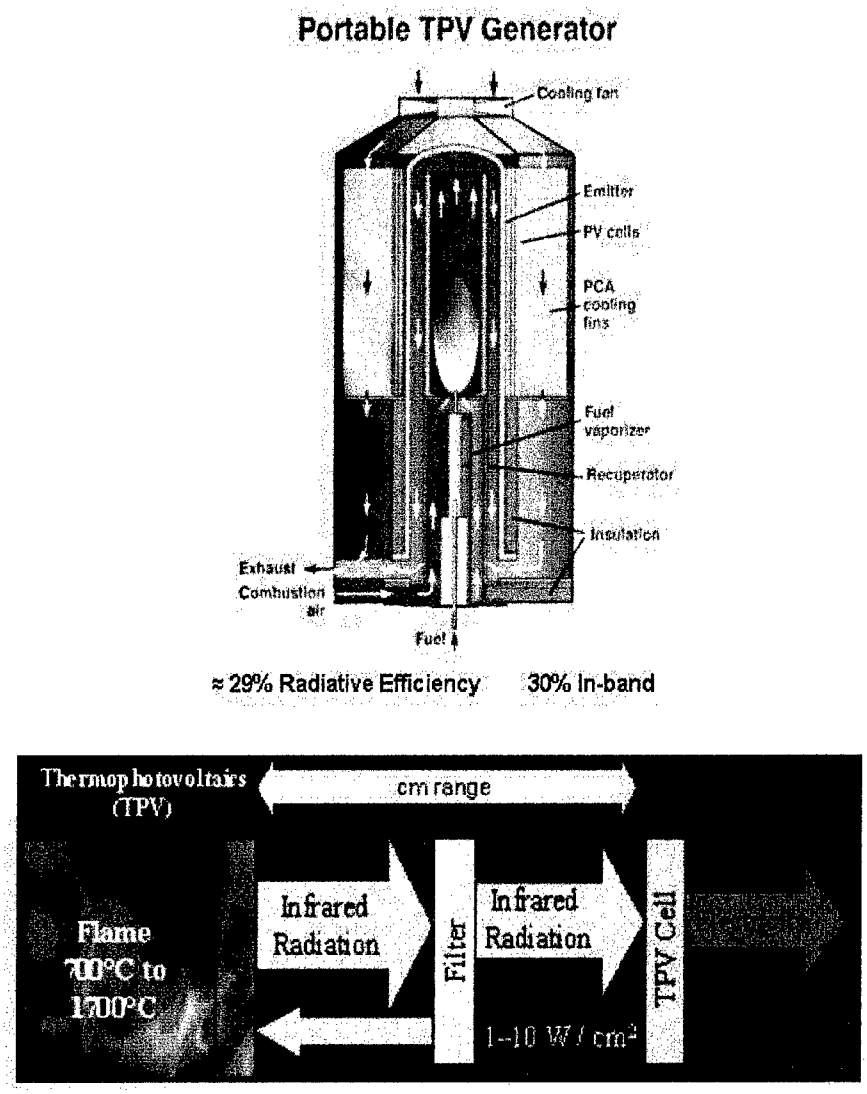

Figure 32: Thermophotovoltaic conversion of fuel into electricity.

Table 8: Summary of demonstration prototype laboratory 20 W thermophotovoltaic convector test results.

Parameter	Propane/Air Combustion		Propane/Air Combustion With Oxgyen Enrichment	
Top PV Array		Blocked		Blocked
Voc - Volts	15.74		15.70	
Isc - Amps	0.156		0.222	
FF	0.5858		0.568	
Power - W	1.44		1.98	
Cell Temperature -C	83		90	
Side PV Array				
Voc - Volts	15.85	16.30	16.00	15.722
Isc - Amps	1.130	1.361	1.823	3.259
FF	0.645	0.542	0.641	0.549
Power -W	11.55	12.02	18.71	28.11
Cell Temperature -C	56	52	62	77
Total Array Power -W	12.99	12.02	20.69	28.11
Emitter (Seperate Test)				
Temperature -K	1287	1287	1458	1458
Broadband Radiation -W	228.2	202.2	452.2	400.8
In-band Radiation -W	69.0	61.1	142.4	126.2
In-Band Fraction	0.2%	30.2%	31.5%	31.5%
Fuel Heat Input -W	694	694	952	952
Heat Sink Load -W	221	196	425	377
Exhaust Heat Content -W	131	141	161	201
BER Efficiency	81.1%	79.7%	83.1%	78.9&
Radiative Efficiency	32.9%	29.1%	47.5%	42.1%
In-Band Array Efficiency	18.8%	19.7%	14.5%	22.3%
Broadband Array Efficiency	5.7%	5.9%	4.6%	7.0&
Gross Efficiency	1.9%	1.7%	2.2%	3.0%

efficiency and in-band values can in principle be improved through better engineering designs, but we saw no approach that would lead to improvements in these values by factors of greater than ≈20–30%.

At 2% net energy efficiency of a TPV system (a level which has not yet been achieved technically) from JP-8, the gross output level of such a system would be 240 W-hr/kg. Furthermore, it should be noted that the remaining 98% of the energy not converted into electrical energy is emitted as heat; thus this 20 W TPV system would emit a 1000 W thermal signature that would be readily detectable.

14.2 AMTEC (Alkali Metal Thermal Energy Conversion)

AMTEC (manufactured by Advanced Modular Power Systems, AMPS) is a heat engine with no intrinsic moving parts. In this respect it resembles a thermoelectric generator (AMTEC will also have slowly flowing alkali metal vapor), and AMTEC and thermoelectrics share advantages of simple, quiet and reliable operation, without complex control architecture or risk of mechanical breakdown. AMTEC is driven by the chemical potential difference between high and low temperature alkali metal (usually sodium, although potassium may also be used) vapor. Free energy is turned into electric power by diffusing the alkali metal, under its chemical potential gradient, through a β-alumina solid electrode (BASE) (Figure 33). This is non-aqueous electrochemistry. In an engineered application a simple cooling fan will be required to dilute the exhaust gases with cool air (to reduce the thermal signature) and to maintain heat transfer from the low temperature (condenser) end of the heat engine to the ambient environment.

Any source of high temperature heat can in principle power an AMTEC device. In the soldier's power and energy application it would be the burning of hydrocarbon fuel. Combustion is steady, so that almost any fuel is sat-

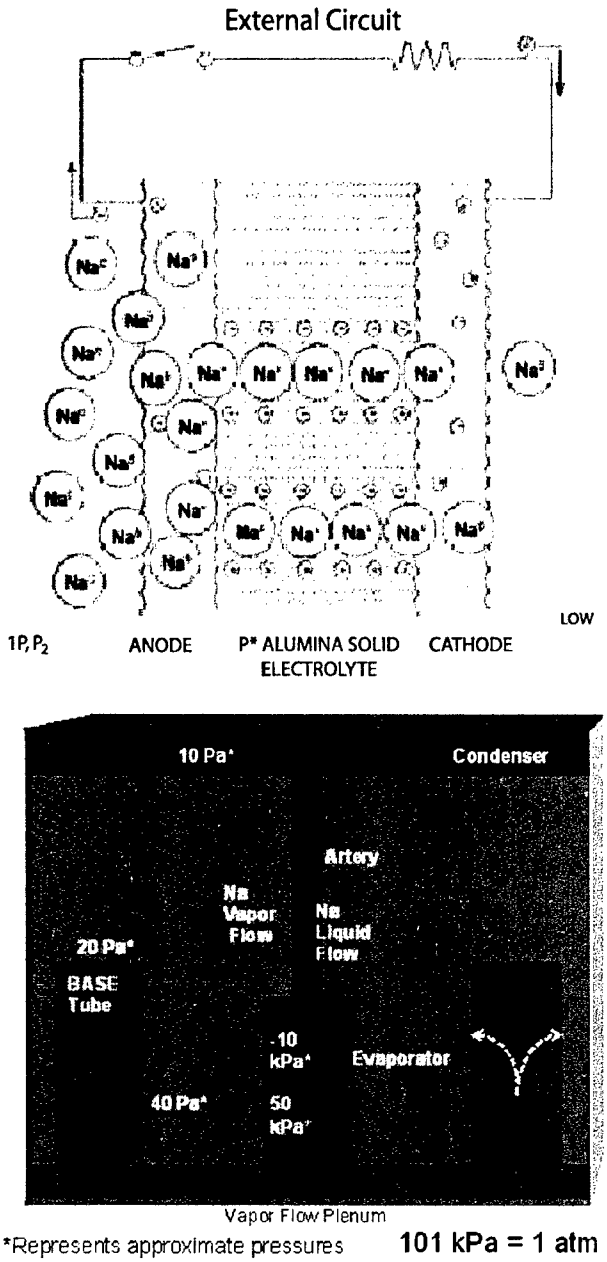

Figure 33: Schematic of the operation of an AMTEC device.

isfactory, including possibly the Army's standard diesel fuel JP-8 (AMPS's 5 W demonstration system used propane, but this is not a significant issue except for the coking of JP-8). The hot and cold ends of the heat engine are typically around 800 °C and 300 °C, respectively, implying a Carnot efficiency of about 47%.

AMPS quotes a system specific energy of 200 W-hr/kg for its 5 W demonstration system [33, 34]. This should be compared to the enthalpy of combustion of propane (the fuel used) of 13,000 W-hr/kg. The reported fuel consumption of 10 gm/hr implies a conversion efficiency of 4.6%, less than a tenth of the Carnot efficiency, or a specific energy of 500 W-hr/kg. Adding a dry mass of 2.1 kg to the 1.68 kg of fuel burned in 1 week of operation (the specified mission duration) reduces the net specific energy to 222 W-hr/kg (rounded to 200 Wh/kg in the presentation).

The large gap between the theoretical (Carnot) and achieved efficiencies has two causes. One is losses in the electrolyte itself—the flow of alkali metal ions is not strictly reversible (its ionic resistivity is not zero), and there are contact resistance losses at the electrodes. Analogous losses occur in thermoelectrics, batteries and fuel cells. It has been estimated that these losses account for roughly a factor of two in efficiency, although we do not have the details to support this estimate.

The remaining inefficiencies, which appear to account for roughly a factor of six in the difference between achieved and Carnot efficiency, are the result of engineering "details" which are, in fact, essential. Coupling of combustion energy to the hot reservoir is highly inefficient. Both the 800 °C hot reservoir and the 300 °C "cold" reservoir suffer extensive heat losses to the environment. There is also a significant parasitic heat flow between these reservoirs, both in the electrolyte itself (properly part of the losses discussed in the preceding paragraph) and between supporting, insulating and other structures at hot and cold temperatures. Thermoelectric generators suffer

similar losses, and typically have end-to-end efficiencies under 6% (although values approaching 20% have been recently reported in experimental systems).

Note that the inefficiencies discussed in the preceding two paragraphs are energy inefficiencies in the conversion of enthalpy of combustion to electricity, and are distinct from the reduction in net specific energy (for operation over a finite time) attributable to the system dry mass.

The important question for AMTEC is how much the specific energy and efficiency can be improved. AMPS has developed a thin, flat planar electrode which will permit a more compact system that is less massive and should have smaller parasitic thermal losses. Further, increasing the power from the 5 W demonstrator to 20 W will tend to reduce the proportion of parasitic losses, and the influence of the fixed dry mass on the specific energy, because these tend to improve as the system is scaled up in size. However, no detailed quantitative thermal analysis of improved designs appears to exist (we saw none), so it is impossible to say by how much the specific energy will improve. Achieving the nearly ten-fold improvement suggested in the AMPS briefing is likely to be very challenging. One possibility that we suggest would be to couple the well thermally-isolated catalytic combustor of Jensen/MIT with the AMTEC convertor system as a method to obtain good heat transfer to the AMPS cell while maintaining the good conversion efficiency of the AMTEC approach to produce electricity from heat.

Some of the difficulty is generic to any system containing components at 800 °C, including some fuel cells. Good thermal insulation is required for at least three reasons—to protect the soldier from injury, to reduce the thermal signature, and to prevent degradation of the efficiency and specific energy. We note that aerogel insulators, although they have excellent thermal properties, may not be mechanically rugged enough for military use.

One difficulty is specific to AMTEC, which requires a large tempera-

ture drop across a thin layer of solid electrolyte (the same difficulty applies to thermoelectric generators). If the electrode were thicker, the developed electric field would decrease in proportion to the temperature gradient, and the electrical loss would be greater. As a result, increasing the size scale will not improve the intrinsic efficiency (the same conclusion applies to thermoelectrics, whose figure of merit is a function of materials properties, not size), although it may reduce losses from heat flow outside the electrode itself.

14.3 Microengines as Energy Conversion Devices

Another approach to energy conversion is to use the combustion of the fuel to power an engine, and couple the mechanical motion of the engine to a generator to produce electrical energy. Of course, such an approach is implemented on larger scales (1 kW or greater) using a variety of commercially available approaches. A range of problems are faced, however, as the engine size is scaled down to the 20 W power level.

Figure 34 depicts the specific fuel consumption and energy efficiency of a large collection of engines of various types as a function of engine output [35]. The engine output in brake horsepower is the power delivered through a load onto the engine output, with 0.0013 hp/W. The energy efficiency of large engines is approximately 25%, and it can be seen that all small engines suffer in energy efficiency, with the losses increasing significantly below 1 hp for all engine types.

The reasons for this behavior involve several kinds of scaling issues. One is heat loss, which is more important for small structures than for large ones. A second is combustion kinetics. A smaller engine has a shorter cycle time. If this approaches the characteristic ignition or burning time of the fuel used, operation becomes difficult and inefficient. A third is mechanical tolerances. The absolute accuracy of fabrication is not much better for small parts than

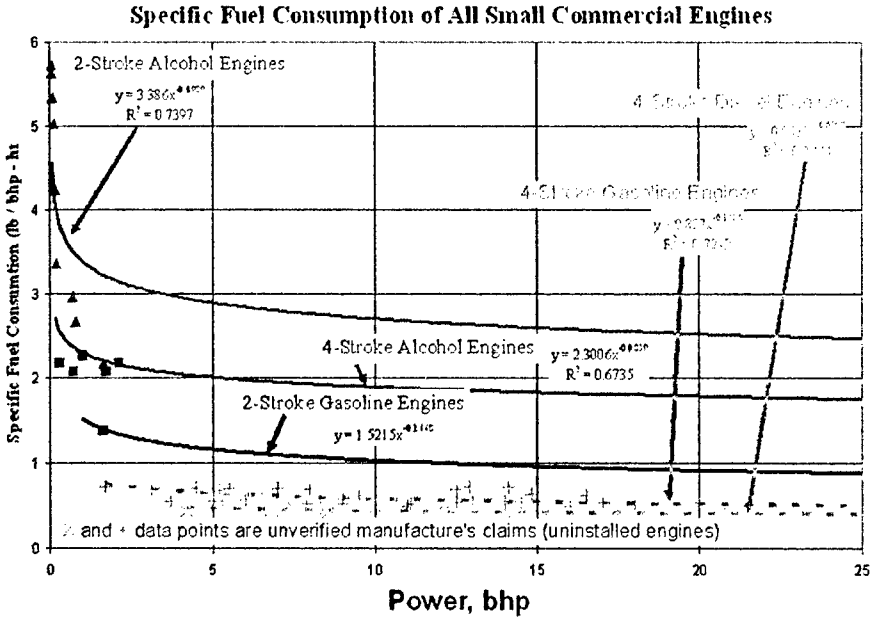

Figure 34: Specific fuel consumption of small engines

for larger ones, so misfits and associated losses at seals are more important for small engines. This reduces the efficiency of both the engine itself (hot gases leak past sliding contacts) and the electrical generator (magnetic flux leaks as well). Estimates generally show that these problems are moderate at electrical power outputs of 100 W, but are severe or prohibitive at 10 W. The task is to push the limit of feasibility as low as possible, or at least as close to 20 W, the power required by an individual soldier, as possible.

Here we discuss three miniature piston engines and a MEMS microturbine. All the reciprocating engines we review use two-stroke cycles because of their lesser weight, greater simplicity and higher power density. These four projects are at very different levels of maturity, so we comment on each without making head-to-head comparisons.

14.3.1 MICE (Miniature Internal Combustion Engine)

The MICE from Aerodyne Research, Inc. is a linear engine, in which a single piston moves along a linear path, with a helical spring providing the restoring force to oppose the pressure of the combustion products (Figure 35). The overall package resembles an ordinary automotive sparkplug

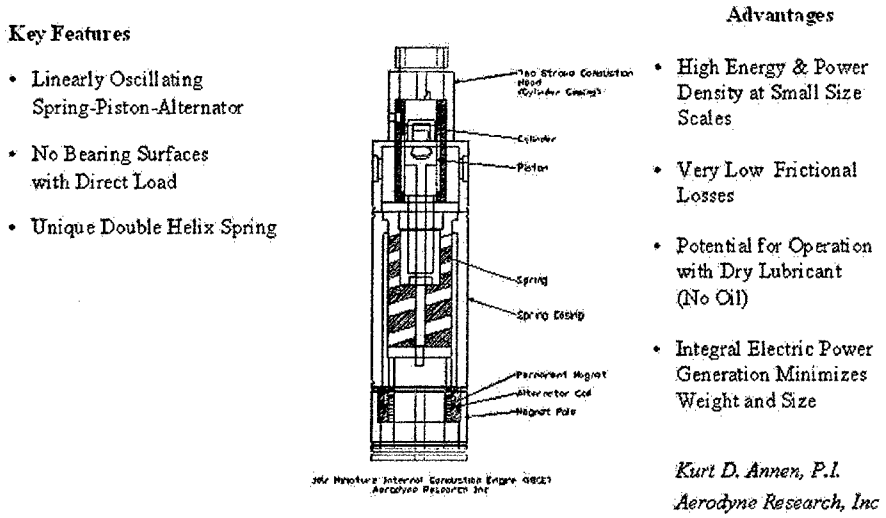

Figure 35: Linearly-Oscillating miniature internal combustion engine

in shape and size. The piston moves on a long shaft extending along the axis of the spring, and an alternator coil is attached to the far end of the shaft; electrical power is generated as this coil moves in the field of a permanent magnet. The most obvious concern is metal fatigue in the spring. Aerodyne reports operation of over 1.5×10^7 cycles without failure, corresponding to 11 hours at a typical operating frequency of 390 cps (23,400 cpm) [36]. This is not sufficient to demonstrate successful operation over a 10 day mission (3.4×10^8 cycles of continuous operation), but we have no reason to expect failure. The phenomenological understanding of metal fatigue is sufficient that, if necessary, straightforward redesign of the spring to reduce peak stresses would likely be capable of solving this problem, should it arise.

At present, MICE is at a very preliminary stage of development. It has run, but less than 1 W of electrical power has been extracted. It depends on a glow plug igniter which must be continually supplied with electric power. Even then, ignition occurs only when the propane fuel is mixed with oxygenated (35%) air. The scavenging ratio is low (the "best guess" is 50%) and very uncertain, and the developers believe this accounts for its inability to support combustion with ambient air. They attribute the poor scavenging to a poorly designed inlet system.

In fact, little detailed design work appears to have been done on this system. It is therefore difficult to say how well it might perform if a systematic development effort, including both quantitative design calculations and an extensive experimental program, were made. In its present configuration MICE burns gaseous or volatile fuel, not JP-8. To burn JP-8 would require a fundamental redesign as a diesel, with correspondingly higher compression ratio to achieve ignition (quite apart from the present issues of inlet design). Existing experimental results indicate that performance degrades as the oscillation amplitude and peak compression ratio increase, probably as a result of leakage at the piston-cylinder seal, even though the builders estimate the fit to be good to 0.00005". This problem is likely to be much worse at compression ratios required for diesel operation.

14.3.2 MICSE (Micro Internal Combustion Swing Engine)

MICSE (University of Michigan) is a swing engine, in which a linear rotor serves as a piston [37, 38]. It oscillates with an amplitude of about 40°. MICSE is thus intrinsically a four "cylinder" engine (though the spaces in which combustion occurs are not cylindrical), with one on each side of each arm of the rotor. There are actually two combustion chambers, each with the geometry of a pie slice about 120° wide. Each arm of the rotor moves in

one of these chambers, dividing it into two subregions in which combustion occurs (Figure 36).

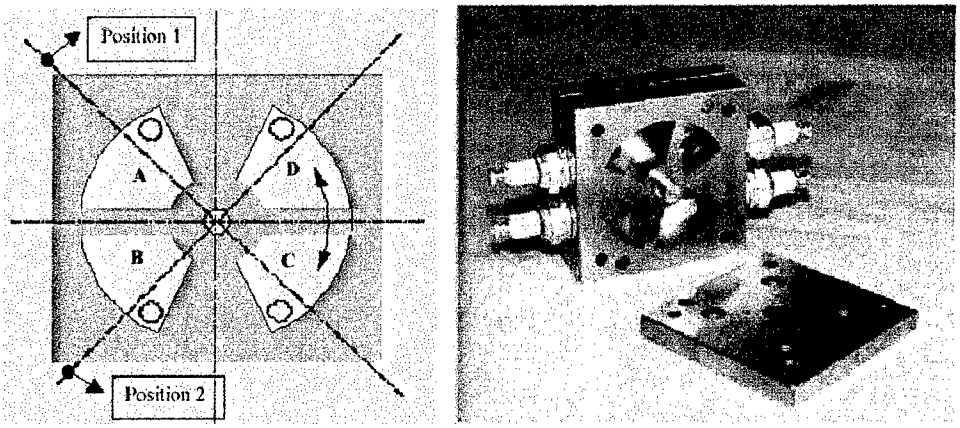

Figure 36: A microswing engine.

MICSE has been the subject of extensive finite element analysis of its thermal, mechanical and (for the generator) electromagnetic properties. This analysis has been the basis for an optimized design which promises 21 W of electrical power with a specific energy (considering fuel mass alone) of 1590 W-hr/kg, burning butane. We were unable to find a design figure for the total dry mass, but estimated component masses are 30 gm for the engine and 140 gm or less for the generator. At the predicted fuel specific energy, in one week of operation 2.24 kg of fuel would be burned. Taking (probably conservatively) 500 gm dry mass would yield a net specific energy of 1230 W-hr/kg. The dry mass is a fairly small fraction of the fuel mass (22% for a one week mission and 16% for a 10 day mission), and its effect on the specific energy is not large. However, the overall energy density will be further reduced if, as is probably necessary, a secondary battery must be provided to smooth over fluctuations in power demand.

Although the design effort has been elaborate, the experimental effort has been much less comprehensive. The initial (sized to 65 W) MICSE0 prototype ignited, but the smaller (20 W) MICSE1 failed to ignite. Extensive

study appears to have identified the cause of this failure as a too small ignition spark, and consequent heat loss from the initial flame "kernel". We have not seen the results of experimental tests (which apparently had not been completed at the time of our briefing in July 2002) of MICSE2 with a redesigned ignition system.

MICSE is designed to run on butane, not the standard logistic fuel JP-8. A fundamental redesign would be required to achieve ignition of the less volatile liquid JP-8. No comparison has been made between the expected performance of the swing engine and the performance of existing small engines such as either Cox hobby model airplane engines or micro-diesel engines discussed in the next section.

The engineering of the MICE and MICSE systems is too preliminary to determine whether they can function at 20 W, but in general a secondary battery will be useful for load management.

14.3.3 Micro-Diesel Engines

The most familiar small engine to hobbyists is the commercial Cox engine series that is used in model airplanes. These consumer products are noisy and are not ruggedized for military use, but nevertheless demonstrate that small engines can function to produce mechanical power that could be coupled to an electrical generator. In some respects, these engines are the benchmarks that other small engine designs need to exceed to prove their usefulness. It should be noted, however, that the Cox engines run on fuel that contains its own oxidizer, nitromethane/alcohol, because of the difficulties involved in sustaining robust combustion on these small length scales with hydrocarbon fuels. In addition, JP-8 diesel fuel in particular forms coke deposits that will quickly force such a small engine to cease functioning.

The microdiesel engine (D-STAR Engineering Co.) is a clean-slate design of a Cox-type engine [35]. The microdiesel engine has been designed to run on JP-8, the standard logistic diesel fuel. Its displacement is 0.050 in^3 and its nominal mechanical power output is 0.1 hp ($\approx$75 W). This engine is the most mature of the micro-engine power sources we studied. This comparative maturity means that more problems have been solved, but also means that more problems have had the opportunity to be identified.

Diesel engines are traditionally heavy, because they require a robust structure to contain the overpressure implied by their high compression ratios (required to heat the fuel-air mixture to ignition). In addition, for this reason diesel engines are traditionally used in applications (heavy trucks, locomotives and ships) in which weight is unimportant, so little effort is expended to make them lighter. There is no royal road to a light diesel engine, but D-STAR's design takes several steps to reducing the engine weight. Ceramic materials have higher strength to weight and stiffness to weight ratios than steel (their higher cost is unimportant in a small engine for soldier power, while it would be prohibitive in traditional diesel applications). A reduced compression ratio reduces the pressure. In future engines a pressure relief valve may further reduce the peak pressure while hardly affecting the rest of the pressure curve. High cycle rates permitted by small sizes increase the power per unit mass and volume. A two-stroke cycle doubles the number of power strokes and reduces frictional losses. Each of these measures (except the use of ceramic materials) exacts some price in efficiency and performance, as does the scaling to small size.

The microdiesel is a fairly mature system which has demonstrated 40 W_e into 27 VDC operating on JP-8. The design goal is 50 W_e. The specific energy, based on fuel consumption alone, is 1810 W-hr/kg, assuming the design power and 15% fuel to electric conversion efficiency are achieved. The presently achieved 10% conversion efficiency would imply a specific energy of about 1200 W-hr/kg. The design specifications include 3 kg of fuel, sufficient

to provide a mean power of 20 W for 11 days. Inclusion of the dry mass of 1 kg would reduce the net specific energy to 1360 W-hr/kg (here and subsequently we assume the goal of 15% efficiency is achieved). For a one week mission at a mean 20 W the net specific energy becomes 1170 W-hr/kg. The dry mass is greater than that of the other microengines considered. This is the price paid for diesel operation, but it is not a large price. In fact, the dry mass is only about 1/3 of the fuel mass for the 11 day mission, and 54% of the fuel mass for a 7 day mission. The microdiesel was designed to provide 50 W of electricity, not the 20 W the soldier needs. This is not an accident, but is a consequence of the increasing difficulty of operating internal combustion engines at smaller sizes. In practice, such an engine would operate intermittently, recharging a secondary battery when the engine was operating. The D-STAR system design proposed 3 kg of secondary batteries, reducing the net system specific energy to 4/7 of the values (including dry mass) cited in the previous paragraph, or to about 780 W-hr/kg for a 11 day mission. The battery mass could be reduced at the price of more frequent on-off cycling of the generator (the 3 kg provide 10 hours of power at the nominal load, permitting cycling as infrequently as three times a day), but some battery capacity is required for cold starting the diesel.

14.3.4 Microturbines

The microturbine (MIT) engine constructed with silicon etch (MEMS) technology is arguably the most radical and innovative engine technology considered for soldier power. It has been the subject of a very elaborate and extensive design and development program [39] –[41]. Because its parameters are far from those of any other engine, this program has depended heavily on CFD and finite element calculation. There was no prior experimental experience at this size scale, but there is now a substantial experimental program.

Turbine engines (macro or micro) have extremely high power densities and low masses, which is why they now dominate aircraft propulsion. The reason for this is that air, fuel and combustion products flow through the engine smoothly at speeds approaching their sound speed, rather than being limited by the requirement of moving massive pistons and shafts. The turbine rotates continuously at a steady rate rather than starting and stopping again with each stroke as a piston does. As a result, the measured power density [39]–[41] in the microturbine (burning hydrogen) is at least 1100 MW/m^3, about 12 times greater than the design power density of 92 MW/m^3 of the microdiesel.

This intrinsically high power density and rapid flow of the burning fuel has advantages (the 200 W thermal microturbine has a rotor 4 mm in diameter and a mass of order a gram) but also has disadvantages. The time available for fuel to burn is very short $\approx 10^{-6}$ sec, even though its flow path is folded rather than straight through as in a full scale aircraft or power generating turbine. As a result, most of the microturbine design work has been done on hydrogen, the fastest burning of all fuels. Ethylene gives a power density of 500 MW/m^3, roughly half that of burning hydrogen, and propane gives a power density of 140 MW/m^3, eight times less than hydrogen.

It is not possible to slow the passage of fuel through the microturbine simply by slowing the rotor, because that would make its compressor stage inefficient. As a result, it would be quite difficult to make a microturbine burn JP-8, and successful operation on propane or butane is uncertain.

Even with hydrogen fuel, the performance may be disappointing. The near-term microturbine design goal is 5% chemical to electrical conversion efficiency at 200 W thermal power. Part of the inefficiency is accounted for by poor generator performance (the small, high speed, low torque rotor makes electrical generation inefficient) and partly by thermal and frictional losses in the turbine itself. Scaling upward in size would make everything easier,

so we will assume the same efficiency at 400 W thermal power to make the 20 W of electrical power needed by the soldier. The 5% efficiency implies three times as much waste heat as produced by the microdiesel. If scaled up yet again to 50 W of electrical power (implying a 40% duty factor, as for the microdiesel) the waste heat would approach 1 kW (although improvements in efficiency which come with increasing size might reduce this). This is a source of significant thermal signature; the solution must go beyond simply mixing hot exhaust gases with cool air and concealing the hot exhaust pipe from view. 1 kW is approximately the mid-day summer Solar insolation of 1 m^2 of ground and is ten times a man's basal metabolism; hence adding this amount of heat to the ambient heat load will produce a substantial plume.

The most critical question for microturbines is whether they can run on hydrocarbon fuels. The best chemical stores of hydrogen contain less than 20% by mass, and these are exotic, temperamental and frequently toxic chemicals. The best pressure vessels for hydrogen gas store (at standard margins of safety) only $\approx$6% of their own mass in hydrogen. If we adopt this number and assume the design 5% chemical to electrical conversion efficiency the resulting specific energy is only 90 W-hr/kg, too small to be useful (no allowance has been made for secondary batteries, some of which will surely be necessary). Even assuming a 20% mass storage fraction raises the specific energy only to 360 W-hr/kg, barely exceeding that of current primary batteries.

It is clear that the usefulness of microturbines depends on their being able to burn hydrocarbon fuels. Table 9 presents some fundamental characteristics of various fuels [36]. This table underscores the important differences between the various fuels, and emphasizes why H_2 is the near-ideal fuel for a turbine engine, whereas other fuels are much more difficult to use in such a system, especially at small scales. The current microturbine engine is designed to run with hot walls, but the much lower autoignition temperature of JP-8 relative to H_2 will impose a limit on the wall temperature that

Table 9: Technology Issues Involving Fuels

	Propane	Butane	Ethylene	Dimethy ether	H_2	JP-8, Diesel
Autoignition Temp, K	777	704	763	623	844	520
Flame Speed cm/s	45	44	79	53	306	40
Quencing Distance, mm	.31	.47	.197	.354	.098	.90 (est)
Min. Ignition Energy, mJ	.305	–	.096	.45	.02	–
Comments	Best Fuels for Small Engines		Potential Small Engine Fuels For Improved Combustion			Feasible at/100 W

can be used and thus will result in additional engine efficiency losses. The flame speed is almost an order of magnitude lower for JP-8 than for H_2, so the combustion kinetics are much less favorable for diesel fuel than for H_2. Perhaps most importantly, the quenching distance of diesel is comparable to the physical size of the microdiesel engine, whereas the quenching distance of H_2 is an order of magnitude smaller. These fundamental properties of the fuel present an imposing challenge to overcome at small engine sizes. We did not see any credible design which was compatible with the efficient, microturbine-based, utilization of diesel fuel on a 20 W engine scale.

We suggest that the design effort, at least for the soldier power application, focus on systems with 50 W electric output which can be directly compared to microdiesels. If microturbines of this size can be made to run on volatile hydrocarbons (ethylene, propane or butane) they might be competitive with microdiesels if the burden of a non-logistic fuel is accepted. It might also be useful to consider yet larger microturbines, planning on a smaller duty cycle of operation; because microturbines are compact and light, and because their high revolution rate increases the power density of the generator, the system dry mass would remain acceptably small even at much higher peak power. The most difficult challenge would be to make a microturbine run on JP-8, as well as the logistics challenge of recharging the

secondary batteries sufficiently often and rapidly to make the system useful. It is important to find out on how small a scale these types of engines can actually be built and run on diesel fuel.

15 CARBON-AIR BATTERIES

We also heard a briefing from J. Cooper of Lawrence Livermore National Laboratory about carbon-air batteries (Figure 37). These are high-

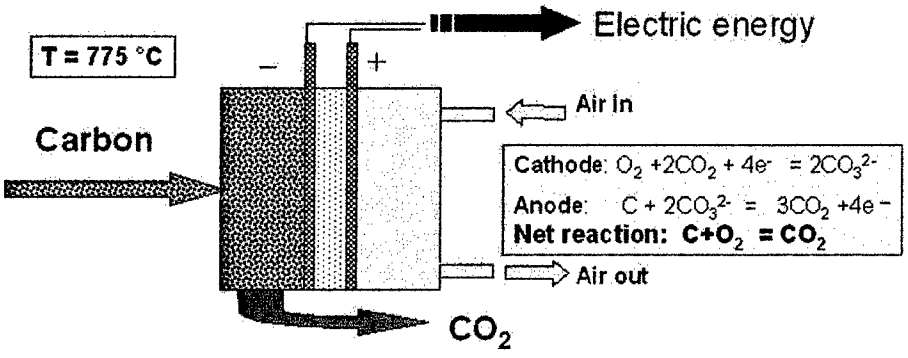

Figure 37: Carbon-air batteries

temperature devices, which instead of burning carbon with oxygen to form CO_2, use a finely divided source of carbon in a fuel cell [43, 44]. Claims have been made that such systems can possibly have very high energy densities, at levels that if achievable would be approximately 10 times higher than the best batteries that have ever been constructed. A key unanswered technical issue to achieve these energy densities concerns what fraction of the carbon that is loaded into the cell is actually utilized and converted into electrical current. The technology concept is very old, dating to the early 1900's, and the apparent advance is the use of a finely divided carbon that produces a higher discharge rate than was available previously. However the fuel utilization fraction has not yet apparently been determined even qualitatively, and no estimates were provided about the energy density that has actually been obtained in test cell configurations, although such values must be available from the data obtained to date and would establish a lower limit on the cell performance. Without these values, we can not speculate further about the potential of this approach, except to say that it will clearly

involve high temperatures (which may possibly be shielded with insulation; vide infra). Another key unknown is what reaction chemistry is taking place at the cathode, since in many cases CO_2 is not supplied and only house compressed air is supplied, contrary to the equations which suggest that CO_2 is needed at the cathode to resupply the charge-carrying ion to the electrolyte. A third question is whether the device could ever be shut off once it was started, or whether such would be necessary to reduce a thermal signature when needed. This technology thus needs better definition of its fundamental behavior before a quantitative assessment of its potential for portable energy production can be made. The packaging requirements and parasitic losses of such a high-temperature energy production system, which requires forced air for the cathode and cooling of the entire structure, will undoubtedly reduce the net energy density significantly from any theoretical values, but we can not estimate these mass and power burdens given the level of unknowns involved with the technology performance at present. These basic performance measurements can be made relatively rapidly so that the judgement on this approach can be carried out expeditiously once the values are available.

16 TECHNOLOGY READINESS LEVELS FOR COMPARING DIFFERENT ENERGY CONVERSION APPROACHES FOR SOLIDER POWER

The technological approaches discussed above are at very different stages of development, and therefore embody a wide range of technical risks with their implementation. It is always difficult to compare that which is known, and which has problems concretely identified, to that which is unknown and which therefore potentially has problems that have not yet been identified. An approach to organize such comparisons is to assess various technologies using Technology Readiness Levels. The Technology Readiness Levels serve to gauge the levels of technical development (and thus remaining technology risk) associated with various technologies. We believe that it is useful to use such a framework to place the various technologies discussed in this report in mutual context.

Figure 38 defines the technology readiness levels as used in this report. This scale was taken from the NASA technology readiness level chart, and appropriate modifications in the wording (changing "flight demonstration" to "field demonstration" etc.) have been performed to make it relevant to the portable energy technology discussion.

Figure 39 presents a summary of the proven and/or potential reasonably estimated performance levels of the various energy conversion approaches discussed in this report, plotted on a common scale on the ordinate in units of output W-hr/kg, as a function of estimated technology risk on the abcissa (with higher TRL values corresponding to lower technology risk levels). Of course, the ordinate is a quantitative scale, whereas the abcissa is a qualitative human value judgement scale that is not necessarily linear as a function of resources required to develop the technology or linearly related to the

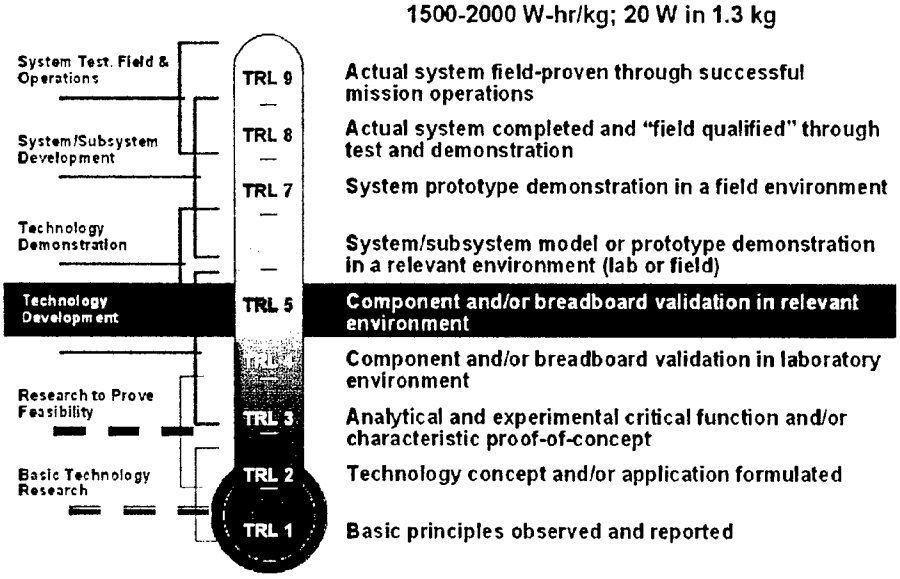

Figure 38: Technology readiness levels.

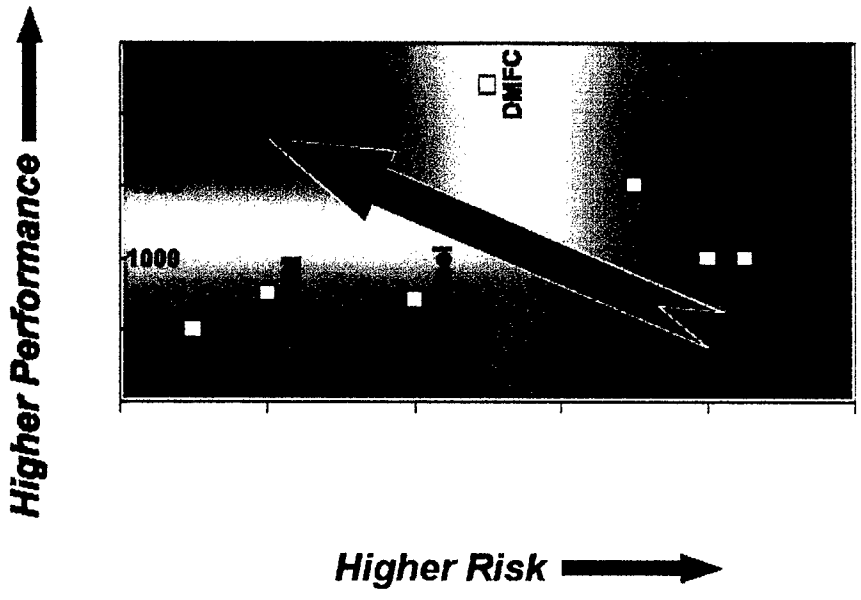

Figure 39: Reasonably expected performance vs technical risk of various energy conversion technologies.

likelihood of attaining the projected practical performance without other serious problems being identified during the process. Nevertheless, such an approach provides a useful method for comparing the various technologies and expected performance levels of the technology approaches discussed in this report. Obviously the goal is to identify technologies that approach the upper left quadrant of the graph, which have very high expected practical performance levels and additionally which have low perceived technical risk of being implemented at those performance levels.

A typical situation would be that the technologies having the highest potential performance would have the highest technical risk of development. However, in the present situation, we observe somewhat different behavior. Clearly at the 20 W level, the DMFC approach seems to stand out singularly on this graph. Prototypes have demonstrated 2000 W-hr/kg of energy density from the fuel, and the fixed mass of the DMFC convertors is, with little technology risk, 1.5 kg as 20 W of output power. For extended missions of the type considered in this study, where most of the mass of the entire system consists of fuel and the mass of the convertor is not so important, the DMFC technology appears to be most attractive for further development.

17 LOGISTICS ISSUES

17.1 Prepackaged Fuel

The Army has expressed a clear commitment to having only one logistics fuel, JP-8, on the battlefield and in the logistics supply chain. Hence the drive has been to have soldier power systems developed to operate on JP-8. As discussed above, no low-noise technology has been identified or perhaps even conceptualized that can use JP-8 and provide a net output energy density even remotely close to that available from current primary batteries.

The issue then is whether another fuel would be acceptable for use for a battery replacement power system. We note that batteries, which in essence contain fuel (Li, SO_2, etc.) are already supplied throughout the logistics supply chain. Hence it would seem acceptable to use an alternate fuel, such as methanol, for example, for soldier power, provided that the fuel was prepackaged, and if necessary even labeled "Battery cartridge". Hence we do not see a compelling need to insist on a device that uses JP-8 to fulfill the requirements of the 20 W extended mission, and believe that the logistics issues involved with use of such a fuel would be very similar to handling the logistics of batteries as they are currently dealt with in the supply chain.

17.2 Mission Operation Issues

The logistics associated with the use of microengines as power sources are somewhat different, however. In most cases, if an internal combustion engine works at all, it will be efficient enough to have a specific energy, measured with respect to its fuel consumption, of between 500-1000 W-hr/kg (i.e. 5-10% energy efficiency from hydrocarbon fuel such as diesel or propane).

The engine's dry mass may be significant, but the chief difficulty is making it work. All internal combustion engines enjoy the very high (about 12,500 Wh/kg) energy content of hydrocarbon fuels. They all must deal with the problem of combustion on a very small scale. Except for possibly microturbines, all must muffle a high level of noise, both in structural vibration and in their exhaust pipes. These fundamental facts have operational implications. If one wishes to provide a soldier with (for example) 20 W of power for a 10 day mission, one must ask whether it is necessary to generate that power continuously, or whether he can carry a secondary battery capable of supplying his power needs for a much shorter time, after which it will be recharged or replaced. This recharge could be by a generator carried by the soldier himself, or he could return to a recharging generator which would supply the electrical energy needs of several (or many) soldiers by maintaining a supply of recharged secondary batteries.

A recharger which supplies the electrical needs of several or many soldiers by recharging secondary batteries is much simpler to design and build than one designed to be carried by and supply the needs of a single soldier because it is a much larger and higher power device, with an electrical output of hundreds of watts, rather than 20 W. Such portable generators are a consumer item. However, the operational constraints implied by making a soldier dependent on a central (even squad-level) recharger are severe, and the consequences of failure to meet them potentially catastrophic: if an operation runs into unexpected delays or obstacles, and its soldiers are cut off from their recharging base, they may become ineffective, or even nearly defenseless. Hence there is good reason to miniaturize power sources so that each soldier carries his own, along with fuel sufficient for an extended time. His effectiveness should not be limited by exhaustion of electric power. It is therefore not clear whether there is a viable need for power systems which do not allow the individual soldier to be autonomous.

18 SAFETY ISSUES

All fuels are hazardous to some extent, in fact those with high energy densities are amongst the most desirable for use in demanding portable power applications such as the one considered herein. Batteries also contain toxic material, but it is robustly packaged so as not to present a significant danger to the user. The same approach should be used for packaging of fuels.

There are however, significant differences in both perceived and real hazard levels associated with different fuels. Hydrogen is arguably safer than gasoline, with a 400% greater lower flammability limit, a 12 times higher diffusion coefficient, and a 52-fold greater (but opposite in sign) buoyancy [17]. Nevertheless it is perceived by many to be unsafe in its compressed gaseous form and indeed has a small minimum ignition energy, making sparking a potential hazard. Ammonia, although not classified by the DOT as explosive, is a toxic gas. Methanol is a toxic, odorless, colorless liquid, than can lead to blindness upon prolonged exposure.

Most new product developments experience both technology risk and market risk. The former involves whether the technology will meet the market needs; the latter involves whether the customer will buy the product even if it does perform well technically. In the case of portable soldier power, the military is both the technology developer and the final market consumer. Hence the market risk ought to be minimal, and it ought to be possible to identify which fuels can be packaged sufficiently safely that they would be considered acceptable in that form for use by a soldier. However, to our knowledge no such study has been done. Because many of the performance differences in the various technologies are factors of 2–3 that can be significantly affected by packaging requirements required to insure the safe use of the fuels, this issue should be addressed as soon as possible by the DoD and systems should be evaluated accordingly. For instance, it may well be the

case that due to the possibility for leaks of a toxic gas, the packaging required to insure an acceptable level of risk for the use of ammonia in the field is so significant that the inherent NH_3 fuel content must be derated by a large factor. In that case, even a 50% efficient PEM fuel cell along with a 90% efficient NH_3 cracker might provide less energy density than that available from primary batteries. This type of user/safety/acceptability analysis ought to be performed as soon as possible, to identify the mass burden associated with acceptable handling of the various fuels, to derate their energy content commensurate with the required mass burden, and to eliminate development of energy conversion systems that would never be adopted by the customer even if they were technically successful. This triaging of technology options should be performed regardless of whether these conversion devices are at the conceptualization stage, the prototype stage, or the field demonstration stage of their development.

19 SIGNATURE ISSUES

19.1 Acoustic Signatures

Noise is a general problem for reciprocating internal combustion engines. Even the tiniest model airplane engines produce noise levels that are above the pain threshold at distances of a few meters. This problem has been addressed, although not yet completely successfully, for the microdiesel. Use of a muffler and a noise enclosure reduces the noise level to an estimated 32 dB(A) at 100 meters [35]. This is at or below typical outdoor ambient levels, and is therefore considered not to produce a detectable signature.

The corresponding level at 1 meter is 72 dB(A), similar to that of a household vacuum cleaner at its user and in excess of conversational speech levels, which are typically around 60 dB(A). This level of noise would be very annoying to its operator, and perhaps intolerable when operated for 10 hours every day, as required for a mean output of 20 W. It would make it difficult to engage in conversation or to communicate by radio, and impossible to listen for the faint noises of enemy infiltrators. Further, there are circumstances in which this noise output would pose an unacceptable risk of detection. For example, in jungle or urban warfare the enemy may be much closer than 100 meters. Also, in certain conditions (typically around dawn or in fog) a surface acoustic propagation duct exists and the noise level falls off less rapidly than the -2 power of the range, so that the noise level at 100 meters can exceed 32 dB(A). It will probably be necessary to achieve an additional 20 dB of acoustic source reduction, and 30 dB would be desirable. This ought to be possible but the mass and other physical variables of an engineering solution are not yet known.

The acoustic signature of a microturbine is unknown. There is very

little structural vibration, the turbine speed is about 20 kHz (essentially inaudible), and the exhaust gases are released in a steady stream, so the chief noise sources of a reciprocating engine are absent. However, the high velocity exhaust jet may generate a great deal of noise (analogous to ordinary jet engine noise) as it enters and mixes with the ambient air. Only experiment can show how loud this engine will be, and how well it can be muffled. We note that this can be done without the engine generating positive power to a load, and suggest that it should be evaluated soon so as to obtain an understanding of the magnitude of the problem that needs to be dealt with.

19.2 Thermal Signatures

Although an oft-cited possible drawback of high-temperature approaches to fuel conversion, such as microengines, AMTEC devices, fuel cells, and carbon-air batteries is a possible thermal signature, very little quantitative analysis appears to have been performed to assess the degree to which the thermal signature can be minimized in such systems. Clearly, if insufficiently shielded, the IR emission from high temperature components – with frequencies much higher than those from the ambient background – could produce an unacceptable advertisement of a soldier's location. In principle, the needed shielding can be achieved with acceptable added weight and volume by, for example, embedding the hot system in an argon filled silica or carbon aerogel to effectively suppress thermal leakage. We discuss the basic engineering design properties for such an approach in this section.

An aerogel with thermal conductivity κ, and thickness d, around a box of volume L^3 and surface area L^2, would give a thermal power leakage P_ℓ between the box surface (temperature T) and its own outer surface (temperature $<< T$)

$$P_\ell \sim \frac{10\,\kappa\,T\,L^2}{d}$$

Typical system parameters might be

$$\begin{aligned} P_\ell &\sim 10 \text{ Watts} \\ L &\sim 10 \text{ cm} \\ T &\sim 10^3 \,^\circ C \\ \kappa &\sim 3 \times 10^{-5} \text{ W/cm}\,^\circ\text{C} \\ d &\sim 2 \text{ cm} \end{aligned}$$

The aerogel covering would increase the total package volume by an additional $10^3\,\text{cm}^3$. The small weight increase (aerogel density $\sim 10^{-1}$ g cm^{-3}) would be 10^2g.

Although a very light, poorly conducting, aerogel can relatively easily sufficiently well isolate the hot part of the system from its environment, it would generally not have enough mechanical strength to hold the contained box in place in the face of mechanical stresses and shocks expected in realistic scenarios. The hot box would need to be held by struts and wires which pass through the gel. These would have to be strong at temperatures up to $T \sim 800$°C, but not conduct more heat outward than the P_ℓ through the gel: they should have a large high temperature "modulus of rupture" (Y_r) but small thermal conductivity (κ_r). Among refractories the ratio κ_r/Y_r is particularly small for Al_2O_3 and Z_rO_2, and there are other refractories for which this ratio is only several times larger (BC, $MoSi_2$). If the electric power generating box of mass M is subject to a large transient acceleration α the total cross-sectional area $\hat{A}$ of the wires and struts which hold it in place should be

$$\hat{A} \sim \frac{M\alpha}{Y_r}$$

For $Al_2\,O_3$ Y_r (800°) $\sim 5 \times 10^3$ kg/cm^2,

$$\begin{aligned} \text{and} \qquad M &\sim 1 \text{ kg} \\ \alpha &\sim 10^3 \times \text{ acceleration of gravity,} \\ \hat{A} &\sim 0.2 \text{ cm}^2. \end{aligned}$$

The heat leakage out through the $Al_2\ O_3$ mechanical holding structure would then be $P_r \sim \kappa \hat{A} T/d \sim 1$ watt, much less than the 10 watts thermal flow through the gel. [The ratio $\frac{P_r}{P_t}$ is roughly proportional to the linear size of the system (L).]

Thus, thermally isolating hot parts in some suggested batteries, fuel cells, and thermal electric generators is not ignorable, but is far from a show stopping problem provided that the mass requiring insulation is not too large.

20 COSTS

It is of course not possible to compare precisely the cost of a system under development to an existing, implemented system such as primary batteries. Nor is it straightforward to value the additional capability that would be obtained if one reduced the mass of the soldier's battery pack and allowed him instead to carry more bullets or become more mobile. Additionally, unlike batteries, whose mass is constant regardless of the state of charge of the battery (and batteries must, by regulation, be brought back and not discarded onto the battlefield even if fully discharged), fuel cell systems become lighter as the fuel is consumed. For the missions of interest, most of the mass is fuel, so this decrease in mass is of significant value even if the total system mass and fuel mass were comparable initially to that of batteries. Nevertheless, neglecting these added functionality and value features, some cost estimates can be made to serve as guidelines as to whether the technologies being considered are likely to be cost-prohibitive for the application of interest.

A key consideration is that fuel cells and the other systems considered above consist of two components; the convertor device, which bears a fixed cost that must be amortized over the operational lifetime of the convertor, and the recurring cost of the expendable, which is the fuel. These costs must be compared to the fully recurring costs incurred with the use of expendable primary batteries as power sources for the solider.

To first order, the fuels are so inexpensive that the recurring cost can be neglected. Figure 40 presents cost curves that amortize various fixed costs for the convertor unit in terms of cost per W of installed power, as a function of the operational lifetime of the convertor unit. Clearly, the longer the conversion unit lasts, the more expensive it can be while still providing an acceptable amortized cost level per unit of energy produced.

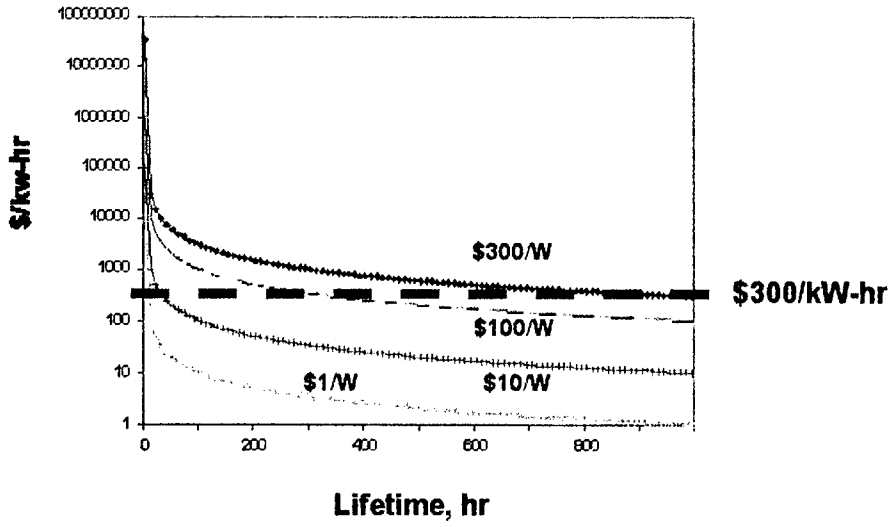

Figure 40: Cost curves for various energy conversion systems.

Figure 40 also presents the recurring cost of current BA-5590 batteries, which is approximately \$300/kW-hr. Since the extended soldier mission is to last at least 7 days, the conversion unit is clearly not of any use if it does not last at least that long; we therefore consider only units that last at least 10 times this value, i.e. on the order of 1000 hr or greater. Clearly, a cost of \$300/W for installed capacity, if the unit only lasts for 10 missions, i.e., 1000 hr, is an amortized cost of approximately (not rigorously because net present value computations have not been included in the calculations, but this does not affect the order of magnitude of the estimation) \$300/kW-hr, which is break-even with the cost per delivered kW-hr of the BA-5590 battery system.

As a guideline, we draw upon recent estimates of the cost of installed capacity for fuel cells for use in vehicular transportation applications [9]. PEM fuel cells in large quantity are estimated to cost \$100/kW of installed capacity, and DMFC's might cost \$200 500/kW due to the larger catalyst loadings and therefore their costs being dominated by catalyst costs. Nevertheless, even these cost levels are 1000-fold lower than the \$300/W level that can be afforded with a 1000 hr convertor lifetime to provide power at a cost/kW-hr

that is comparable to current military primary battery prices. Hence there appears to be no impediment to developing an affordable energy generation system based on any of the technologies discussed above, when the cost comparison is framed with respect to competing with existing military battery costs per delivered kW-hr to the soldier.

21 EXTENSION OF THE TECHNOLOGY APPROACH TO OTHER MISSIONS

It is important to point out that the evaluation performed in this study specifically addressed the mission of interest specified in the charge to the JASONs, which was for extended (7 days or greater) missions for which soldiers currently carry over 15–20 kg of batteries, and at a mean power level of approximately 20 W. Different mission types will impose different constraints that will likely affect the recommended technical solutions.

For example, higher power capacity would require more fixed mass in the convertor of a DMFC unit. As an example, a 100 W DMFC would have a mass of approximately 4.5 kg; hence unless the mission had very large energy demands, it would be difficult at this power level to overcome the fixed mass penalty of a DMFC relative to use of primary batteries (e.g. see Figure 41). Still higher power levels, or a distribution of 20 W power sources,

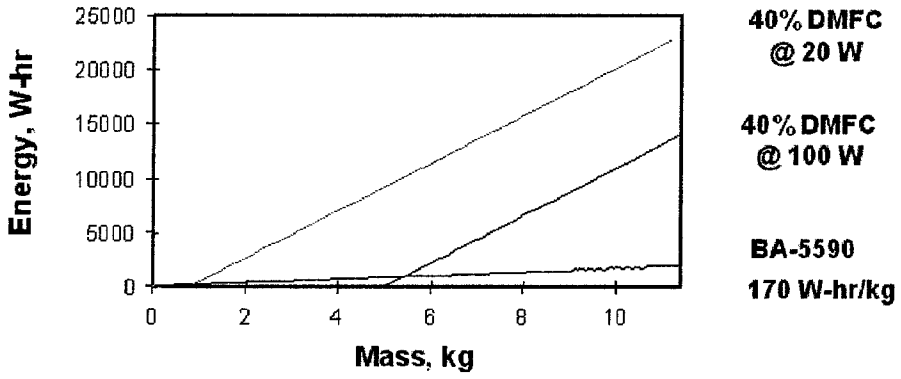

Figure 41: Energy vs mass as a function of the power level of DMFC's relative to batteries.

would disfavor the DMFC approach still more due to the penalty of having the mass of the convertor unit increase commensurately.

At the other extreme, very small power levels, such as those appropriate for cellphones, typically come with additional constraints on the volume and mass that can be allocated to the power source. Such constraints impose tradeoffs on the efficiency of the balance of plant for the conversion device and/or on the amount of fuel that can be carried. At present, such limitations disfavor DMFC technology or PEM fuel cell technology compared to primary or even secondary batteries.

Finally, at very high power levels, for instance, those of relevance to vehicular transportation applications, DMFC's simply are not affordable due to their high catalyst costs. Additionally, the relatively low power density of DMFC's imposes a significant weight penalty on the vehicle to achieve the required capacity of the power plant. Hence at these higher power levels the tradeoff for vehicular fuel cell technology generally favors reformers used in conjunction with H_2-fueled PEM fuel cells as opposed to DMFC's.

An additional consideration is whether DMFCs will be useful in the short-term for shorter duration missions. Note that for a 24 hr mission, satisfying a 20 W mean power load does not require 15 kg of batteries, and in fact supplying the 480 W-hr of energy with the Land Warrior v0.6 (285 W-hr/kg) battery will require only 1.7 kg of batteries. It hardly seems worth the effort to replace this system by a higher energy density source that might have a mass of 0.5 kg for the convertor and 0.5 kg for the fuel, especially given the difficulties in scaling down the technology to these levels. Furthermore the overall mass burden on such soldiers is approximately 45 kg, so the overall effect would be a reduction of the mass burden by perhaps 0.7 kg out of 45 kg. For these reasons, it seems that the "sweet spot" for application of DMFC technology and perhaps fuel cell technology in general is the 20 W power level for extended range missions. Other missions might well be best satisfied using existing battery technology and hybrids or improvements therein.

22 TECHNOLOGY LEVERS

In this section, we briefly identify some basic R&D issues that would potentially significantly enhance the performance of the energy conversion devices described above. These areas, amongst others, would seem to be appropriate for investment at the DoD 6.1 level to try to achieve significant eventual performance improvements relative to the existing technology options.

- Improved performance at fuel cell cathodes (oxygen reduction); all of the fuel cells suffer kinetic overpotential losses at the cathode and improved cathode catalysts would have a global impact on the efficiency of such devices
- Improved anodes for methanol oxidation in DMFCs; obviously, higher energy efficiencies would be obtained if the kinetic overpotential for methanol oxidation could be reduced to levels comparable to that of H_2 in a PEM fuel cell
- CO and S-tolerant H_2 PEM catalysts; such catalysts would avoid the need for water-gas shift and preferential oxidation catalysts and significantly simplify systems that used steam reforming in conjunction with PEM fuel cells
- Materials that enable "passive" fuel cell operation with less active control loops, which would greatly simplify the balance of plant in fuel cell systems

At the 6.2–6.3 funding levels, technology development and demonstration is needed to evaluate what can be achieved for

- Thermal and acoustic isolation for small engines

- Systems engineering for small H_2 generators, using micromachining concepts

At the systems level, the safety and packaging requirements and associated limitations for the fieldability of various fuels should be addressed.

Finally, we recommend that prototypes be evaluated rapidly with field personnel so that feedback as to the ultimate utility of what is being developed can be obtained in an expedient fashion.

References

[1] National Research Council, *Energy-Efficieint Technologies for the Dismounted Soldier*; National Academy Press: Washington, D.C., 1997; Vol. http://books.nap.edu/books/0309059348/html/R1.html#pagetop.

[2] Feldman, S., Land Warrior Briefing.

[3] Stockel, J., Private Communication to JASONs.

[4] Appleby, A. J.; Foulkes, F. R. *Fuel Cell Handbook*; Krieger Publishing Co.: Balabar, FL, 1993.

[5] Larminie, J.; Dicks, A. *Fuel Cell Systems Explained*; John Wiley and Sons: West Sussex, UK, 2000.

[6] Bard, A. J.; Faulkner, L. R. *Electrochemical Methods*, 2 ed.; John Wiley and Sons: New York, NY, 2000.

[7] Gulzow, E. *Journal of Power Sources* 1996, **61**, 99.

[8] Heinzel, A. et al. *Electrochimica Acta* 1998, **43**, 3675.

[9] Kalhammer, F. R.; Prokopius, P. R.; Roan, V. P.; Voecks, G. E. "Status and Prospects of Fuel Cells as Automobile Engines," State of California Air Resources Board, 1998.

[10] Zawodzinski, T. A.; Derouin, C.; Radzinski, S.; Sherman, R. J.; Smith, V. T.; Springer, T. E.; Gottesfeld, S. *Journal of the Electrochemical Society* 1993, **140**, 1041.

[11] Hirschenhofer, J. H.; Stauffer, D. B.; Engelman, R. R.; Klett, M. G. "Fuel Cell Handbook," Parsons Corp. for US DOE, 1998.

[12] Hirschenhofer, J. "Status of Fuel Cell Commercialization Efforts"; American Power Conference, 1993, Chicago, IL.

[13] Maru, H. C.; Paetsch, L.; Pigeaud, A. "Proceedings of the Symposium on Electrochemical Modeling of Battery, Fuel Cell and Photoenergy Conversion Systems"; Meeting of the Electrochemical Society, 1984.

[14] Bevc, F. *Proceedings of the Institution of Mechanical Engineers* 1997, **211A**, 359.

[15] Schmidt, J.; Quakenbush, T. "Fuel for Portable Power Systems Program Final Report," Ball Aerospace, 2002.

[16] Schmidt, J., Briefing to JASONs.

[17] James, B. D.; Baum, G. N.; Lomax Jr., F. D.; Thomas, C. E.; Kuhn, I. F. "Comparison of Onboard Hydrogen Storage for Fuel Cell Vehicles," Directed Technologies, Inc., 1996.

[18] Monsler, M.; Hendricks, C.; Walsh, T. "Energy Film: A Safe Portable Source of Hydrogen"; Workshop on Hydrogen Storage and Generation Technologies, 1997, Orlando, FL.

[19] Teitel, R. J.; Powers, J. "Microcavity Systems for Automotive Applications, Final Progress Report," R. J. Teitel Associates, 1979.

[20] Dengel, O. M.; Beckert, W. F. "Chemical Hydrides"; Workshop on Storage and Generation of Hydrogen, 1997, Orlando, FL.

[21] Bloomfield, D., Briefing to JASONs.

[22] Millenium Cell, http://www.millenniumcell.com/index.pl, 2002.

[23] Narang, S. C.; Sharma, S. K. "Development of Portable Hydrogen Source," SRI International, 2002.

[24] Rostrup-Nielsen, J. R. *Catalysis Today* 1993, **18**, 305.

[25] Twigg, M. *Catalyst Handbook*, 2 ed.; Wolfe: London, U.K., 1989.

[26] Palo, D., Briefing to JASONs.

[27] Palo, D. R.; Holladay, J. D.; Rozmiarek, R. T.; Guzman-Leong, C. E.; Wang, Y.; Hu, J. L.; Chin, Y. H.; Dagle, R. A.; Baker, E. G. *Journal of Power Sources* 2001, **108**, 28.

[28] Wildhaber, B.; Schmidt, J. "Final Report fo the Pacific Northwest National Laboratories and Ball Aerospace and Technologies Corp Integrated Fuel Processor-Fuel Cell Study," Pacific Northwest National Laboratory, Batelle Memorial Institute, 2002.

[29] Surampudi, S.; Narayanan, S.; Vamos, E.; Frank, H.; Halpert, G.; Laconti, A.; Kosek, J.; Prakash, G.; Olah, G. *Journal of Power Sources* 1994, **47**, 377.

[30] Ren, X.; Zelenay, P.; Thomas, S.; Davey, J.; Gottesfeld, S. *Journal of Power Sources* 2000, **86**, 111.

[31] Hallmark, J., Briefing to JASONs.

[32] Doyle, E.; Shukla, K.; Metcalfe, C. "Development and Demonstration of a 25 Watt Thermophotovoltaic Power Source for a Hybrid Power System," Thermo Power Corp., 2001.

[33] Mussi, E.; Hunt, T. K., Briefing to JASONs.

[34] Pantolin, J. E.; Sievers, R. K.; Giglio, J. C.; Tomczak, D. R.; Shuck, Q. Y.; Thomas, B. K. "Advanced AMTEC Converter Development"; Proceedings of IECEC01, 36th Intersociety Energy Conversion Engineering Conference, 2001, Savannah, GA.

[35] Dev, S. P., Briefing to JASONs.

[36] Annen, K., Briefing to JASONs.

[37] Dahm, W. E. "Briefing to JASONs," 2002.

[38] Dahm, W. J. A.; Ni, J.; Mijit, K.; Mayor, J. R.; Quao, G.; Dyer, S. W.; Benjamin, A. G.; Gu, Y.; Lei, Y.; Papke, M. L. "Micro Internal Combustion Swing Engine (MISCE) for Portable Power Generation, Paper No. 2002-0722"; 40th AIAA Aerospace Sciences Meeting, 2002, January 14-17, 2002, Reno, NV.

[39] Epstein, A. H.; Senturia, S. D. *Science* 1997, **276**, 1211.

[40] Epstein, A. H., Briefing to JASONs.

[41] Epstein et al., A. H. "Micro-Heat Engines, Gas Turbines, and Rocket Engines: The MIT MicroengineProject, Paper AIAA 97-1773"; 28th AIAA Fluid Dynamics Conference and the 4th AIAA Shear Flow Control Conference, 1997, Snomass Village, CO.

[42] Fréchette, L. G.; Jacobson, S. A.; Breuer, K. S.; Ehrich, F. F.; Ghodssi, R.; Khanna, R.; Wong, C. W.; Zhang, X.; Schmidt, M. A.; Epstein, A. H. "Demonstration of a Microfabricated High-Speed Turbine Supported on Gas Bearings"; Solid-State Sensor and Actuator Workship, 2000, Hilton Head Island, SC.

[43] Cooper, J.; Cherepy, N.; Barry, G.; Pasternak, A.; Surles, T.; Steinberg, M. "Direct Carbon Conversion: Application to the Efficient Conversion of Fossil Fuels to Electricity, Paper No. 50, UCRL-JC-140629"; Fall Meeting of the Electrochemical Society, 2000, Phoenix, AZ.

[44] Cooper, J. "Briefing to JASONs," 2002.

DISTRIBUTION LIST

Director of Space and SDI Programs
SAF/AQSC
1060 Air Force Pentagon
Washington, DC 20330-1060

CMDR & Program Executive Officer
U S Army/CSSD-ZA
Strategic Defense Command
PO Box 15280
Arlington, VA 22215-0150

DARPA Library
3701 North Fairfax Drive
Arlington, VA 22203-1714

Assistant Secretary of the Navy
(Research, Development & Acquisition)
1000 Navy Pentagon
Washington, DC 20350-1000

Principal Deputy for Military Application [10]
Defense Programs, DP-12
National Nuclear Security Administration
U.S. Department of Energy
1000 Independence Avenue, SW
Washington, DC 20585

Superintendent
Code 1424
Attn: Documents Librarian
Naval Postgraduate School
Monterey, CA 93943

DTIC [2]
8725 John Jay Kingman Road
Suite 0944
Fort Belvoir, VA 22060-6218

Strategic Systems Program
Nebraska Avenue Complex
287 Somers Court
Suite 10041
Washington, DC 20393-5446

Headquarters Air Force XON
4A870 1480 Air Force Pentagon
Washington, DC 20330-1480

Defense Threat Reduction Agency
Attn: Dr. Arthur T. Hopkins [12]
6801 Telegraph Road
Alexandria, VA 22310

IC JASON Program [2]
Chief Technical Officer, IC/ITIC
2P0104 NHB
Central Intelligence Agency
Washington, DC 20505-0001

JASON Library [5]
The MITRE Corporation
WA549
7515 Colshire Drive
McLean, VA 22102

U. S. Department of Energy
Chicago Operations Office Acquisition and
Assistance Group
9800 South Cass Avenue
Argonne, IL 60439

William Acker
431 New Karner Road
Albany, NY 12205

Dr. Allen Adler
Director
DARPA/TTO
3701 N. Fairfax Drive
Arlington, VA 22203-1714

Dr. Jane Alexander
Office of Naval Research
800 North Quincy Street
Arlington, VA 22217-5000

Dr. A. Michael Andrews
Director of Technology
SARD-TT
Room 3E480
Research Development Acquisition
103 Army Pentagon
Washington, DC 20310-0103

Kurt Annen
45 Manning Road
Billerica, MA 01821-3976

Dr. William O. Berry
Director
Basic Research ODUSD(ST/BR)
4015 Wilson Blvd
Suite 209
Arlington, VA 22203

Mr. David Bowman
Los Alamos National Laboratory
Mailstop D411
Los Alamos, NM 87545

Dr. Albert Brandenstein
Chief Scientist
Office of Nat'l Drug Control Policy Executive
Office of the President
Washington, DC 20500

Ambassador Linton F. Brooks
Under Secretary for Nuclear Security/
Administrator for Nuclear Security
1000 Independence Avenue, SW
NA-1, Room 7A-049
Washington, DC 20585

Dr. Steve Buchsbaum
DARPA/STO
3701 N. Fairfax Drive
Arlington, VA 22203-1714

Dr. Darrell W. Collier
Chief Scientist
U. S. Army Space & Missile Defense Command
PO Box 15280
Arlington, VA 22215-0280

John F. Cooper
7000 East Avenue
Livermore, CA 94550-9234

Prof Werner J. Dahm
Aerospace Engineering
3056 Fxb, 2140
Ann Arbor, MI 48109

Dr. James F. Decker
Principal Deputy Director
Office of the Director, SC-1
Room 7B-084
U.S. Department of Energy
1000 Independence Avenue, SW
Washington, DC 20585

Dr. Patricia M. Dehmer [5]
Associate Director of Science for Basic Energy Sciences, SC-10
Office of Science
U.S. Department of Energy
19901 Germantown Road
Germantown, MD 20874

Ms. Shirley Derflinger [15]
Technical Program Specialist
Office of Biological & Environmental Research, SC-70
Office of Science
U.S. Department of Energy
19901Germantown Road
Germantown, MD 20874

Paul Dev
4 Armstrong Road
Shelton, CT 06484

Alan H. Epstein
77 Massachusetts Avenue
31-265
Cambridge, MA 02139

Dr. Martin C. Faga
President and Chief Exec Officer
The MITRE Corporation
Mail Stop N640
7515 Colshire Drive
McLean, VA 22102

Mr. Dan Flynn [5]
Program Manager
DI/OTI/SAG
5S49 OHB
Washington, DC 20505

Ms. Nancy Forbes
Senior Analyst
DI/OTI/SAG 5S49 OHB
Washington, DC 20505

Dr. Paris Genalis
Deputy Director
OUSD(A&T)/S&TS/NW
The Pentagon, Room 3D1048
Washington, DC 20301

Mr. Bradley E. Gernand
Institute for Defense Analyses
Technical Information Services
Room 8701
4850 Mark Center Drive
Alexandria, VA 22311-1882

Dr. Lawrence K. Gershwin
NIC/NIO/S&T
2E42, OHB
Washington, DC 20505

Brigadier General Ronald Haeckel
U.S. Dept of Energy
National Nuclear Security Administration
1000 Independence Avenue, SW
NA-10 FORS Bldg
Washington, DC 20585

Jerry Hallmark
Manager Energy Technologies Lab
7700 S. River Parkway
ML28
Tempe, AZ 85284-1808

Robert Hamlen
ATTN: AMSEL-LC-AMC
Building 2700
Fort Monmouth, NJ 07703-5011

Dr. Theodore Hardebeck
STRATCOM/J5B
Offutt AFB, NE 68113

Dr. Robert G. Henderson
Director, JASON Program Office
The MITRE Corporation
7515 Colshire Drive
Mail Stop W950
McLean, VA 22102

Klavs Jensen
Department of Chemical Engineering
Room 66-566
Cambridge, MA 02139

Dr. Bobby R. Junker
Office of Naval Research
Code 31
800 North Quincy Street
Arlington, VA 22217-5660

Dr. Andrew F. Kirby
DO/IOC/FO
6Q32 NHB
Central Intelligence Agency
Washington, DC 20505-0001

Rich Masel
Chemical Engineering
213 RAL Box C3, MC 712
600 S. Mathews
Urbana, IL 61801

Dr. Anne Matsuura
Army Research Office
4015 Wilson Blvd
Tower 3, Suite 216
Arlington, VA 22203-21939

Dr. Maureen I. McCarthy
Homeland Security
Anacostia Naval Annex
Building 410
250 Murray Lane, SW
Washington, DC 20509

Mr. Gordon Middleton
Deputy Director
National Security Space Architect
PO Box 222310
Chantilly, VA 20153-2310

Dr. Thomas Meyer
DARPA/ATO
3701 N. Fairfax Drive
Arlington, VA 22203

Ed Mussi
Advisory Engineer
4370 Varsity Drive, Suite A
Ann Arbor, MI 48108

Dr. Julian C. Nall
Institute for Defense Analyses
4850 Mark Center Drive
Alexandria, VA 22311-1882

Dr. C. Edward Oliver [5]
Associate Director of Science for Advanced
Scientific Computing Research, SC-30
U.S. Department of Energy
19901Germantown Road
Germantown, MD 20874

Mr. Raymond L. Orbach
Director, Office of Science
U.S. Department of Energy
1000 Independence Avenue, SW
Route Symbol: SC-1
Washington, DC 20585

Dan Palo
P.O. Box 999
MS K8-93
Richland, WA 99352

Dr. Ari Patrinos [5]
Associate Director
Biological and Environmental Research
SC-70
US Department of Energy
19901 Germantown Road
Germantown, MD 20874-1290

Dr. John R. Phillips
Chief Scientist, DST/CS
2P0104 NHB
Central Intelligence Agency
Washington, DC 20505-0001

Records Resource
The MITRE Corporation
Mail Stop W115
7515 Colshire Drive
McLean, VA 22102

Jeff Schmidt
1600 Commerce Street
Boulder, CO 80301

Dr. John Schuster
Submarine Warfare Division
Submarine, Security & Tech
Head (N775)
2000 Navy Pentagon, Room 4D534
Washington, DC 20350-2000

Dr. Ronald M. Sega
DDR&E
3030 Defense Pentagon,
Room 3E101
Washington, DC 20301-3030

Dr. Richard Spinrad
US Naval Observatory
Naval Oceanographers Office
3450 Massachusetts Ave, NW
Building 1
Washington, DC 20392-5421

Jack Taylor
Defense Research and Engineering
(DDR&E)
3030 Defense Pentagon
Washington, DC 20301-3030

Mr. Anthony J. Tether
DIRO/DARPA
3701 N. Fairfax Drive
Arlington, VA 22203-1714

Dr. George W. Ullrich [3]
OSD [ODUSD(S&T)]/WS
Director for Weapons Systems
3080 Defense Pentagon
Washington, DC 20301-3080

Dr. Bruce J. West
FAPS
Senior Research Scientist
Army Research Office
P. O. Box 12211
Research Triangle Park, NC 27709-2211

Dr. Linda Zall
Central Intelligence Agency
DS&T/OTS
3Q14, NHB
Washington, DC 20505-000